REPELLENT FINISH

AND LAYERING ORDER STUDIES OF SURGICAL FACE MASKS

by

HONGQING SHEN

(Under the Direction of Karen K Leonas)

ABSTRACT

A surgical face mask is an important medical device used to protect both a surgical patient and an operating room personnel from transfer of microorganisms, body fluids and particulate material. In this research, effects of repellent finish and layering order on the fluid resistance, filtration ability and differential pressure of surgical face masks were studied. Results have demonstrated that repellent finish, fluid pressure and layering order all affect fluid resistance of surgical face masks significantly. A statistical model was developed to describe the relationship between fluid resistance and repellent finish, and fluid pressure and layering order. In determining the filtration ability of surgical face masks, techniques using Laser Scanning Confocal Microscopy (LSCM) were used to determine particle capture. Small particles present on/in nonwoven fabrics were located using LSCM. Then, image analysis was used to quantify the small particles by total area to evaluate the filtration ability. The results show that the filtration layer is the primary contributor to the barrier effectiveness of the surgical face mask. Statistical analysis was performed and the results showed that although repellent finish decreased the filtration ability of the cover layer, it did not affect the filtration ability of the filtration layer. Although layering order varied in this study, the filtration layer always stopped the penetration of the small particles. Differential pressures of face masks were also evaluated and the results

showed that repellent finish did not affect the breathability of face masks while the layering order influenced the breathability significantly. Although face masks with layering order of cover fabric, filtration fabric and shell fabric provided better breathability than face masks with other layering orders, all three layering orders offered acceptable breathability. Finally, a new face mask with optimum fluid resistance, filtration ability and breathability was statistically generated according to repellent finish and layering order. This would be a face mask treated with 4.5% add-on level of Zonyl® PPR protector on the cover fabric and a layering order of cover fabric, support fabric, filtration fabric and shell fabric.

INDEX WORDS: Medical Textiles, Nonwovens, Surgical Face Mask, Repellent Finish, Layering Order, Fluid Resistance, Filtration, Differential Pressure

REPELLENT FINISH AND LAYERING ORDER STUDIES OF SURGICAL FACE MASKS

by

HONGQING SHEN

B.E., China Textile University, Shanghai, China, July, 1994

M.E., China Textile University, Shanghai, China, March, 1997

A Dissertation Submitted to the Graduate Faculty of The University of Georgia in Partial Fulfillment of the Requirements for the Degree

DOCTOR OF PHILOSOPHY

ATHENS, GEORGIA

2005

REPELLENT FINISH

AND LAYERING ORDER STUDIES OF SURGICAL FACE MASKS

by

HONGQING SHEN

Major Professor:	Karen K. Leonas
Committee:	Mark A. Farmer
	J. Nolan Etters
	Helen H. Epps
	Lionel A. Carreira

Electronic Version Approved:

Maureen Grasso
Dean of the Graduate School
The University of Georgia
August 2005

DEDICATION

This dissertation is dedicated to my father, Guangqi, my mother, Zifen, and my wife, Shuqiong, for their loves and supports.

ACKNOWLEDGEMENTS

This dissertation would never have been completed without help and support of many people, who are gratefully acknowledged here.

I would like to express my deep appreciation to Dr. Karen K Leonas, my major professor, for her invaluable guidance, assistance, encouragement and kindness.

I am very grateful to Dr. Mark A. Farmer, Dr. J. Nolan Etters, Dr. Helen H. Epps, and Dr. Lionel A. Carreira for instructions, providing helpful suggestions and support, and being on my committee.

I would like to extend thanks to faculty, staff, and students in TMI department who supported me with their assistance and friendship over the past five years.

I am grateful to BBA, Vikon and Ciba for providing fabrics and chemicals. Acknowledgements are given to AATCC Student Research Award Review Board for providing funding for this project.

TABLE OF CONTENTS

Page

LIST OF TABLES

Page

LIST OF FIGURES

Page

CHAPTER 1

INTRODUCTION

Medical textiles is a growing area within technical textiles and its value is expected to account for almost 12% of the global technical textile market in 2005. As well as a production increase, the variety of possible application of medical textiles continues to expand and research in the medical textiles area has been stimulated by its growth potential. [1] There are commonly five different kinds of medical textiles: (1) bandaging, (2) health care, (3) hygiene, (4) wound care and (5) implanted devices. This research highlights the study of the surgical face mask, one of the health care medical textiles.

The surgical face mask is a device intended to be worn by operating room personnel during surgical procedures to protect both the surgical patients and the operating room personnel from transfer of microorganisms, body fluids and particulate material. [2] According to the definition of medical device by the Food and Drug Administration (FDA): “any article which is intended for use in the cure, mitigation, treatment or prevention of disease in man and which does not achieve any of its intended purposes through chemical action in the body or is dependent upon metabolism (i.e., a drug)”, the surgical face mask is a medical device and regulated by the FDA.

Infection control in the hospital is very important for the safety of both health care workers and patients. One of the established routines in operating theatre is the use of surgical face masks to minimize the risk of infection. In the United States, standards and guidelines related to this have been published by several organizations. The Association of periOperative

Registered Nurses (AORN) has published recommendations related to standard precautions. Standard precautions to prevent pathogen transmission should be used during all invasive procedures. Standard precautions include the use of protective barriers and prompt and frequent hand washing to reduce the risk of exposure to potentially infectious materials. Personal protective equipment (PPE) for standard precautions includes intact gloves, gowns, masks, and eye protection (eg, face shields, goggles, glasses with side shields). Leg coverings, shoe covers, and other PPE may be used where indicated. [3] The Centers for Disease Control (CDC) has published a prevention recommendation that includes the following: "Surgical masks should be used to prevent the respiratory secretions of the person wearing the mask from entering the air." [4] Use of protective apparel, face masks and other equipment is also recommended by the Occupational Safety and Health Administration (OSHA). The OSHA Occupational Exposure to Bloodborne Pathogens: Final Rule (1991) requires all employers to supply personal protective equipment to employees. The equipment must provide protection against all reasonable anticipated occupational exposure and must not permit blood or other potentially infectious materials to pass through or reach the empolyee's work clothes, street clothes, undergarments, skin, eyes, mouth or other mucous membranes under normal conditions of use. [2] In recent years, several new ASTM standards specifically relating to face masks and their evaluation (ASTM F 1862-00 [5] and ASTM F 2101-01 [6]) were also approved.

Significance of Study

Health care workers, involved in treating and caring for injured or sick individuals, can be exposed to biological liquids capable of transmitting disease. These diseases, which may be caused by a variety of microorganisms, can pose significant risks to life and health. This is

especially true of blood-borne viruses which cause Hepatitis and Acquired Immune Deficiency Syndrome. [5] Surgical face masks are used to reduce the liquid exposure. The same workers can also be exposed to biological aerosols capable of transmitting disease. These diseases can pose significant risks to life and health. Since engineering controls can not eliminate all possible exposures, attention is placed on reducing the potential of airborne exposure through the use of medical face masks. [6] Therefore the primary functions of surgical face masks are to protect individuals from blood splash or spatter and from microorganism transfer.

The ASTM F 1862-00 test method allows for the assessment of the fluid resistance of surgical face masks, but only the pass or fail of the face mask is reported. Although there are some reported studies [7,8] relating applying repellent finish to other PPE devices such as surgical gowns, there's no known literature that reports applying repellent finish to the surgical face mask. Therefore, in this research a repellent finish was applied to the cover fabric of the surgical face mask and its influence on the performances of the face mask was studied. Although there are a variety of surgical face mask styles in the current market, the layered face mask is one of the most common types. Within the available layered face masks, there are a variety of different layering orders. Some of the masks have three layers, and the filtration layer, the layer with the high packing density, is between the outside cover layer and the inner shell layer. Others have four layers and the position of filtration layer changes in the layer arrangement of the four-ply face mask. The filtration layer may be behind the outside cover layer or proceed the inner shell layer. Although nonwoven manufactures have shown much interest [9] in the layering order, there are no published papers about the effect of layering order on the properties of surgical face masks. In the research presented here, the effect of layering order on the performances of face masks was studied too. Finally, a new face mask with optimum

performances was statistically generated according to repellent finish and layering order. The results of this study can provide significant information for health care workers and medical product manufacturers.

Research Objectives

The objective of this dissertation is to study the effects of repellent finish and layering order on the performances of surgical face masks. This overall objective is divided into the following:

1. Evaluate the impacts of repellent finish and layering order on the fluid resistance of surgical face masks,

2. Evaluate the impacts of repellent finish and layering order on the filtration ability of surgical face masks against small particles,

3. Evaluate the impacts of repellent finish and layering order on the differential pressure of surgical face masks,

4. Locate the small particles captured on and/or in the structure of face masks using Laser Scanning Confocal Microscopy (LSCM),

5. Complete the quantitative analysis on the small particles using the Image Processing and Analysis in Java (ImageJ),

6. Statistically generate the specifications of a face mask that has optimum fluid resistance, filtration ability and breathability based on repellent finish and layering order.

CHAPTER 2

LITERATURE REVIEW

It is necessary to first introduce surgical face masks and the primary published research that is available in this area so that the background of this study can be well understood. To study the effects of repellent finish and layering order on the fluid resistance, filtration ability and differential pressure of surgical face masks, an understanding of the theories of repellent property and filtration are also essential. The mechanisms of particle capture by filters are also introduced to obtain a good understanding about this research. Moreover, evaluation of aerosol filtration and use of LSCM in relative areas are also reviewed. An attempt has been made in this chapter to provide an understanding of these topics.

Surgical Face Mask

The surgical face mask is a medical device intended to be worn by operating room personnel during surgical procedures to protect both the surgical patients and the operating room personnel from the transfer of microorganisms, body fluids and particulate material. [2] Therefore the primary functions of surgical face masks are to protect individuals from blood splash or spatter and from microorganism transfer. Mikulicz, in 1896, was the first surgeon to use a mask to protect wounds from mouth bacteria. [10] Since the end of the nineteenth century wearing a surgical face mask by those caring for patients has been recognized as a necessity. [11] The early masks consisted of several layers of gauze or linen and were reused after sterilization. Masks were later improved by the insertion of paper or cellophane between the linen layers to

provide an impervious barrier. In the early 1960's, synthetic fibers such as polyester and polypropylene were first used to produce nonwoven surgical face masks. [12] Now surgical face masks are commonly produced from disposable nonwoven fabrics. Surgical face masks have a variety of styles such as flat-fold, tie-on, cone shaped, duckbill, flat-fold with shields and duckbill with shields.

Although there are a variety of surgical face mask styles currently in the market, the layered face mask is one of the most common types. Within the available layered face masks, there are a variety of different layering orders. Some of them have three layers, and the filtration layer, the layer with the high packing density, is between the outside cover layer and the inner shell layer. Others have four layers and the position of filtration layer changes in the layer arrangement of the 4-ply face mask. The filtration layer may be behind the outside cover layer or proceed the inner shell layer. [9, 13]

That there is little doubt that the routine use of surgical masks in the 1920's helped to suppress the large numbers of postsurgical wound infections caused by streptococci. Streptococci isolated from puerperal fever and wound infections were identical to those carried in the throats of the obstetric and surgical teams. [12] However the use of surgical face masks has been questioned in the past decade. Orr studied the relationship between the use of surgical masks and the rate of surgical site infections. No increase in postoperative surgical site infection rates was found in an initial one month pilot study during which no surgical face masks were worn in the operating theatre of a British hospital. [14] Tunevall examined the effect of wearing surgical face masks on the postoperative surgical site infection rate of 3088 patients during a two-year period in acute and elective general surgery. The surgical site infection rate was 4.7% when masks were worn and the rate was 3.5% when masks were not worn. The difference in rates was not

statistically significant. There was also no significant difference in the number of wound cultures growing staphylococci or streptococci between these two cases. [15]

There have been a number of reports [16-21] citing experimental evidence about the effectiveness of the surgical face mask. Greene developed a sampling chamber to evaluate the effectiveness of the surgical face mask. In his experiment, the subject inserted his head into the chamber and distinctly pronounced the words "sing and chew" at ten-second intervals for one minute. Samples were collected on blood agar with an Anderson sampler and then incubated at 37^{o} C for 24 hours. The results showed that the airborne microorganisms expelled by the masked subject were significantly less than those expelled by the unmasked subject during talking. [16] Madsen found that many thousands of bacteria can be expelled in a single cough or sneeze. In this study four commonly used masks, a Filtron® mask, an Aseptex® mask, a Bardic Deseret Filtermask® and a paper mask, were selected for evaluation. Then these masks were placed over the nose and mouth of a manikin that was placed in a special counting chamber. A known number of bacteria were blown from manikin through the mask simulating a human sneeze or cough. Bacteria in the chamber were collected by an Anderson sampler and counted. The bacterial retaining efficiencies were 98.8%, 98.4%, 97.3% and 92.7% for the Filtron® mask, the Aseptex® mask, the Bardic Deseret Filtermask® and the paper mask respectively. [17] Quesnel used similar chamber to evaluate five different types of surgical masks including Aseptex®, Cestra®, Surgine®, Filtermask® and Filtron®. The contaminated particles escaping through or around the mask during speech by the wearer were collected. The results showed that all the masks had a high degree of efficiency of about 99% in particle filtration. [18] Ford [19,20] and Rogers [21] used a different testing device to evaluate the efficiency of surgical face masks. The experimental testing device is composed of four components: (1) Anderson sampler, (2) a glass

cylindrical chamber, (3) a nebulizing flask, and (4) a compressed air source. This device was used to collect the bacterial particles filtering through masks. Nine types of masks, Aseptex®, 3M® 1818, Surgine®, White Knight®, Luxan Medex®, Macarthys Macro®, Macarthys®, Robinson® and SNS®, were evaluated. The results demonstrated that all tests through masks produced lower bacterial particle counts than the unmasked controls did.

Today, there are a variety of test methods specifically relating to face masks and their evaluation. ASTM F 1862-00: Standard Test Method for Resistance of Surgical Mask to Penetration by Synthetic Blood can be used to evaluate fluid resistance. Fluid resistance is the ability of the mask's material to inhibit the penetration of blood and body fluids. [5] ASTM F2101-01: Standard Test Method for Evaluating the Bacterial Filtration Efficiency (BFE) of Medical Face Mask Materials, Using a Biological Aerosol of Staphylococcus aureus can be used to measure bacterial filtration efficiency. BFE is a measure of the ability of the mask's material to prevent the passage of aerosolized bacteria. BFE is expressed in the percentage of a known quantity that does not pass the mask material at a given aerosol flow rate. [6] Differential pressure (Delta-P) is the measured pressure drop across a surgical face mask material and is used to determine breathing resistance. Differential pressure is expressed as a pressure per unit area. The differential pressure of surgical face masks can measured according to the Military Specification (MIL-M36945C 4.4.1.1.1): Surgical Masks, disposable. [22] Differential pressure relates to the breathability and comfort of the surgical face mask. The lower the differential pressure, the better the breathability and comfort of the surgical face mask. The requirement of differential pressure for surgical face masks is determined in the ASTM F 2100 Standard Specification for Performance of Materials Used in Medical Face Masks [23]. The face mask can offer acceptable breathability as long as its differential pressure is lower than 4.0 mmH_2O/cm^2.

Nonwoven Fabrics Used for Surgical Face Masks

Today surgical face masks are commonly produced from nonwoven fabrics. Nonwovens are defined as " web structures made directly from melts or from fibers which are at least 0.2 mm long and are held together by systems other than hydrogen bonding." [24] In general, the manufacture of nonwoven fabrics consists of four steps: (1) selecting fibers, (2) forming some type of mat structure, (3) mechanically, chemically, or thermally bonding the matted fibers, and (4) finishing and converting the formed integral matted structure. [24]

Dry-laid, wet-laid and melt spun are the three primary systems of nonwovens manufacturing. [24] The dry-laid system is based on well known textile processes. In this system, bales of fibers are torn open by an opener and then fed to a card which will separate and comb the fibers to form a thin web. The wet-laid system is derived from paper making. Forming of mat structure in this system is composed of the following three steps: (1) dispersion of fibers in water, (2) continuous web forming on a wire cloth through filtration, and (3) consolidation, drying and batching up the web. [24] Synthetic polymers can be used to produce nonwovens using the third system, melt spun in which meltable polymers can be used to make nonwovens directly from the melt without necessarily first spinning textile fibers. There are two primary methods within the melt spun system, meltblown and spunbonded. In the meltblown method, melted polymers are forced through a die with 20-40 small orifices per inch of width. High temperature air is impinged at both sides of the melted film. The high velocity air stretches the film into fibers along the length. These fibers are then deposited onto a collector screen to form the web. [25] The meltblown method has a cost advantage over other methods because the web is formed without controlled stretching. [24] The very fine diameter fibers (three microns on average) formed by melt blowing gives the nonwoven high density and cover factor. This

structure is very valuable in the filtration system, therefore many filtration media and medical/surgical products are commonly produced from meltblown nonwoven fabrics. [25] The disadvantage of the meltblown method is the need for large capacity compressors to provide the extremely high air velocities and inability to properly stretch the fractured fibers so as to obtain good fiber strength and controlled elongation. [24] In the spunbonded method, the thermoplastic polymer is extruded through the spinnerettes. The polymer streams are cooled and attenuated by air or by mechanical rollers to achieve the filament. The filaments are deposited onto a conveyor belt and a bonding step forms the nonwoven web of continuous filament fibers in the 15-20 micron range. Spunbonded nonwoven fabrics offer greater strength than meltblown nonwoven fabrics and can be used as diaper overstock, roofing substrates, automotive and carpet tile backing and medical disposables. [25] Today, nonwoven fabrics used for surgical face masks are commonly produced using the melt spun method.

Repellent Properties

In general, liquid repellent fabrics are those that resist being wet out by liquids. Wetting of a fabric results from contact of a liquid with the fabric surface under specific conditions. [26] A fabric's resistance to a liquid will depend on the surface relationship between the liquid and the fabric. A fabric is repellent if the critical surface energy of surface of the fabric is lower than surface tension of the challenge liquid.

Surface Tension and Contact Angle

The surface tension of a liquid is the force acting on its surface, which allows its surface area to be minimized. The surface tension of water is 72 dyne/cm. The surface tension of blood

is 42 dyne/cm and that of isopropyl alcohol is 22 dyne/cm. [26] A liquid with a low surface tension has better wetting ability than a liquid with a high surface tension. The critical surface energy of a solid is defined as the surface tension of a liquid that just completely spreads on the surface. [26] The relationship between the surface energy of the solid and the surface tension of the liquid determines whether the solid is repellency. Liquids with surface tension below the critical surface energy of a solid will spread on the surface of the solid.

When a drop of liquid on a solid surface does not spread, the drop will assume a shape that appears constant and exhibits an angle θ, called the contact angle (Figure 2-1 [26]). The contact angle is due to the mechanical equilibrium of the liquid resting on a solid surface. γ_{LV} represents the surface tension at the interface of the liquid and vapor phases, γ_{SL} at the interface of the solid and liquid, and γ_{SV} at the interface of the solid and vapor. Young's Equation describes the equilibrium forces: [26]

$$\gamma_{SV} - \gamma_{SL} = \gamma_{LV} Cos\theta \qquad 2\text{-}1$$

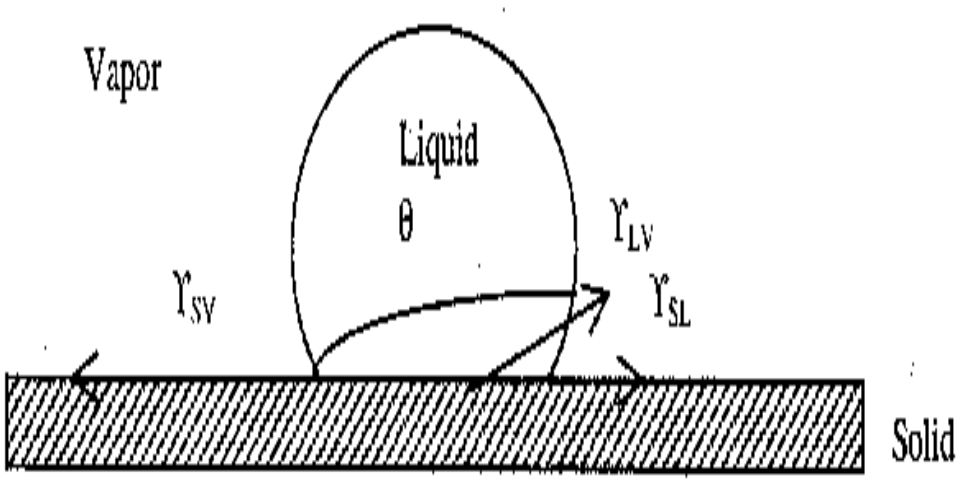

Figure 2-1. Spreading of liquids on smooth surfaces [26]

The contact angle is a useful inverse measure of the ability of a solid to be wet out. When θ is greater than 90°, it is relatively difficult for the liquid to spread on the surface and the solid is generally considered as repellent to this liquid. When θ is less than 90°, the liquid can spread on the surface and the solid is generally considered as non-repellent to this liquid.

Sometimes the measurement of a single static contact angle to characterize the interaction is not adequate as there exists a range of contact angles between a given solid and a liquid. When the drop has recently expanded the angle represents the 'advancing' contact angle that is the maximum value. When the drop has recently contracted the angle represents the 'receding' contact angle that is the minimum value. If the liquid/solid/vapor boundary is in actual motion the angles produced are known as Dynamic Contact Angles and are referred as 'advancing' and 'receding' angles. [27]

Repellent Finishes

There are a variety of repellent finishes used on textiles including fiber reactive hydrocarbon hydrophobes, silicone water repellents and fluorochemical repellents. Fluorochemical repellents are unique in that they confer both water and low surface tension fluids repellent to fabrics. This property is important because low surface tension liquids such as blood and alcohol often exist in the operating room. Therefore, a fluorochemical finish was used in this study. The ability of fluorochemicals to repel low surface tension liquids is related to their low surface energy. The fluorochemical finishes are organic fluorine-containing compounds in which a majority of the hydrogen atoms are replaced by fluorine. When these compounds are applied to fabric followed by drying and curing, the fluorochemical tails orient themselves away from the fibers to produce a very low surface energy barrier. The degree of repellency depends

on the number of fluorines, the orientation of the fluorocarbon segment of the molecule, the add-on levels, and the distribution and coverage of fluorocarbon on the surface. [26]

Filtration

Introduction

Filtration is a process in which a material collects and retains particles while allowing the fluid carrying the particles to pass through. Filtration efficiency can be expressed in terms of the number (E) or the mass (E_m) of particles by the following equations: [28]

$$E = \frac{N_{in} - N_{out}}{N_{in}} \qquad 2\text{-}2$$

where E = filtration efficiency in terms of the number,

N_{in} = number concentration of particles entering the filter,

N_{out} = number concentration of particles leaving the filter,

$$E_m = \frac{C_{in} - C_{out}}{C_{in}} \qquad 2\text{-}3$$

where E_m = filtration Efficiency in terms of the mass,

C_{in} = mass concentration of particle entering the filter,

C_{out} = mass concentration of particles leaving the filter.

The filtration efficiency of a material may also be expressed by the penetration of particles through it by the following equations based on the number (E) or the mass (E_m) of particles: [28]

$$P = 1 - E = \frac{N_{out}}{N_{in}} \qquad 2\text{-}4$$

$$P_m = 1 - E_m = \frac{C_{out}}{C_{in}} \qquad 2\text{-}5$$

where P = penetration of particles in terms of the number,

P_m = penetration of particles in terms of the mass.

Aerosol Filtration Characteristics of Surgical Face Masks

Weber et. al, selected eight surgical masks that had different filter materials and mask shapes (molded cone vs flat) from four manufacturers and tested for aerosol particle penetration. A Laser Aerosol Spectrometer was used in this study to measure the corn oil aerosol particles in the range of 0.1 to 1 μm and an Aerodynamic Particle Sizer was used to measure the corn oil aerosol particles in the range of 1 to 4 μm. Both instruments recorded the number concentration of particles by specific sizes. One advantage of these instruments is that filtration efficiency can be measured for each particle size, in contrast to other methods that yield only an overall efficiency for a particle size distribution with a given mean size and spread. The results showed that the percentage of filter penetration ranged from 20% to nearly 100%. When the surgical masks had artificially induced face-seal leaks, the concentration of particles inside the mask increased slightly. [29] In another study, Chen et. al, selected five masks and respirators, including Aseptex® sub-micron molded surgical mask, 3M® healthcare particulate respirator, 3M® dust/mist respirator, 3M® dust/welding fume respirator and 3M® high efficiency respirator, and evaluated them against mycobacterial aerosols. In the designed test apparatus, mycobacterial aerosol was generated with a nubulizer from a specific concentration of Mycobacteria chelonae. Aerosol concentrations were measured with Anderson samplers upstream and downstream of the test masks and respirators. The results showed that even the least efficient mask tested had a

filtration efficiency of more than 97% against particles less than 1 μm and the filtration efficiency ranged from 97% to 99.99%. The same samples were also evaluated against the polystyrene latex spheres (PLS) with the size of 0.8 μm and the results showed an extremely high correlation between microbiologic data and the data for the PLS. [30] In the study by Willeke, bacterial penetration of different bacterial shapes through a surgical mask and a respirator were studied. A Filtron® high-performance surgical mask and a dust/mist respirator were selected, and both masks were evaluated against four bacteria: Streptococcus salivarius with a single-cell spherical form and an aspect ratio (length to width ratio) of 1, Bacillus megatherium with an aspect ratio of 2.6, Pseudomonas fluorescents with an aspect ratio of 3.0 and Bacillus alcalophilus an aspect ratio of 4.4. The concentrations of bacteria upstream and downstream of the test devices were measured with an aerodynamic size spectrometer. The results showed that rod-shape bacteria whose aspect ratio are greater than 1 penetrated less. The penetration difference between the spherical and rod-shape bacteria was dependent on the aspect ratio of the bacteria. For an aspect ratio of 4, the penetration of rod-shaped bacteria was about half that of spherical ones. [31]

In June 1995 the National Institute for Occupational Safety and Health (NIOSH) issued a new regulation (42 CFR Part 84). [32] The regulation distinguishes filters with three efficiency levels, 95%, 99% and 99.97%. Qian et. al, measured the filtration efficiency of the most commonly used respirator with certified 95% efficiency. The respirators were challenged with NaCl aerosols whose particle sizes range from 0.1 μm to 0.3 μm. The filtration efficiency was measured with particle-size spectrometers. The results showed that the respirators had higher filtration efficiencies than those of non-certified surgical masks. [33] In 1997, Qian et. al, also studied the reaerosolization of bacteria on N95 respirators. If a respirator does not contain an

exhalation valve, and the respirator wearer sneezes or coughs, one may expect previously collected particles to be reaerosolized. This may be of special concern in environments contaminated with airborne microorganisms. In that study, the percentages of reaerosolization were measured in a test setup where the number of reaerosolized particles were registered by dynamic aerosol size spectrometry relative to the number of previously collected particles or bacteria. The results showed that the reaerosolization of particles and bacteria collected on the fibrous filters of N95 respirators was insignificant at conditions encountered in respirator wear. [34]

Two studies [35,36] completed on the bacterial aerosol collection efficiency of surgical face masks and respirators under varying conditions were found. In these studies aerosols were generated by nebulization before combining with dilution air. All aerosols were measured using the Aerodynamic Particle Sizer. Biological aerosols were also measured with a viable particle sampler. The Anderson six stage viable particle sampler was modified by the addition of a seventh stage and dilutor to sample at lower flows. Aerosol was sampled upstream and downstream of the sample. The collection efficiency was determined in the same way as the filtration efficiency. Brosseau et. al, used Mycobacterium abscessus and 0.55 μm latex sphere aerosols to measure the collection efficiencies of 16 respirators and five surgical masks from different manufactures. These samples were evaluated under two flow rates, 45 L/min and 85 L/min. The results showed that higher flow rate resulted in higher penetration. [35] In another study, McCullough et. al, studied the collection efficiencies of different surgical masks against three bacteria, Mycobacterium abscessus, Staphylococcus epidermidis and Bacillus subtilis. The bacterial collection efficiency was determined at two flow rates (45 L/min and 85 L/min) and two relative humidity levels (30% and 70%). Aerosols were measured with a total-particle,

direct-reading spectrometer and a viable particle cascade impactor. Measurements upstream and downstream of the mask were used in determining aerosol penetration. The results showed that the effect of flow rate was significant for all bacteria and higher flow rate resulted in significantly greater penetration. The effect of humidity was significant for only Mycobacterium abscessus. Mycobacterium abscessus penetrated more at the lower relative humidity condition, while the other two organisms were largely unaffected by relative humidity. [36]

Filtration Efficiency Tests of Surgical Face Masks

There are two commonly used methods to measure the filtration efficiency of surgical face masks: (1) Bacterial Filtration Efficiency (BFE) and (2) Filtration Efficiency Test (FET).

Bacterial Filtration Efficiency (BFE)

Bacterial Filtration Efficiency (BFE) is a measure of the ability of the mask's material to prevent the passage of aerosolized bacteria. BFE is expressed in the percentage of a known quantity that does not pass the mask material at a given aerosol flow rate. [6] Two methods, in vitro BFE and in vivo BFE, are used to perform the bacterial filtration efficiency test.

In Vitro BFE

The in vitro BFE test requires the surgical face mask to be challenged with a mist produced by aerosolizing Staphylococcus aureus bacteria with peptone water in a standard nebulizer. The Standard Test Method ASTM F 2101-01, Standard Test Method for Evaluating the Bacterial Filtration Efficiency (BFE) of Medical Face Mask Material, Using a Biological Aerosol of Staphylococcus aureus is a typical in vitro BFE test method. The Bacterial Filtration Efficiency can be determined using the apparatus shown in Figure 2-2 [6], which consists of a

continuous drive mechanism, an aerosol chamber, a six-stage sampler, a condenser, a flow meter and a vacuum pump. The aerosol is drawn through the controls and the test specimen clamped in the holder at a flow rate controlled by the flow meter. The aerosols penetrating the controls and the test specimen are collected by the six-stage agar plates, then agar plates are incubated at 37 ± 2°C for 48 ± 4 h. All bacterial colonies for the controls and the test specimens from each of the six plates are counted. The percent particle penetration, P, and filtration efficiency, E, are determined by comparing the particle count with and without the specimen using the following equations: [6]

$$E = \frac{C - T}{C} \times 100 \qquad 2\text{-}6$$

Where C = average plate count total for test controls,

T = plate count total of test sample.

$$P = 1\text{-}E. \qquad 2\text{-}7$$

In Vivo BFE

In the in vivo BFE tests, a face mask worn by a person is challenged with the aerosol emitted by a person while speaking or simulating a cough several times. Figure 2-3 [16] is a typical test apparatus for the in vivo BFE. The primary components are a sampling chamber and the Anderson sampler. Air samples are taken from the empty chamber to determine the "background" microbial and particulate. Air samples from the chamber with the masked subject present, but silent, are taken to determine the "subject-background" contaminant level. Air samples are also collected when the subject wearing a mask pronounced "sing and chew" at ten-second intervals for one minute. Samples are collected on blood agar with an Anderson sampler. The samples are incubated at 37^{o} C for 48 hours, and then at 20^{o} C for an additional 24 hours.

Bacterial colonies can be counted or calculated according to the positive conversion table [37] that was developed by Anderson in 1958. The efficiency of the mask in retaining both microbial and particles can be determined and evaluated by the counts. [16]

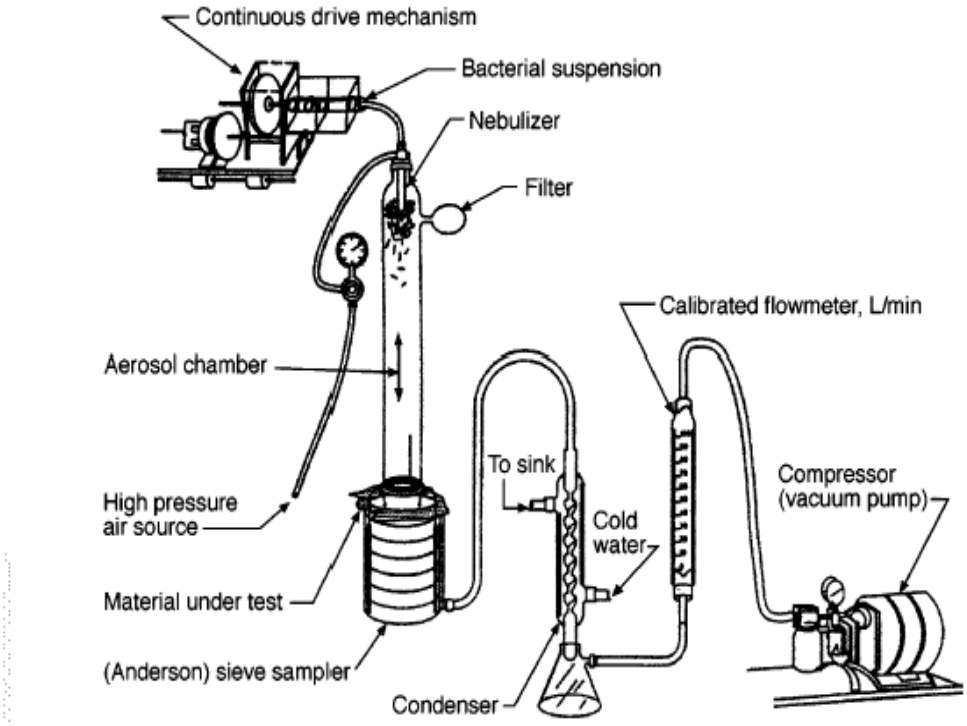

Figure 2-2. In vitro bacterial filtration efficiency test apparatus [6]

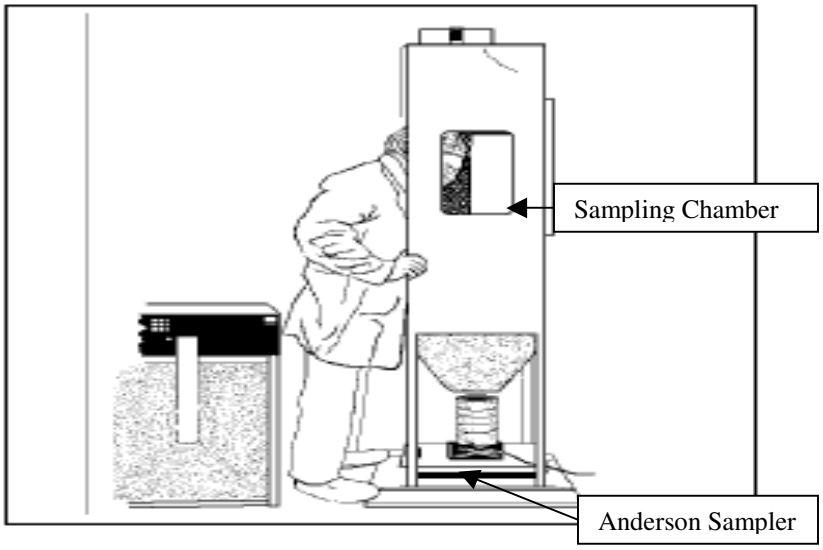

Figure 2-3. In vivo bacterial filtration efficiency test apparatus [16]

Filtration Efficiency Test (FET)

In 1983, Wadsworth and Davis [33, 34] developed a simulated BFE test known as the filtration efficiency test (FET). The FET apparatus is shown in Figure 2-4 [38]. In the FET test latex particles are substituted for the bacteria and an optical particle counter (OPC) is used to count the number of latex particles. As shown in Figure 2-4, a water suspension of latex microspheres with an average diameter of 0.8 μm is drawn to a standard nebulizer. From the nebulizer the aerosol passes into a mixing chamber. From the mixing chamber the aerosol is drawn through the T-shaped tube down through the filter media sealed in a circular sample holder. The aerosol penetrating the filter is drawn into a drying tube. The filtration efficiency is calculated from the number of particle counts measured at the OPC with and without the filter. The filtration efficiency measured by the FET is found to correlate with that of the BFE test with a correlation coefficient value of greater than 0.95. The FET has several advantages over the BFE tests. Its test time is about 5 minutes compared with a 2-day test for the BFE. FET is more reproducible than the BFE test. Thousands of different types of particles can be used in FET rather than approximately 100 types of bacteria that can be used in BFE. It can provide rapid feedback in the production of the filter media. [38]

Particle Capture Mechanisms by Filters

The filtration mechanisms of aerosol particle captured in filters are principally based on the "single-fiber" model. Several partial mechanisms are combined in integral particle collection on the surface of a fiber. (Figure 2-5 [39]) Mechanisms of interception, inertial impaction, diffusion, gravity, electrostatic capture and combined effects of these mechanisms are discussed briefly in the following sections.

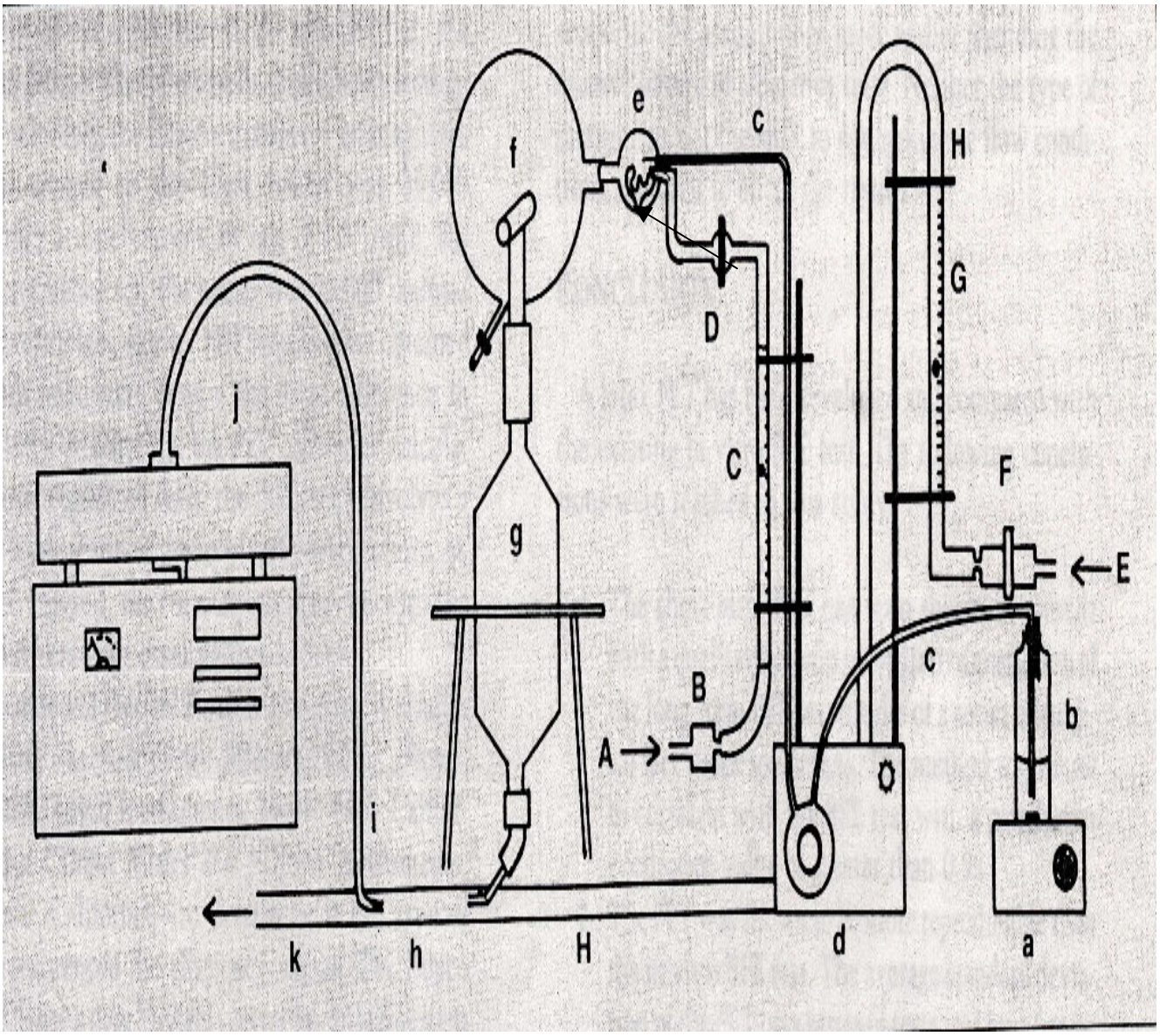

Figure 2-4. Latex FET apparatus: a, magnetic stirrer; b, test suspension; c, tubing to nebulizer; d, peristaltic pump; e, nebulizer; f, mixing chamber; g, sample holder; h, drying tube; I, tubing to particle counter; j, optical particle counter; k, exhaust line; A, inlet air to nebulizer; B, Millipore filter (25 mm); C, flowmeter (nebulizer air); D, three-way stopcock; E, dilution air to drying tube; F, Millipore filter (45 mm); G, flowmeter (dilution air); H, line to drying tube [38]

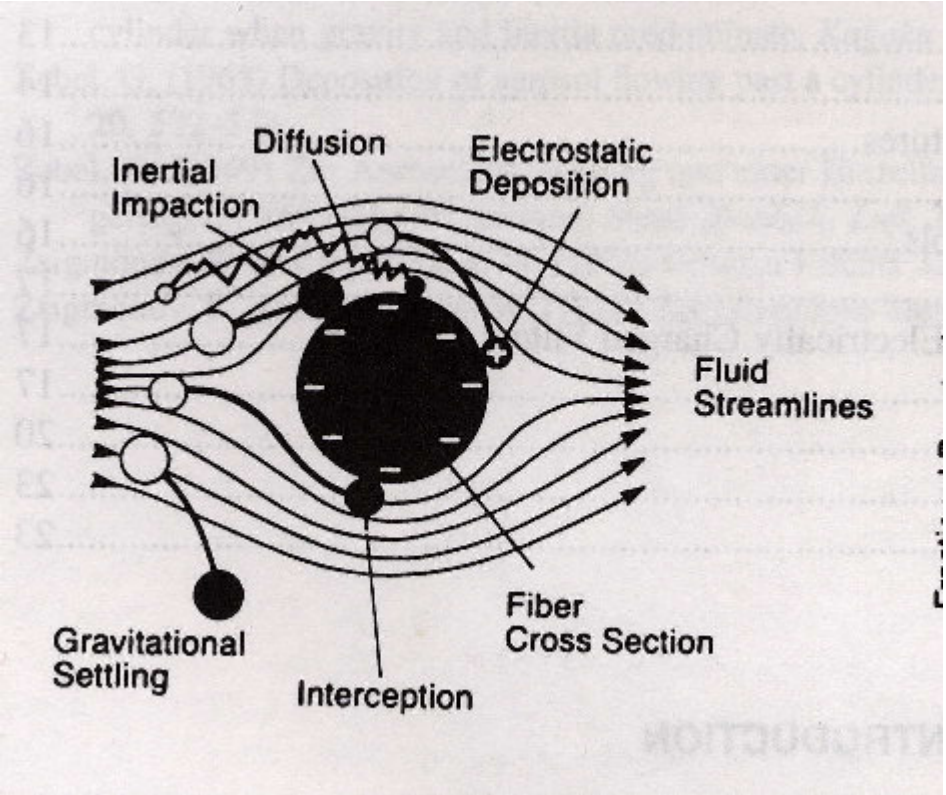

Figure 2-5. Particle-capture mechanisms [39]

Theory of Single Fiber Efficiency

The single fiber efficiency is defined as the quotient of the number of particles actually removed and the number that would be removed by a 100% efficient fiber. [40] Single fiber efficiency (E_s) has the value,

$$E_s = \frac{2y}{d_f} \qquad 2\text{-}8$$

where the parameters y and d_f are illustrated in Figure 2-6 [40]. This definition is satisfactory provided that the fiber is isolated and that a limiting trajectory can be defined in such a way that particles originating nearer to the axis than this trajectory will be captured and those originating further away will not be captured. [40]

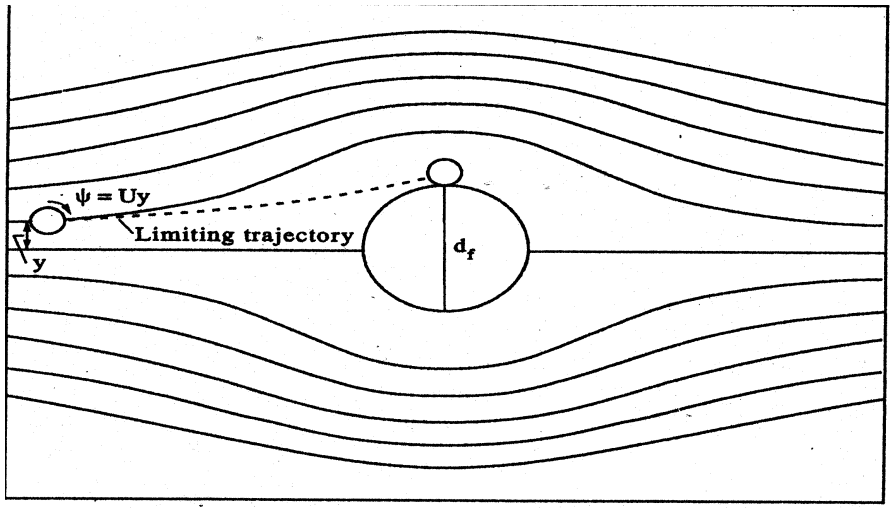

Figure 2-6. Single fiber efficiency [40]

Interception

Interception involves a particle following a stream and then being captured if this results in it coming into contact with the fiber. [40] Interception occurs when particles are subject neither to inertial effects nor to diffusive motion. As shown in Figure 2-7 [40], the particle touching the fiber at the point $\theta = \frac{\pi}{2}$ is on the limiting streamline. The single fiber efficiency for capture by interception, E_R, can be expressed as following expression: [40]

$$E_R = \frac{2\psi}{Ud_f} \qquad 2\text{-}9$$

where $\psi =$ stream function,

$U =$ the velocity of approach,

$d_f =$ diameter of fiber.

For the Kuwabara model [40], the most popular of the single fiber models,

$$E_R = \frac{1}{2Ku}\left\{2(1+N_R)\ln(1+N_R) - (1+N_R)(1-c) + (1+N_R)^{-1}(1-\frac{c}{2}) - \frac{c}{2}(1+N_R)^3\right\} \quad 2\text{-}10$$

where N_R = the dimensionless parameter describing capture by interception,

Ku = Kuwabara's hydrodynamic factor,

c = packing density.

Equation 2-10 is a complete expression and it can be reduced to a simple form [40]:

$$E_R = \frac{(1-c)N_R^{\,2}}{Ku(1+N_R)}. \quad 2\text{-}11$$

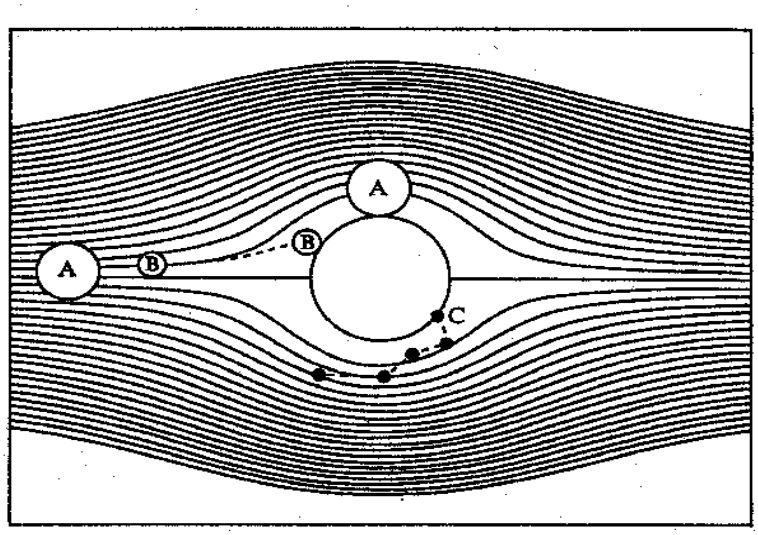

Figure 2-7. Particle-capture mechanisms: A, particle capture by interception, B, particle captured by inertial impaction, and C, particle captured by diffusional deposition [40]

Inertial Impaction

In inertial impaction the capture is affected by the deviation of a particle because of its own inertia. Particles may deposit on the fiber due to their inertia. A particle with zero inertia will be taken past the fiber and the single fiber efficiency for inertial capture, E_I, will be zero. A

particle of infinite inertia will ignore the flow and the E_I will be unity. The particles with high mass or velocity will be most susceptible to this mechanism. The efficiency of this mechanism depends on the Stoke drag force on the particles. The Stokes number is used to evaluate the Stoke drag force. [40]

The relationship between single fiber efficiency and Stokes number is shown in Figure 2-8 [36]. In general, the single fiber efficiency increases with the increasing of the Stokes number. When the Stokes number is large, the single fiber efficiency approaches unity asymptotically. Fitting analytical expressions to data obtained for filtration efficiency by inertial impaction is more difficult than it is for other filtration processes. In inertial impaction, theory gives an analytical description only in limiting situations, and description of the Stokes number requires curve-fitting. The following equation is fitted to the calculations based on an isolated fiber model [40]:

$$E_I = \frac{St^3}{St^3 + 0.77St^2 + 0.22} \qquad 2\text{-}12$$

where $St =$ Stokes number.

Diffusion

In diffusional deposition, the combined action of airflow and Brownian motion brings a particle into contact with a fiber. Capture due to this mechanism occurs because of the diffusion motion of the very small particles. These small particles follow the flow lines around the fiber and may contact with the fiber surface due to the diffusion motion, as shown in Figure 2-7 [40]. The capture of particles by this mechanism will depend on the relative magnitude of the diffusional motion and the convective motion of the air past the fiber. The Peclet number, Pe,

relates to these. The particle capture efficiency by diffusion will decrease when the Peclet number increases. [40]

The exact calculation expression of the single fiber efficiency requires the solution of a complicated transport equation, therefore a simple approximation has been made to understand this mechanism. The single fiber efficiency for diffusional capture, E_D, can be expressed by the following equation [40]:

$$E_D = 2.9\zeta^{-1/3} Pe^{-2/3} \qquad 2\text{-}13$$

where ζ = Hydrodynamic factor.

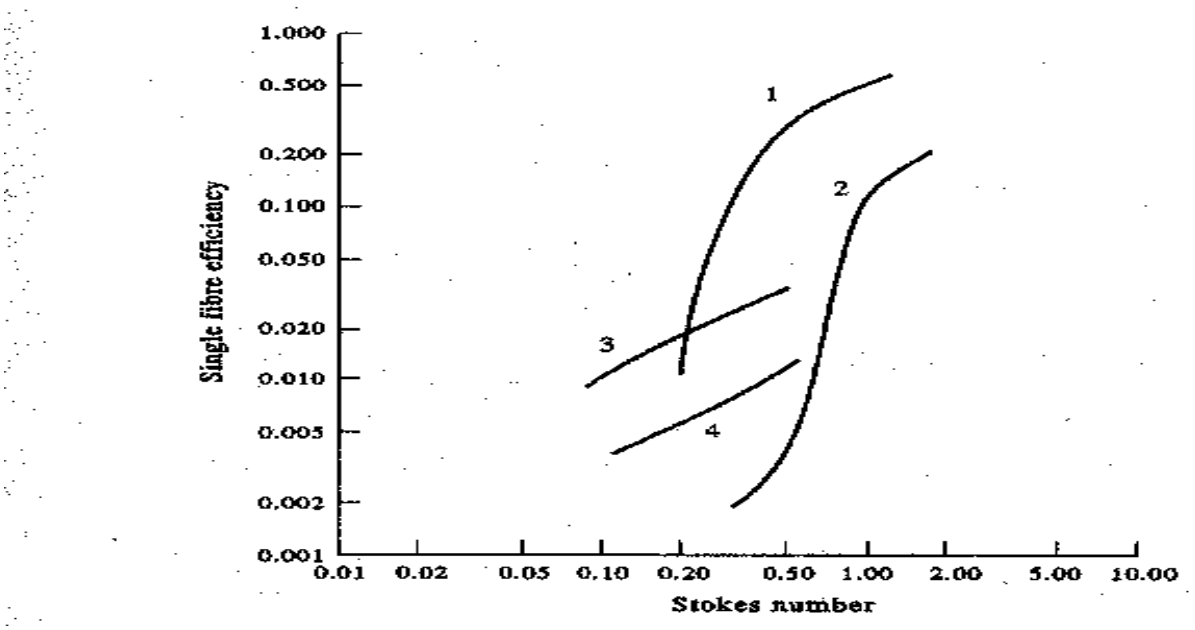

Figure 2-8. Calculated values of single fiber efficiency by inertial impaction: (1) c=0.11, (2) c=0.01, (3) c=0.1, N_R=0.05, and (4) c=0.01, N_R=0.05 [40]

Gravity

In gravity capture, the aerosol particles will tend to settle out under the influence of gravity. The effect of gravity during filtration will depend on the direction of airflow, with the

result of that gravitational settling may either augment or diminish the transport of the particles towards the fibers. [40]

Hinds defines a dimensionless number, G, which controls the deposition due to gravitational settlings: [28]

$$G = \frac{\rho_p d_p^2 C_c g}{18\eta V} \qquad 2\text{-}14$$

where C_c = Cunningham slip correction factor,

ρ_p = particle density,

d_p = particle diameter,

η = viscosity of air,

V = aerosol velocity,

g = acceleration due to gravity.

When the flow is vertically downward, the single fiber efficiency for gravitational capture, E_G, is:

$$E_G = G(1 + \frac{d_p}{d_f}) . \qquad 2\text{-}15$$

When the flow is vertically upward, the E_G is:

$$E_G = -G(1 + \frac{d_p}{d_f}) . \qquad 2\text{-}16$$

When the flow is horizon, the E_G is:

$$E_G = G^2 . \qquad 2\text{-}17$$

Electrostatic Capture

The particles and the fibers of a filter often carry electrostatic charges that may influence particle deposition considerably. The electrostatic charge on the fibers, in the majority of cases, is not stable and decreases with time mainly owing to the following factors: (1) conductivity of the fibers, (2) passage of ionized gases, (3) X or radioactive irradiation, (4) deposition of the charged particles, and (5) humidity. The charge on fibers and particles may influence the process of filtration in two ways: (1) the particles may be attracted to the fibers surface from a greater distance, and (2) the charge makes the particles "adhere" to the fiber surface. [41]

The electrostatic capture mechanism applies only to electrically charged particles. Davies uses the following equation to express the single fiber efficiency due to electrostatic capture: [42]

$$E_q = \left(\frac{\omega - 1}{\omega + 1}\right)^{1/2} \left[\frac{q^2}{3\pi\eta d_p d_f^2 V (2 - \ln \mathrm{Re}_t)}\right] \qquad 2\text{-}18$$

where $\omega =$ Dielectric constant of the particle,

$q =$ Charge on the particle,

$\mathrm{Re}_t =$ Flow Reynolds number.

Combined effects of two or more capture mechanisms

In investigative work to validate a theoretical prediction, it is best to arrange filtration parameters so that one mechanism acts alone; but in reality several mechanisms usually work together. It is difficult to express such a situation if those processes are exclusive. The simplest approach is to assume that the two processes are independent. If this assumption is correct, and the processes have calculated single fiber efficiencies E_1 and E_2, then a fraction (1- E_1) would escape capture by the first process if it acted alone. A fraction (1- E_1)(1- E_2) will escape capture

by both processes. The total single fiber efficiency E_{12} can be expressed by the following equation: [40]

$$E_{12} = E_1 + E_2 - E_1 E_2 \qquad 2\text{-}19$$

and for several independent processes, [40]

$$1 - E_{1\ldots j} = \prod_{i=1}^{j} (1 - E_i) \qquad 2\text{-}20$$

where E_i = the single fiber efficiency of ith process,

j = jth process.

Diffusion and interception

The particle capture by diffusion alone can be extended to the situation where interception is included, because with the assumption that it is possible to define a limiting trajectory, which ends not at the rear stagnation point but at a distance of one particle radius above the fiber surface. The single fiber efficiency for capture by diffusion and interception, E_{DR}, can be expressed as following expression: [40]

$$E_{DR} = \frac{1}{\zeta R^2}\left[\frac{3D\zeta R^2 \pi}{2U} + \left(\frac{d_p}{2}\right)^3\right]^{2/3}. \qquad 2\text{-}21$$

One particular value of this equation is that it indicates the existence of a most penetrating particle size, which is that value of d_p that gives the minimum of the expression.

Gravity and Interception

The relationship between gravity and interception depends on the fiber diameter because the single fiber efficiency of interception is inversely proportional to the square of the diameter

while the single fiber efficiency of gravity is independent of the square of the diameter. Therefore the fine fibers are more likely to exhibit these two mechanisms together. [40]

The single fiber efficiency for capture by gravity and interception, (E_{GR}), can be expressed as following equations [40]:

$$E_{GR} = E_R(1 + 2 \wedge COS\theta_G + \wedge^2)^{1/2} \qquad 2\text{-}22$$

where $\wedge = \frac{N_G(1+N_R)}{E_R}$,

θ_G = the velocity vector of gravity,

N_G = the dimensionless parameter describing capture by gravity.

When $\theta_G = 0$, the flow is downward, and the E_{GR} is:

$$E_{GR} = E_R + N_G(1+N_R). \qquad 2\text{-}23$$

When $\theta_G > N_G$, the flow is upward, and the E_{GR} is:

$$E_{GR} = E_R - N_G(1+N_R). \qquad 2\text{-}24$$

When $\theta_G = \pi/2$, the flow is cross, and the E_{GR} is:

$$E_{GR} = [E_R{}^2 + N_G^2(1+N_R)^2]^{1/2}. \qquad 2\text{-}25$$

Laser Scanning Confocal Microscopy

Mellors and Silver developed the concept of automated scanning using a fluorescence microscope in 1951. [43] In their study, cancer cells were scanned with a narrow excitation beam and the emitted light was detected and quantified. The use of a narrow beam enabled one to irradiate only one small area at a time. The confocal microscope was first introduced in 1957, when Marvin Minsky submitted a patent application for a microscope that used a stage-scanning

confocal optical system. [44] However, the lack of an adequate light source prevented full development of the confocal microscope at that time. Advancements in laser technology in the 1960's stimulated the development of confocal microscope. Lasers are well suited for microscopy work because they produce light beams with a high degree of monochromacity and polarization. [45] With continued advancements in video technology, it became possible to store the images produced by scanning. Advances in computer technology have allowed for large enough memory to store the images produced and to complete image manipulation and enhancement. [46] During the 1970's, a laser-illuminated confocal microscope was developed. This had a significant influence on the field of cellular biology and soon thereafter the first Laser Scanning Confocal Microscopes were made commercially available by Sarastro, Olympus, Zesis and Leitz. [44] LSCM has been extensively used in numerous applications of cellular biology. Considerable interest now exists in the use of LSCM as a diagnostic and therapeutic tool. For example, LSCM can help to elucidate drug interactions at the cellular and molecular levels by dividing the signals from probes spatially into three dimensions (3D). [43]

LSCM has had limited uses in the material sciences, including the textile area. In 1998, Leonas [44] discussed the history, principles and advantages of LSCM, and also studied the feasibility of using LSCM to investigate the three dimensional structure of the fabric. In a later study, Leonas and Huang used LSCM to evaluate the movement of small particles through fabrics traditionally used in surgical gowns and drapes. Four fabrics, two Spunbond/Meltblown/Spunbond (SMS) type polypropylene composites, a spunbond high-density polyethylene and a spunbond nonwoven fabric laminated with a microporous polymeric membrane, were selected. The fabrics were exposed to a solution containing fluorescently tagged microspheres similar in size to common bacteria found in hospitals. Cross-sectional specimens of

the exposed fabric were prepared and evaluated using LSCM. The results showed that it was possible to evaluate the movement of microsphere particles through fabrics commonly used in surgical gowns and drapes using LSCM. The particles were forced from the face and upper surfaces of the fabric to the back of the fabric as the pressures applied to the fabric were increased. Fabric construction influenced the movement of the particle through the fabric. The two fabrics with the SMS construction had particle strikethrough adjacent to the bond point. The microporous film prevented penetration of the particles. [47]

LSCM is a valuable tool for obtaining high resolution images and 3-D reconstructions of a variety of specimens. Figure 2-9 [46] shows the optics of a typical LSCM. In a LSCM the laser beam passes through a beam splitter and is moved in a raster pattern by a set of pivoting mirrors. These mirrors cause the beam to move in an X and Y pattern. The beam then passes through a tube lens and then an objective lens that focuses it on the specimen. This produces a diffraction limited light spot only in one plane of the specimen. The mixture of reflected light and emitted fluorescent light is captured by the same objective and is focused onto a photomultiplier via a diachronic mirror. The reflected light is deviated by the diachronic mirror while the emitted fluorescent light passes through to the direction of photomultiplier. A pinhole is placed in front of the photodetector so that only illumination from the one point in the focal plane is brought to focus.

LSCM has several advantages over the conventional optical microscopy, they are: [46]

1. Contrast and resolution are improved since out of focus information is greatly reduced,

2. Images can be acquired as single planes to produce three-dimensional representations of serial optical sections,

3. LSCM can use a variety of excitation illuminations and change the scan pattern,

4. Non-destructive examination of surface topography can be done using LSCM.

However, LSCM has two disadvantages: [46]

1. The real time imaging is impossible because the raster pattern is established by physically moving mirrors,

2. The operator can only see the resultant image as it is presented on the CRT.

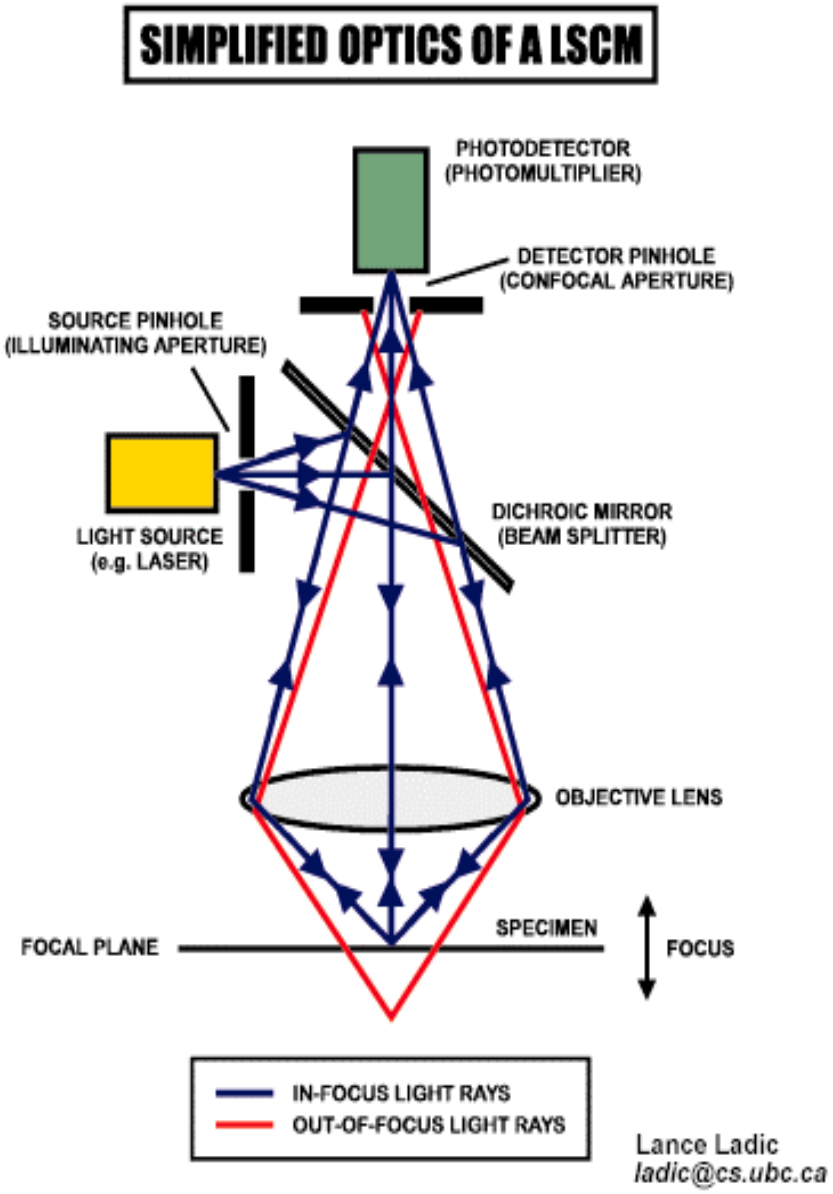

Figure 2-9. Simplified optics of a LSCM [46]

CHAPTER 3

MATERIALS AND METHODS

Nonwoven Fabrics and Repellent Finish

An investigation conducted by Leonas [13] identified those surgical face masks currently available on the market. Fourteen surgical face masks, representative of varying fabric structures, were reported and descriptions of each are shown in Table 3.1. Face mask characterization tests (Table 3.2) including weight, thickness, water repellency spray, hydrocarbon resistance, dynamic contact angle and fluid resistance were preformed. The results of that investigation were reviewed and the types and the weight range of nonwoven fabrics were found. Based on this information, categories and target weights of nonwoven fabrics used for this study were selected. Since the primary objective of this research is to study the impacts of repellent finish and layering order on the properties of face masks, other variables such as the type and the weight of nonwoven fabrics were fixed in this study. Four nonwoven fabrics were obtained from the industry, including one polypropylene meltblown nonwoven fabric the weight of which is about 20 g/m^2 for the filtration layer, one polypropylene spunbonded nonwoven fabric the weight of which is around 26 g/m^2 for the support layer, one polypropylene spunbonded nonwoven fabric the weight of which is around 20 g/m^2 for the cover layer and one polypropylene spunbonded nonwoven fabric the weight of which is about 18 g/m^2 for the shell layer. Types of these nonwoven fabrics were selected as same as those found and reported by Leonas.

To enhance the resistance of the surgical face mask to penetration by fluid, a fluorochemical finish was applied to the fabric to be used as the outside layer (cover layer) of the simulated surgical face masks to be prepared in this study. Fluorochemical repellents are unique in that they confer both water and oil repellency to fabrics. This property is important because low surface tension liquids such as alcohols often exist in the operating room. Zonyl® PPR Protector is a low curing temperature oil and water repellent fluoropolymer available from Ciba Specialty Chemicals. [48] It can provide excellent oil and water repellent properties to a range of products such as protective wear, sportswear/active wear, upholstery, home furnishings and even technical textiles. [49] It is a typical fluorochemical finish and mainly applied to polypropylene. Therefore Zonyl® PPR Protector was used in this study.

Nonwoven Fabric Property Tests

A previous study [47] showed that nonwoven fabric properties including thickness, weight, repellency and contact angle were related to barrier effectiveness. In this study, these nonwoven fabric properties were measured. Fabric thickness was measured in accordance with ASTM D 1777-96, Standard Method for Thickness of Textile Materials [50]. Fabric weight was measured according to ASTM D 3776-96, Standard Method for Mass per Unit Area (Weight) of Fabric [51].

The repellency of the fabric was determined according to standard tests AATCC 22-1996 Water Repellency: Spray Test and AATCC 118-1997 Oil Repellency: Hydrocarbon Resistance Test [52]. Water repellency was measured to give an indication of the ability of a fabric to resist wetting by water. A zero rating reflects complete wetting of whole upper and lower surfaces of the fabric. A rating of 100 reflects no sticking or wetting of the upper surface of the fabric. Oil

repellency was measured to give an indication of the ability of a fabric to resist wetting by oily liquids. A zero rating reflects no resistance to wetting for an oily liquid of the highest surface tension, Kaydol. A rating of 8 reflects no resistance to wetting by an oily liquid of low surface tension, n-heptane. A fabric with a high rating has a lower surface energy than one with a low rating and will resist wetting better.

The contact angle of the nonwoven fabric was measured using the Dynamic Contact Angle (DCA) analyzer manufactured by Cahn Instruments and following the manual. The fabrics were cut to 5 mm width and 10 mm length. In this study, synthetic blood was used as the challenge liquid because it often exists in the operating room and it is also the challenge liquid used in the fluid resistance test for face masks. The advancing angle indicates the wetting ability of the fabric. One hundred and eighty degrees is the highest value and any value above 90 degrees indicates non-wetting of the fabric. The receding angle reflects how the liquid reacts after the fabric has been wet out. The lower receding angle value indicates adhesion.

Two-way Factorial Design

There are two independent factors in this study, the repellent finish and the layering order of the face mask. Therefore a two-way factorial design was used. The add-on level of the repellent finish is critical to impart the desirable properties to products. In the study of Huang and Leonas [8], a fluorochemical finish add-on range, 0% to 1.75%, was applied to hydrophobic nonwoven surgical gown fabrics. Therefore, three fluorochemical finish add-on levels, 0%, 0.6% and 1.2%, were initially selected in this study.

Table 3.1. Face mask descriptions [13]

Code	Name	Manufacturer	Description
1	Aseptex Fluid Resistant Molded Surgical Face Mask	3M Healthcare	Molded
2	Tie-on Surgical Face Mask	3M Healthcare	3-ply, pleated
3	Surgine Face Mask	Johnson & Johnson Medical Inc	3-ply, pleated
4	Softloop Extra Protection Mask	Johnson & Johnson Medical Inc	3-ply, pleated
5	Barrier Extra Protection Mask	Johnson & Johnson Medical Inc	4-ply, pleated
6	Surgine II Soft Arch Mask	Johnson & Johnson Medical Inc	3-ply, pleated
7	Surgine II Cone Mask	Johnson & Johnson Medical Inc	Molded
8	Surgical Grade Cone Style Mask	Cellucap/Melco Manuf.	Molded
9	Classic Surgical Mask	Kimberly-Clark	3-ply, pleated
10	TECNOL* FLUIDSHIELD* Fog-Free Surgical Mask / Orange	Kimberly-Clark	4-ply, pleated
11	TECNOL* FLUIDSHIELD* Fog-Free Surgical Mask with WrapAround Splashguard* Visor/ Orange	Kimberly-Clark	4-ply, pleated
12	TECNOL* FLUIDSHIELD* Fog-Free Procedure Mask / Orange	Kimberly-Clark	4-ply, pleated
13	Fluid Resistant Earloop Mask	3M	4-ply, pleated
14	Respirator N95 Particulate	3M	4-ply, pleated

Table 3.2. Face mask characterization tests [13]

Test Description	Method Number	Title
Thickness	ASTM D1777-96	Standard Test Method for Thickness of Textile Materials
Weight	ASTM D 3776-96	Standard Test Method for Mass per Unit Area (Weight) of Fabric
Water Repellency	AATCC 22-1996	Water Repellency Spray Test
Oil Repellency	AATCC 118-1997	Hydrocarbon Resistance Test
Dynamic Contact Angle	Following the manual of the CAHN Dynamic Contact Angle Analyzer	

The fluorochemical finish, Zonyl® PPR protector with 1.2% of add-on, was first applied to the cover layer polypropylene fabric to determine the effect of this repellent finish. The dynamic contact angle of the treated fabric was measured to assess whether the 1.2% add-on repellent finish offered the desired repellent properties. The dynamic contact angles of the treated cover fabric are reported in Table 3.3.

The results in Table 3.3 show that the advancing contact angle of the treated cover fabric for synthetic blood is 85.03 degrees which is smaller than 90 degrees, indicating that the expected repellency has not been achieved by the 1.2 % add-on level. Therefore, higher add-on levels than initially thought were required. Other add-on levels greater than 1.2% were selected for application and evaluated to find the desired repellent finish. 3%, 6%, 9% and 12% add-on levels were selected, then the fluorochemical finish was applied to the cover layer polypropylene fabric at those add-on levels. Finally, dynamic contact angles at 3%, 6%, 9% and 12% add-on levels were measured to assess whether the finish offered the desired repellent properties. The dynamic contact angles of these treated cover fabrics are reported in Table 3.4.

Table 3.3 Contact angle of cover fabric treated with 1.2% add-on level of Zonyl® PPR protector for synthetic blood

Replication	Advancing (Degree)	Receding (Degree)	Replication	Advancing (Degree)	Receding (Degree)
1	85.23	76.24	**7**	84.54	78.60
2	84.92	74.57	**8**	85.32	75.88
3	82.88	75.67	**9**	88.21	74.78
4	84.32	72.65	**10**	84.97	75.28
5	86.11	75.89	**Mean**	85.03	75.38
6	83.79	74.21	**CV (%)**	1.68	2.06

The results in Table 3.4 show that the higher the add-on level, the greater the advancing contact angle of the treated cover fabric. When a 3% add-on level of the repellent finish was applied to the cover fabric, the advancing contact angle, 87.68 degrees, was still smaller than 90 degrees. When a 6% add-on level of the repellent finish was applied to the cover fabric, the advancing contact angle, 91.22 degrees, was greater than 90 degrees. From this preliminary work where limited add-on levels of the repellent finish were evaluated, the 6% was the lowest add-on level where repellency was achieved. Therefore, 6% was selected as the low level of repellent finish that would be applied to the cover fabric to obtain the repellent property. However, 6% is not necessary the lowest level of add-on where repellency is achieved. In this study, three add-on levels of repellent finish were used to study the effect of repellent finish on the properties of face masks. An add-on level of 0% was used as the control. Although 9% add-on level could offer greater advancing contact angle (92.76 degrees) than 6% add-on level, 12% was selected as the high level repellent finish that would offer much better repellent property because it offered much greater advancing contact angle (96.62 degrees) to the cover fabric than the 9% add-on level.

To determine the effect of layering order on the properties of face masks, the following three layering orders* [9] were used:

1) Three-layer face mask and a layer arrangement of cover fabric, filtration fabric and shell fabric from outside to inside,

2) Four-layer face mask and a layer arrangement of cover fabric, filtration fabric, support fabric and shell fabric from outside to inside,

3) Four-layer face mask and a layer arrangement of cover fabric, support fabric, filtration fabric and shell fabric from outside to inside.

Table 3.4 Contact angle of cover fabric treated with additional add-on levels of Zonyl® PPR protector for synthetic blood

Add-on Level of Repellent Finish		**3%**	**6%**	**9%**	**12%**
Advancing Contact Angles of Ten Replications	**1**	88.35	91.52	91.16	93.15
	2	82.95	90.55	83.82	94.6
	3	84.46	91.51	92.18	101.42
	4	86.79	89.94	90.75	98.67
	5	87.53	91.51	91.57	95.94
	6	89.54	90.55	92.66	95.53
	7	88.53	90.29	93.15	95.94
	8	92.39	91.41	92.74	98.67
	9	88.42	90.86	107.25	95.43
	10	87.86	94.08	92.36	96.48
Mean		87.68	91.22	92.76	96.62
S.D.		2.6	1.15	5.76	2.37
CV (%)		2.97	1.26	6.21	2.45
Receding Contact Angles of Ten Replications	**1**	78.45	70.35	83.67	62.25
	2	75.62	85.04	69.23	83.25
	3	64.58	57.23	80.78	60.45
	4	75.06	82.83	55.02	72
	5	75.94	57.23	83.43	73.93
	6	74.31	85.14	56.09	71.81
	7	85.39	81.61	76.45	73.93
	8	72.32	78.59	79.87	72.06
	9	75.54	74.35	73.89	70.05
	10	73.96	75.07	72.66	68.77
Mean		75.12	74.74	73.11	70.85
S.D.		5.15	10.41	10.36	6.36
CV (%)		6.86	13.93	14.17	8.98

Based on the repellent finish add-on level and the layering order, the following two-way factorial design (Table 3.5) was used. This two-way factorial design has three repellent add-on levels and three different layering orders. Nine simulated face masks can be formed in

accordance to the two-way factorial design and the codes of these face masks are also listed in Table 3.5.

Table 3.5. Two-way factorial design and the codes of nine simulated face masks

Layering Order of the Face Mask	**Repellent Finish Add-on (%)**		
	0	**6**	**12**
Order One (Three layers): Cover layer, Filtration layer and Shell layer (From outside to inside)	0-1	6-1	12-1
Order Two (Four layers): Cover layer, Filtration layer, Support layer and Shell layer (From outside to inside)	0-2	6-2	12-2
Order Three (Four layers): Cover layer, Support layer, Filtration layer and Shell layer (From outside to inside)	0-3	6-3	12-3

Application of Repellent Finish and Evaluation of Repellent Property

The pad-dry-cure method was used to apply the repellent finish to the cover fabric. There are three steps in this method: (1) applying the fluorochemical finish by passing the fabric through the chemical bath and then the padder (padding), (2) removing of excess water (drying) and (3) heating the treated fabric to a temperature that causes crosslinking between the fabric and the chemical (curing). [26].

A Cromax$^{@}$ laboratory padder was used and the cover fabric was passed through a bath, and then one pair of rubber rollers twice (two dips and two nips) at 60 psi and a rate of 2.5 m/min.

The concentration of repellent finish necessary in the solution to achieve the desired add-on level was determined using the following formula:

$$\text{g/l} = \frac{add-on(\%)}{wetpick-up(\%)} \times 1000 . \qquad 3\text{-}1$$

To calculate the concentration of the fluorochemical dye bath, the wet pick-up of the cover fabric was determined first using the following formula:

$$WetPick-up(\%) = \frac{WetWeight - DryWeight}{DryWeight} . \qquad 3\text{-}2$$

The results are reported in Table 3.6. The mean wet pick-up was 200% with a standard deviation of 2.92%. Therefore wet pick-up 200% was used in equation 3-1. Then the necessary chemical concentration was calculated according to the wet pick-up and the desired add-on level. In this study, 30 g/l and 60 g/l concentrations of repellent finish were prepared to obtain the 6% and 12% add-on levels respectively. Fabrics were passed through the fluorochemical finish bath using the parameters described above. Finally, the fabrics were dried at 176^{o} F for two minutes and then cured at 250^{o} F for two minutes in a Mathis laboratory curing oven according to the Zonyl® PPR Protector Technical Bulletin [48].

Table 3.6 Wet pick-up determinations

Replication	Dry Weight (gram)	Wet Weight (gram)	Wet Pick-Up (%)
1	2.74	8.15	197
2	2.75	8.3	202
3	2.93	8.73	198
4	3.04	9.25	204
5	3.07	9.19	199
Mean	2.91	8.72	200
S.D.	0.16	0.5	2.92
CV (%)	5.5	5.73	1.46

Order Fabric Layers to Simulate Face Masks

After the application of the repellent finish, the treated cover fabric layer and filtration layer, support layer and shell layer were arranged to simulate different face masks according to the predetermined layering orders. There are three layering orders and three add-on levels of repellent finish, therefore nine (three × three) different simulated face masks were formed. For each of the nine face masks, a minimum of 39 specimens were formed for the evaluation of different properties.

Evaluation of Fluid Resistance

The fluid resistance of the face masks was evaluated according to the Standard Test Method ASTM F 1862-00, Standard Test Method for Resistance of Surgical Mask to Penetration by Synthetic Blood [5]. Prior to the evaluation of fluid resistance, the simulated face masks were conditioned for a minimum of four hours in conditions of 21 $\pm$ 5^{o}C and a relative humidity of 85 $\pm$ 5%. The resistance to synthetic blood was evaluated by the apparatus shown in Figure 3-1, of which the primary components are a plastic box, a pneumatic control valve, a valve controller, a valve control switch and a fluid reservoir. The three pressures identified in the test method, 80 mmHg, 120 mmHg, 160 mmHg, were used in the testing and two mls of solution was delivered. Since the fluid resistance was tested at specific pressures, the effect of fluid pressure as well as repellent finish and layering order was studied. The following two equations [5] were used to determine the necessary velocity and the valve time to deliver two mls of fluid.

$$v = [(2.0081 \times 10^{6})P]^{0.5}, \qquad 3\text{-}3$$

where P = blood pressure, mmHg,

v = stream velocity, in/s.

$$t = 3620 / v, \qquad \text{3-4}$$

where t = time for delivery of 2 mL synthetic blood.

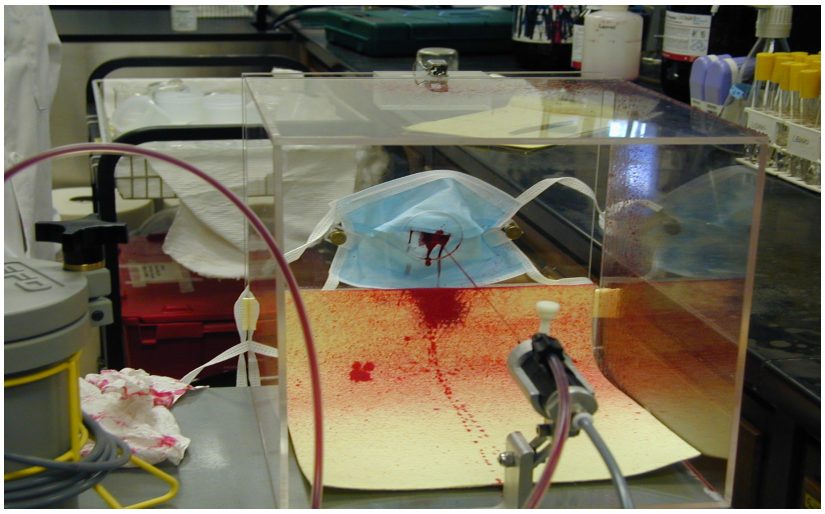

Figure 3-1. Fluid resistance test apparatus

Evaluation of Filtration

In chapter two, filtration and particle capture mechanisms were introduced. One of the objectives of this research is to study the impact of repellent finish and layering order on filtration ability of face masks, so the method used in this study to evaluate filtration of face masks is described in this section.

Evaluation of filtration was composed of three steps: (1) exposure of the face mask to challenge aerosol containing small particles, (2) LSCM examination, and (3) image analysis. First, the face masks were exposed to a challenge aerosol composed of synthetic blood and small particles. Then techniques using LSCM were used to determine particle capture. Small particles present on/in nonwoven fabrics were located using LSCM to determine that the particles were

captured. Finally, the image analysis was used to quantify the number of small particles by area to evaluate the filtration ability of the face mask.

Exposure of the Face Mask

The face masks were exposed to a challenge aerosol by modifying Standard Test Method ASTM F2101-01, Standard Test Method for Evaluating the Bacterial Filtration Efficiency (BFE) of Medical Face Mask Materials, Using a Biological Aerosol of Staphylococcus aureus [6]. Prior to the exposure, the simulated face masks were conditioned for a minimum of 4 hours in conditions of 21 $\pm$ 5^{o}C and a relative humidity of 85 $\pm$ 5%. The test apparatus is shown in Figure 3-2. To study the filtration ability of face masks against small particles, a challenge liquid containing small particles rather than a S. aureus suspension was used to generate the aerosol. This challenge liquid was composed of latex microspheres and synthetic blood. The spheres are fluoresbirte^{TM} carboxylate microspheres (Polysciences, Inc.) the average size of which is 1.0 micron, and they are round in shape. These physical properties are similar to that of bacteria S. aureus, and spheres were used in previous studies [13,47] to simulate S. aureus. The concentration of this solution is 2.5×10^{-4} .

LSCM Examinations

After the exposure of the face mask to the challenge aerosol, the face mask specimen was examined with a Leica TCS SP2 Spectral Confocal Microscope to locate the small particles present on/in the structure of the face mask. To study the effect of the repellent finish on the filtration ability of face masks, the LSCM was used to examine the surfaces of individual layers

of the face masks. The LSCM surface examination of small particles on various layers of the face masks was composed of the following steps:

1. A one square inch specimen that contained an exposed area was removed by cutting from the face mask,

2. Then specimen was immediately frozen using liquid nitrogen,

3. The layers of each specimen were separated and individually placed on glass slides, then covered with cover slips,

4. The surfaces of specimens were examined using LSCM.

For each face mask, three specimens were examined and for each specimen, five different locations of the surfaces of the face masks were randomly selected and examined using LSCM.

To study the effect of layering order on the filtration ability of face masks, the transmission of small particles through the entire face mask is necessary and the LSCM surface examination did not provide appropriate information for this component of the study. Therefore, a technique involving LSCM cross sectional examination was used to study the impact of layering order on filtration ability.

The LSCM cross sectional examination on the face mask was composed of the following steps (Figure 3.3):

1. The face mask was cut into one square inch specimen that contains the exposed area,

2. The specimen was immediately frozen by liquid nitrogen,

3. The specimen was mounted and kept in the liquid nitrogen,

4. A cross section of the specimen was cut when it was still in the frozen status,

5. The cross section was observed using LSCM.

For each face mask, three specimens were examined and for each specimen, five different locations of the cross sections of the face masks were examined using LSCM.

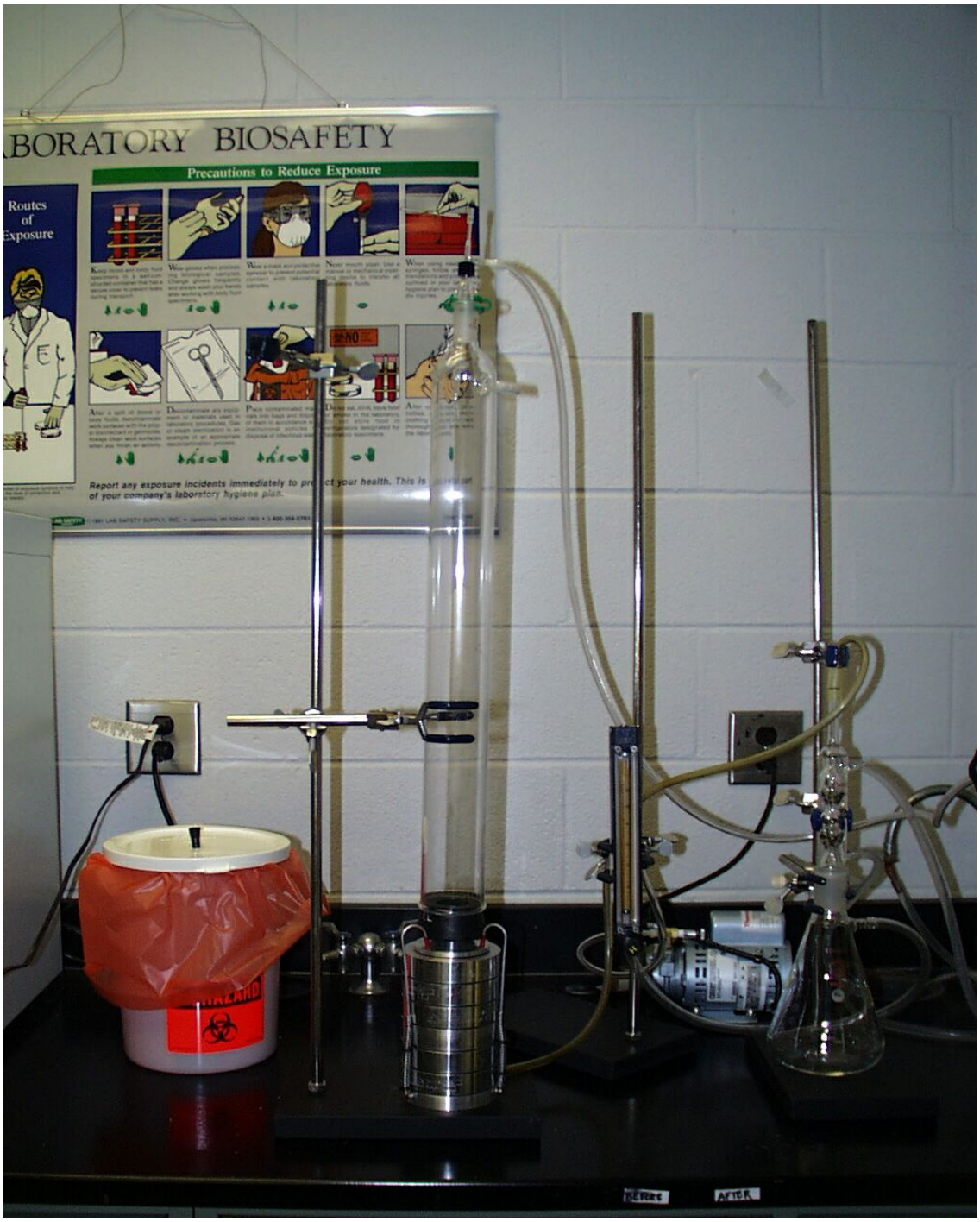

Figure 3-2. Bacterial filtration efficiency test apparatus

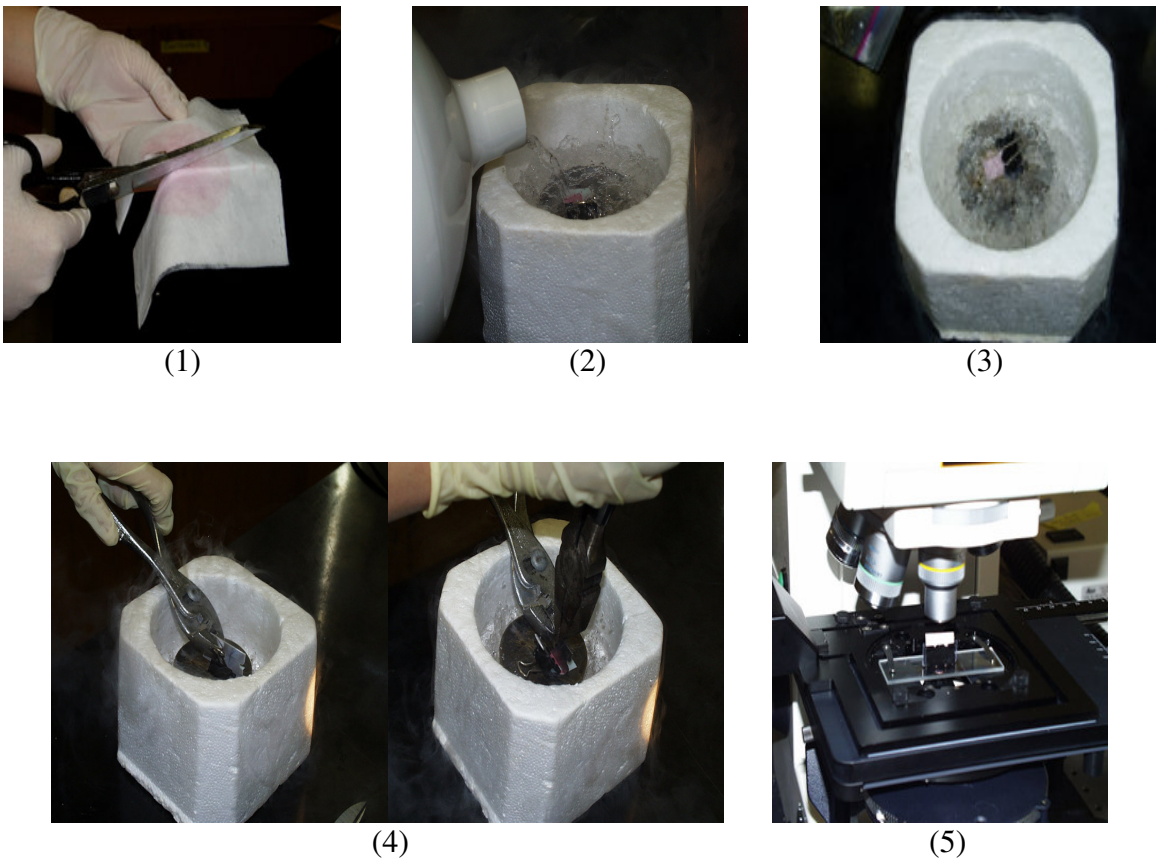

Figure 3.3 Procedure for the cross sectional observation technique; (1) cut specimen, (2) freeze specimen, (3) mount and preserve specimen, (4) prepare a cross section, and (5) observation

Image Analysis

Image Processing and Analysis in Java (ImageJ) was used to complete the image analysis. ImageJ was selected because it is a pubic domain Java image processing program that can analyze 8-bit, 16-bit and 32-bit images and read a variety of image formats. The area represented by pixel value statistics of a selected area can be calculated using ImageJ. ImageJ also supports standard image processing functions such as contrast manipulation, sharpening, smoothing, edge detection and median filtering. [53] Total area (as determined by square pixels)

was used to represent the small particles captured on the surface of individual fabric layers of face masks. The total area was calculated by the product of the number of particle spots with the mean area of all particle spots. The procedure of image analysis was composed of the following steps and depicted by the micrograph in Figure 3.4:

1. The original LSCM image was obtained,

2. The original image was adjusted using a threshold with parameters of 100 pixels to 255 pixels,

3. The adjusted image was analyzed to obtain the simulated image. The minimum analysis size was 1 pixel and the maximum was 9999 pixels,

4. The number of particle spots and the mean area of all particle spots in the simulated image were determined.

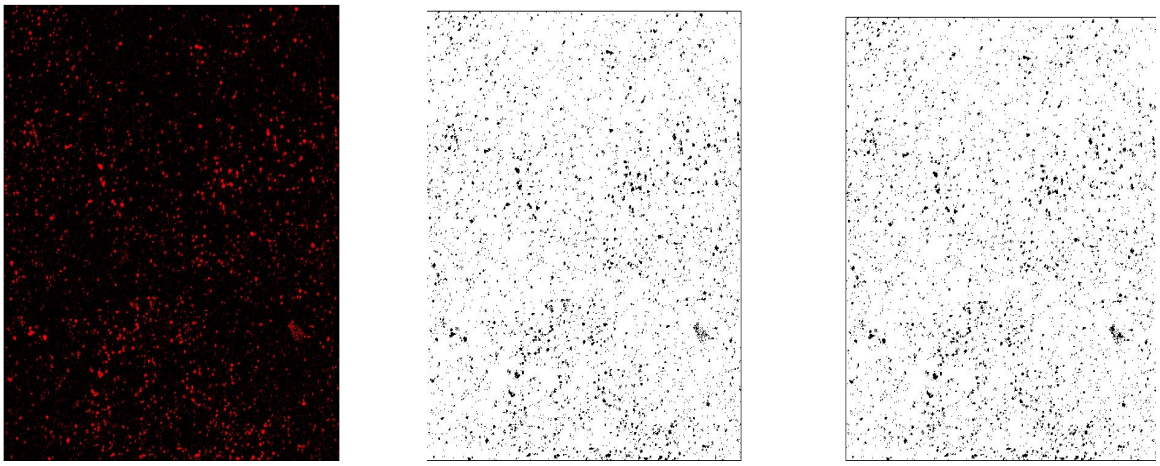

(a) Original image (b) Adjusted image (c) Simulated image

Figure 3.4. Three images in the image analysis process

Evaluation of Differential Pressure

Differential pressure (Delta-P) is the measured pressure drop across a medical face mask material. Delta-P is used to determine the breathing resistance of a surgical face mask.

Differential pressures of the nine simulated face masks were determined at Nelson Laboratory, Salt Lake City, Utah. Two replications of each of the nine face masks were sent to Nelson Laboratory for determination of the differential pressure.

Statistical Analysis

Statistical analysis was performed on the properties of fluid resistance, filtration ability and differential pressure of face masks using the SAS system. Add-on levels of repellent finish and the different layering orders of face masks were the independent variables. The fluid resistance, filtration ability and differential pressure were the dependent variables respectively. All statistical analyses were conducted using 1% significance level.

Statistical Analysis of Fluid Resistance

A particular type of regression, logistic regression, was used. In logistic regression, the response variable is an indicator variable and the predictor variables can be either continuous or class variables. In this study, the response variable, fluid resistance, is an indicator variable. If the face mask passes the fluid resistance test (ASTM 1862-00), the response variable is 1. If the face mask fails the test, the response variable is 0. Since the fluid resistance was tested at specific pressures, the effect of fluid pressure as well as repellent finish and layering order was studied. Therefore, the predictor variables are the add-on level of repellent finish, the layering order of face masks and the fluid pressure. They are different types of variables. The layering order of face masks is a class variable because it only has three levels. Level one is cover layer, filtration layer and shell layer. Level two is cover layer, filtration layer, support layer and shell layer. Level three is cover layer, support layer, filtration layer and shell layer. However, both the fluid

pressure and the add-on level of repellent finish are continuous variables that in theory can be any number between zero and infinite. Therefore, logistic regression fits very well with this study.

In addition, the logistic regression was used because it overcomes many of the restrictive assumptions of the linear regression: [54]

1. Logistic regression does not assume a linear relationship between the dependents and the independents. However, it is also possible and permitted to add explicit interaction and power terms as variables on the right-hand side of the logistic equation, as in linear regression,

2. The dependent variable need not be normally distributed,

3. There is no homogeneity of variance assumption,

4. Normally distributed error terms are not assumed,

5. Logistic regression does not require that the independents be interval,

6. Logistic regression does not require that the independents be unbounded.

Statistical Analysis of Filtration Ability

To study the impact of repellent finish on filtration ability of face masks, assumptions of Analysis of Variance (ANOVA) were tested first to determine whether it is an appropriate method for this study. ANOVA is based on the following assumptions:

1. The samples should be independent,

2. The populations from which the samples were obtained should be normally or approximately normally distributed,

3. The variances of the populations should be equal.

Therefore, these assumptions were tested first before ANOVA were applied. The nonparametric techniques will be used instead if any of the three assumptions of ANOVA does not fit with this study.

Statistical Analysis of Differential Pressure

To study the impacts of repellent finish and layering order on the differential pressure of face masks, assumptions of two-way ANOVA were tested first to determine whether it is an appropriate method for this study. The nonparametric techniques will be used if any of the three assumptions of ANOVA does not fit with this study.

CHAPTER 4

RESULTS AND DISCUSSION

The results and discussion are presented in five sections. The first section is the results of the nonwoven fabric property tests; the second section is the application of the repellent finish and the order of various nonwoven fabric layers to simulate face masks; the third section includes the results of the fluid resistance of face masks and the statistical analysis of the impacts of repellent finish, layering order and fluid pressure on the fluid resistance; the fourth section includes LSCM surface examination, image analysis, LSCM cross sectional examination and the statistical analysis of impact of repellent finish on the filtration ability; and the fifth section is the results of differential pressure of face masks and the statistical analysis of impacts of repellent finish and layering order on the differential pressure.

Nonwoven Fabric Property Tests

Nonwoven fabric properties related to the barrier effectiveness were measured in this study and the results are presented in Tables 4.1 - 4.5. The results of fabric thickness are shown in Table 4.1. The mean thickness of the polypropylene spunbonded cover fabric is 0.236 mm with a standard deviation of 0.027 mm. The mean thickness of the polypropylene spunbonded support fabric is 0.247 mm with a standard deviation of 0.008 mm. The mean thickness of the polypropylene meltblown filtration fabric is 0.190 mm with a standard deviation of 0.007 mm. The mean thickness of the polypropylene spunbonded shell fabric is 0.201 mm with a standard deviation of 0.012 mm. For the same type of nonwoven fabric, barrier effectiveness improves

with increased thickness because small particles need to transmit deeper to penetrate through a thicker fabric.

Fabric weights are reported in Table 4.2. The mean weight for the polypropylene spunbonded cover fabric is 21.98 g/m^2 with a standard deviation of 2.24 g/m^2. The mean weight for the polypropylene spunbonded support fabric is 25.95 g/m^2 with a standard deviation of 1.08 g/m^2. The mean weight for the polypropylene meltblown filtration fabric is 19.33 g/m^2 with a standard deviation of 0.92 g/m^2. The mean weight for the polypropylene spunbonded shell fabric is 18.84 g/m^2 with a standard deviation of 1.14 g/m^2. For the same type of nonwoven fabric, greater weight indicates more fibers. According to the "single-fiber" model, more fibers can provide better filtration ability because each fiber has the same single fiber efficiency.

Oil repellency of the fabric is reported in Table 4.3. The oil repellency rating for all fabrics is 0, indicating that all those nonwoven fabrics offer the minimum oil repellency.

Water repellency of the fabric is reported in Table 4.4. The water repellency rating for all fabrics is 80 which reflects wetting of upper surface at spray points and indicates that all those nonwoven fabrics offer median water repellency.

Contact angle is reported in Table 4.5 which contains the advancing and receding contact angles for all nonwoven fabrics used in this study. The receding angles for these nonwoven fabrics ranged from 71.62 degrees to 76.10 degrees, indicating that the adhesion is high. The advancing angles of these nonwoven fabrics for the synthetic blood ranged from 81.56 degrees to 84.18 degrees. All advancing angles are lower than 90 degrees, indicating that synthetic blood can wet out those nonwoven fabrics. Therefore, repellent finish should be applied to offer them the ability to resist synthetic blood.

Table 4.1 Thickness of nonwoven fabrics

Replication	Thickness (mm)			
	Cover Fabric	Support Fabric	Shell Fabric	Filtration Fabric
1	0.236	0.252	0.207	0.188
2	0.259	0.245	0.190	0.197
3	0.247	0.239	0.203	0.197
4	0.287	0.245	0.183	0.199
5	0.236	0.237	0.191	0.180
6	0.241	0.262	0.205	0.187
7	0.211	0.253	0.214	0.180
8	0.190	0.253	0.186	0.190
9	0.218	0.239	0.211	0.195
10	0.237	0.241	0.215	0.193
Mean	0.236	0.247	0.201	0.190
S.D.	0.027	0.008	0.012	0.007
CV (%)	11.220	3.280	5.990	3.420

Table 4.2 Weight of nonwoven fabrics

Replication	Weight Mass Per Unit Area (Gram Per Square Meters)			
	Cover Fabric	Support Fabric	Shell Fabric	Filtration Fabric
1	21.04	26.32	19.52	18.96
2	19.04	25.84	17.68	18.80
3	22.24	26.08	18.72	20.32
4	22.40	24.88	18.32	20.64
5	22.08	27.68	18.72	18.88
6	19.20	25.44	18.08	19.12
7	24.16	26.88	17.84	18.48
8	26.16	26.72	18.80	18.56
9	23.36	25.84	21.68	18.64
10	20.08	23.84	19.04	20.88
Mean	21.98	25.95	18.84	19.33
S.D.	2.24	1.08	1.14	0.92
CV (%)	10.19	4.16	6.05	4.76

Table 4.3 Oil repellency of nonwoven fabrics

Replication	Oil Repellency Rating			
	Cover Fabric	Support Fabric	Shell Fabric	Filtration Fabric
1	0	0	0	0
2	0	0	0	0
Result	0	0	0	0

Table 4.4 Water repellency of nonwoven fabrics

Replication	Water Repellency Rating*			
	Cover Fabric	Support Fabric	Shell Fabric	Filtration Fabric
1	80	80	80	80
2	80	80	80	80
3	80	80	80	80
Result	80	80	80	80

* AATCC 22-1996 Water Repellency Rating: 0 - complete wetting of whole upper and lower surfaces of the fabric, 100 - no sticking or wetting of the upper surface of the fabric.

Table 4.5 Contact angle of control nonwoven fabrics for synthetic blood

Fabric		Cover Fabric	Support Fabric	Shell Fabric	Filtration Fabric
Advancing Contact Angle of Ten Replications (Degree)	**1**	85.83	80.96	82.26	87.87
	2	82.34	83.21	77.67	84.09
	3	82.20	79.87	82.54	86.61
	4	82.67	82.15	84.31	83.77
	5	79.67	82.30	85.32	81.22
	6	78.94	84.63	82.77	81.98
	7	81.75	82.33	83.24	81.59
	8	81.45	79.48	76.06	82.50
	9	89.00	80.26	81.81	82.54
	10	88.72	83.10	79.62	89.66
Mean		83.26	81.83	81.56	84.18
S.D.		3.48	1.65	2.92	2.9
CV (%)		4.18	2.02	3.58	3.44
Receding Contact Angle of Ten Replications (Degree)	**1**	79.96	71.25	73.90	78.94
	2	74.56	69.34	63.90	73.91
	3	74.35	72.72	74.51	74.64
	4	71.80	71.61	70.80	73.20
	5	72.88	70.55	75.34	73.03
	6	71.82	77.44	74.93	71.67
	7	75.83	76.40	69.50	74.32
	8	76.18	74.69	65.38	74.97
	9	81.30	70.38	74.33	74.07
	10	82.28	70.40	73.60	74.40
Mean		76.10	72.48	71.62	74.32
S.D.		3.84	2.78	4.13	1.89
CV (%)		5.05	3.84	5.77	2.54

Application of Repellent Finish and Order Various Fabric Layers to Simulate Face Masks

Add-on levels of 6% and 12% of fluorochemical finish Zonyl® PPR protector were applied to the cover fabric using the pad-dry-cure method as previously described in the chapter of Materials and Methods.

After the application of the fluorochemical repellent finish, the treated cover fabric was ordered with support fabric, filtration fabric and shell fabric to simulate different face masks according to the two-way factorial design. Three layering orders and three add-on levels of repellent finish were used, therefore nine (three × three) different simulated face masks were formed. The codes of those face masks are listed in Table 3.5 in the chapter of Materials and Methods. For each of the nine face masks, a minimum of 38 specimens were formed for the evaluation of fluid resistance, filtration ability and differential pressure.

Evaluation of Fluid Resistance of Simulated Face Masks

Fluid resistance of the simulated face masks was evaluated according to the Standard Test Method ASTM F 1862-00, Standard Test Method for Resistance of Surgical Mask to Penetration by Synthetic Blood [5]. In this study, three pressures (80 mmHg, 120 mmHg and 160 mmHg) were used to measure the fluid resistance test of each face mask. Ten replications of each of the nine face masks were tested at each pressure. The results of fluid resistance are reported in Tables 4.6 - 4.14. The letter “P” indicated that the face mask passed the fluid resistance test at the specific pressure. The letter “F” indicated that the face mask failed the fluid resistance test at the specific pressure.

Table 4.6 Fluid resistance (ASTM F 1862-00) of face mask 0-1

Replication		**1**	**2**	**3**	**4**	**5**	**6**	**7**	**8**	**9**	**10**
Pressure (mmHg)	**80**	P*	P	P	P	P	P	P	P	P	P
	120	F**	F	F	F	F	F	F	F	F	F
	160	F	F	F	F	F	F	F	F	F	F

* P: The face mask passed the fluid resistance test at the specific pressure;

** F: The face mask failed the fluid resistance test at the specific pressure.

Table 4.7 Fluid resistance (ASTM F 1862-00) of face mask 0-2

Replication		**1**	**2**	**3**	**4**	**5**	**6**	**7**	**8**	**9**	**10**
Pressure (mmHg)	**80**	P	P	P	P	P	P	P	P	P	P
	120	F	P	F	F	F	F	P	F	F	F
	160	F	F	F	F	F	F	F	F	F	F

Table 4.8 Fluid resistance (ASTM F 1862-00) of face mask 0-3

Replication		**1**	**2**	**3**	**4**	**5**	**6**	**7**	**8**	**9**	**10**
Pressure (mmHg)	**80**	P	P	P	P	P	P	P	P	P	P
	120	P	P	P	P	P	P	F	P	P	P
	160	P	F	P	P	F	P	P	F	P	P

Table 4.9 Fluid resistance (ASTM F 1862-00) of face mask 6-1

Replication		**1**	**2**	**3**	**4**	**5**	**6**	**7**	**8**	**9**	**10**
Pressure (mmHg)	**80**	P	P	P	P	P	P	P	P	P	P
	120	P	P	F	P	P	P	P	F	P	P
	160	F	F	F	F	F	F	F	F	F	F

Table 4.10 Fluid resistance (ASTM F 1862-00) of face mask 6-2

Replication		1	2	3	4	5	6	7	8	9	10
Pressure (mmHg)	80	P	P	P	P	P	P	P	P	P	P
	120	P	P	P	P	P	P	P	P	P	P
	160	F	F	F	P	F	F	F	F	F	F

Table 4.11 Fluid resistance (ASTM F 1862-00) of face mask 6-3

Replication		1	2	3	4	5	6	7	8	9	10
Pressure (mmHg)	80	P	P	P	P	P	P	P	P	P	P
	120	P	P	P	P	P	P	P	P	P	P
	160	P	P	P	P	P	P	P	P	P	P

Table 4.12 Fluid resistance (ASTM F 1862-00) of face mask 12-1

Replication		1	2	3	4	5	6	7	8	9	10
Pressure (mmHg)	80	P	P	P	P	P	P	P	P	P	P
	120	P	P	P	P	P	P	P	P	P	P
	160	F	F	F	F	F	F	F	F	F	F

Table 4.13 Fluid resistance (ASTM F 1862-00) of face mask 12-2

Replication		1	2	3	4	5	6	7	8	9	10
Pressure (mmHg)	80	P	P	P	P	P	P	P	P	P	P
	120	P	P	P	P	P	P	P	P	P	P
	160	P	P	P	P	P	P	P	P	P	P

Table 4.14 Fluid resistance (ASTM F 1862-00) of face mask 12-3

Replication		**1**	**2**	**3**	**4**	**5**	**6**	**7**	**8**	**9**	**10**
Pressure (mmHg)	**80**	P	P	P	P	P	P	P	P	P	P
	120	P	P	P	P	P	P	P	P	P	P
	160	P	P	P	P	P	P	P	P	P	P

Statistical Analysis of Fluid Resistance

Logistic regression was used to analyze the impacts of repellent finish, layering order and fluid pressure on the fluid resistance of face masks. A SAS program (Appendix A, Fluid Resistance Logistic Model) was developed and used to complete the analysis. Effects of parameters are shown in Table 4.15 and parameters estimates are shown in Table 4.16. The following null hypotheses were tested to study the main effects of the continuous variables, repellent finish and fluid pressure, and the class variable, layering order:

Hypothesis 1: H_0: The main effect of repellent finish was not significant,

The results show that the P value of repellent finish is smaller than 0.0001. Therefore, the hypothesis was rejected and it was concluded that the finish influenced the fluid resistance.

Hypothesis 2: H_0: The main effect of fluid pressure was not significant,

The results show that the P value of fluid pressure is smaller than 0.0001. Therefore, the hypothesis was rejected and it was concluded that fluid pressure influenced the fluid resistance.

Hypothesis 3: H_0: The main effect of layering order was not significant,

The results show that the P value of layering order is smaller than 0.0001. Therefore, the hypothesis was rejected and it was concluded that the layering order influenced the fluid resistance.

Table 4.15 Effects of parameters of fluid resistance logistic model

Variable	DF	Chi-Square	Pr>Chi-Square
Finish	1	21.5636	<.0001
Order	2	25.6027	<.0001
Pressure	1	25.9681	<.0001

Table 4.16 Parameter estimates of fluid resistance logistic model

Parameter	DF	Standard Estimate	Error	Chi-Square	Pr>Chi-Square
Intercept	1	18.6602	3.7286	25.0456	<.0001
Finish	1	0.9267	0.1996	21.5636	<.0001
Pressure	1	-0.1959	0.0385	25.9681	<.0001
Order 2 - Order 1	1	4.1486	1.1896	12.1609	0.0005
Order 3 - Order 1	1	13.1485	2.6545	24.5343	<.0001

Since all three parameters had significant main effects on the fluid resistance, the following model could be obtained according to the results in Table 4.16:

$$\ln (P/Q) = 18.6602 + 0.9267\ \text{Finish} - 0.1959\ \text{Pressure} + 4.1486\ (\text{Order 2} - \text{Order 1}) + 13.1485\ (\text{Order 3} - \text{Order 1}) \quad 4\text{-}1$$

Where: P = Probability of a specific face mask passes the fluid resistance test,

Q = 1-P,

Finish = Add-on level (%) of repellent finish,

Pressure = Fluid pressure (mmHg),

Order 1 = Layering order one,

Order 2 = Layering order two,

Order 3 = Layering order three.

This model clearly describes the impacts of repellent finish, layering order and fluid pressure on the fluid resistance qualitatively as well as quantitatively. A positive coefficient of

finish indicates that the fluid resistance pass probability of face masks is increased with increasing add-on level of repellent finish. Therefore, a face mask treated with the 12% add-on of repellent finish on the cover fabric would provide greater pass probability than a face mask treated with 6% add-on of repellent finish on the cover fabric. However, a face mask treated with the 6% add-on level repellent finish on the cover fabric would provide greater pass probability than a control face mask without any repellent finish on the cover fabric. The higher the add-on level of repellent finish applied to the cover fabric, the better the fluid resistance of the face mask. In addition, the model shows that fluid resistance pass probability is linear related to 0.9267 of the add-on level of repellent finish.

Transmission of a fluid into a fabric involves three steps: (1) the fluid contacts the surface of the fabric, (2) the fluid wets out the surface of the fabric, and (3) the fluid transmits into the fabric. Since the surface energy of the fabric is decreased by repellent finish to a point below the surface tension of the fluid, synthetic blood, the ability of the fabric to resist being wetted out is increased by repellent finish. It is difficult for the fluid to transmit into the finished fabric because it is harder for the fluid to wet out the treated fabric. Therefore, the fluid resistance of the fabric is improved by repellent finish.

A negative coefficient of pressure indicates that the fluid resistance pass probability of a face mask is decreased with increasing pressure of the fluid. Therefore, the pass probability of the face mask tested at the pressure of 160 mmHg is lower than the pass probability of the face mask tested at the pressure of 120 mmHg. However, the pass probability of the face mask tested at the pressure of 120 mmHg is lower than the pass probability of the face mask tested at the pressure of 80 mmHg. The fluid resistance of the face mask decreases with increased fluid pressure. In addition, the model shows that fluid resistance pass probability is linear related to

0.1959 of the pressure. The force behind the impacting fluid is increased by fluid pressure, therefore the fluid resistance of the fabric is decreased by increased fluid pressure.

The coefficient of difference between orders level two and level one, 4.1486, indicates that the pass probability of the face mask with order level two is greater than the pass probability of the face mask with order level one and the fluid resistance pass probability is linear related to 4.1486 of the difference between orders two and one. The coefficient of difference between orders level three and level one, 13.1485, indicates that the pass probability of the face mask with order level three is greater than the pass probability of the face mask with order level one and the fluid resistance pass probability is linear related to 13.1485 of the difference between orders three and one. Since 13.1485 is greater than 4.1486, the difference between orders level three and one is greater than the difference between orders level two and one. Therefore, the pass probability of the face mask with order level three is the greatest. So face masks with layering order of cover fabric, support fabric, filtration fabric and shell fabric can provide the best fluid resistance.

Compared with the face masks with layering order one, there is one more layer, the support layer, in the face masks with layering order two or three. The increased strength offered by the spunbonded fabric provides the support layer a greater ability to resist the penetration of fluid. Therefore, the layering orders two and three can provide better fluid resistance to the face mask than the layering order one. The only difference between layering order two and three is the location of the support layer. In layering order three, the support layer is before the filtration layer. Therefore, the support layer can take full advantage of its great ability to resist the penetration of fluid. The lower strength provided by the meltblown nonwoven fabric offers the filtration layer smaller ability to resist fluid. However, with the protection of the support layer,

the filtration layer can use more of its potential to resist the penetration of the fluid. Therefore, the layering order three can offer better fluid resistance to the face mask than the layering order two.

This model can also be used to predict the fluid resistance pass probability of a face mask with specific parameters. Table 4.17 shows the results. For example, with 3.0% add-on level of repellent finish on the cover fabric and a layering order two, the pass probability is 88.85% at pressure of 120 mmHg. Optimum parameters can also be estimated using this model. The statistical analysis shows that layering order three can offer the best fluid resistance. To reduce the cost, the minimum add-on level of repellent finish for desired effectiveness can be determined. Table 4.18 shows that 4.5% is the minimum add-on level of repellent finish for a 100% pass probability of fluid resistance at pressure of 160 mmHg. Therefore, according to repellent finish and layering order, a face mask treated with 4.5% add-on of Zonyl® PPR protector on the cover fabric and layering order of cover fabric, support fabric, filtration fabric, then shell fabric would provide a 100% pass probability of fluid resistance at 160 mmHg with the lowest cost.

Table 4.17 Results of parameter prediction

Specific Parameters	Layering Order	Pressure (mmHg)	Predicted Parameter
Add-On Level of Repellent Finish = 3%	2	120	Pass Probability=88.85%
Pass Probability = 100%	3	160	Minimum Add -on Level of Repellent Finish=4.5%

Evaluation of Filtration Ability of Simulated Face Masks

Both individual fabric layers and the entire face mask of each of these nine simulated face masks were examined to evaluate the filtration ability. LSCM surface examination was used

to study the filtration ability of individual fabric layers and LSCM cross sectional examination was used to study the filtration ability of entire face masks.

LSCM Surface Examination

To locate the latex microspheres on/in the structure of nonwoven fabrics, a variety of combinations LSCM parameters were evaluated to determine those that produced the most effective images for this study. Table 4.18 shows the parameters actually used in this study. To locate the small particles on/in nonwoven fabrics, two detectors were used to identify different components by selective signal detection. Therefore, there were three images obtained by LSCM for each specimen. The left image was obtained by PMT one that was optimized to show the fabric. The middle image was obtained by PMT two that was optimized to show the small particles. The right image was the merged image that combined the left and the right images to show the distribution of small particles on the fabric.

The liquid used to generate the challenge aerosol was first examined by the LSCM with the parameters in Table 4.18 and the results are shown in Figure 4.1. In these color micrographs*, the microspheres are represented by red. When these three images are evaluated, it is apparent that nothing is identified by detector one while latex microspheres are clearly identified by detector two and the merged image is the same as the image obtained by detector two. This was expected as only the liquid that contains small particles was examined.

The cover fabric, filtration fabric, support fabric and shell fabric were also examined by the LSCM with the same parameters and the results are shown in Figure 4.2 - 4.5. In these color micrographs*, the fabrics are represented by shades of gray. The left images in Figures 4.2, 4.4 and 4.5 clearly show the structures of the spunbonded cover fabric, support fabric and shell

fabric. Both fibers and the diamond-shaped bonding point were identified by LSCM. The left image in Figure 4.3 clearly shows the structure of the meltblown filtration fabric. When all these images are evaluated, it is apparent that the structure of fabrics is clearly identified by detector one while nothing is identified by detector two and the merged images are the same with the images obtained by detector one. This was expected as only control fabrics were examined.

Table 4.18 Parameters of LSCM

Laser	**Source**	Ar/He Ne
	Excitation Wavelength (nm)	100% 476
	Emission Wavelength of PM 1 (nm)	478-493
	Emission Wavelength of PM 2 (nm)	499-576
Dichroic Mirror		TD 488/543/633
Beam Expander		Beam Exp 3
Pinhole (micron)		459.26
Zoom		1
Image Dimension (micron*micron)		1.50*1.50
Voxel Size (micron*micron)		1.46*1.46
Objective Lens		20
Scan Mode		xyz
Speed (HZ)		400
Format		512*512
Gain PMT 1 (V)		503
Offset PMT 1 (%)		0
Gain PMT 2 (V)		799
Offset PMT 2 (%)		0

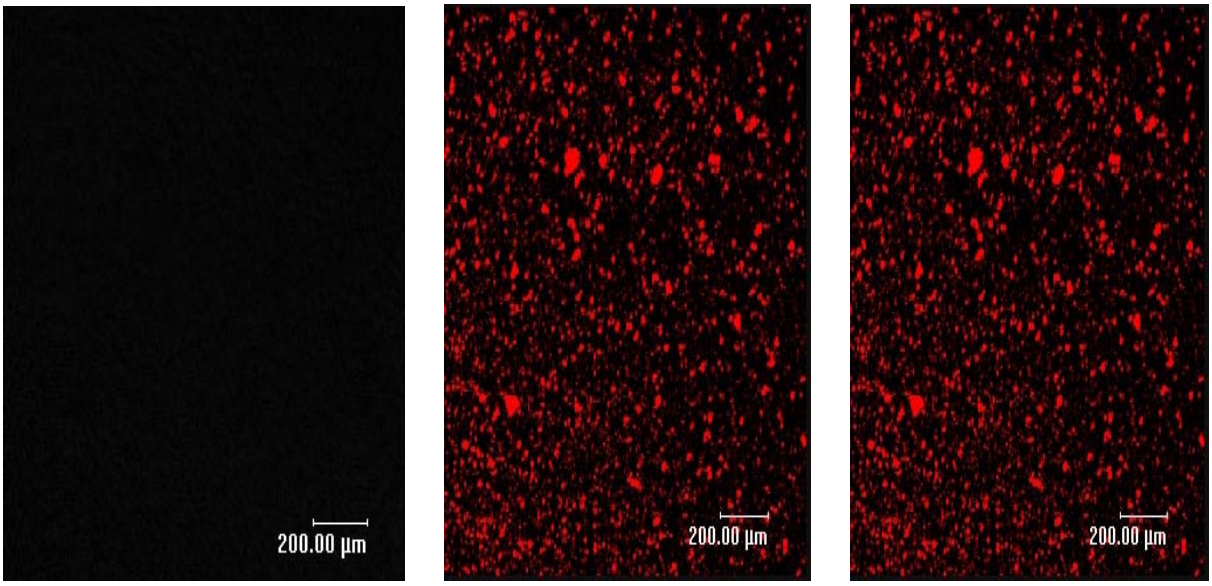

(a) (b) (c)

Figure 4.1 LSCM image of challenge liquid which was composed of synthetic blood and microspheres; (a) image obtained by PMT one, (b) image obtained by PMT two, and (c) merged image

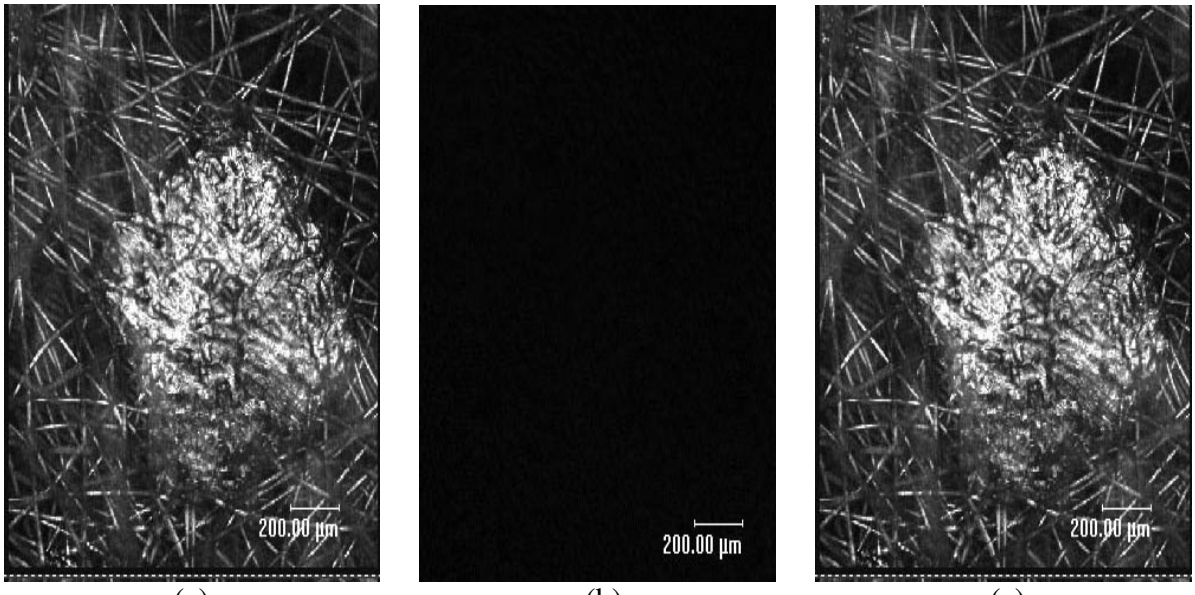

(a) (b) (c)

Figure 4.2 LSCM image of cover fabric; (a) image obtained by PMT one, (b) image obtained by PMT two, and (c) merged image

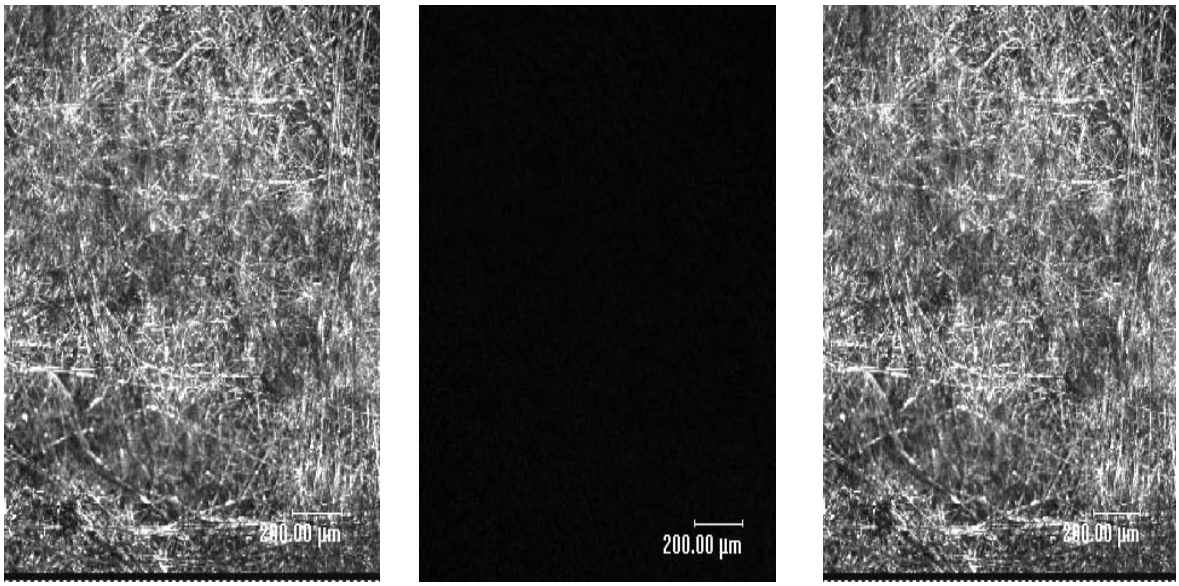

(a) (b) (c)

Figure 4.3 LSCM image of filtration fabric; (a) image obtained by PMT one, (b) image obtained by PMT two, and (c) merged image

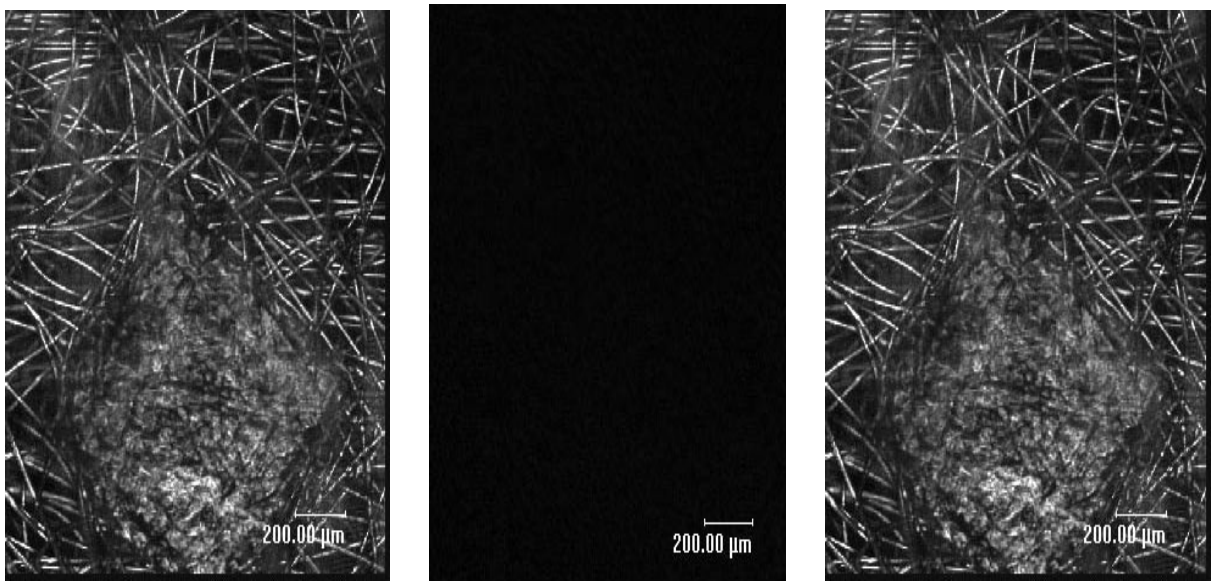

(a) (b) (c)

Figure 4.4 LSCM image of support fabric; (a) image obtained by PMT one, (b) image obtained by PMT two, and (c) merged image

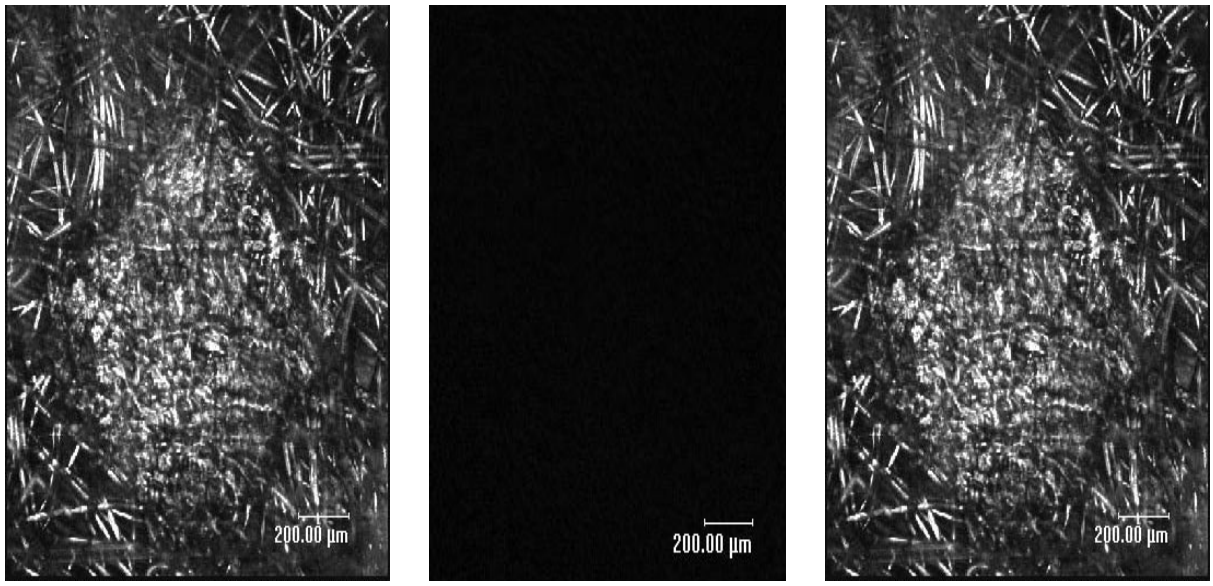

(a) (b) (c)

Figure 4.5 LSCM image of shell fabric; (a) image obtained by PMT one, (b) image obtained by PMT two, and (c) merged image

All simulated face masks were then exposed to the challenge aerosol using the method as previously described in the chapter of Materials and Methods, each individual layer was examined by LSCM, and the results are presented in Figures 4.6 - 4.26. In these color micrographs*, the microspheres are represented by red and the fabrics are represented by shades of gray. When all of these images are evaluated, it is apparent that the structure of fabrics is clearly identified by detector one while the small particles are clearly identified by detector two. Moreover, the merged images show the distribution of small particles on fabrics. To study how the small particles transmit through the face mask, the two detectors were used to select the signal of the microspheres from that of nonwoven fabric. When this method was used, the fabric and small particles could be determined independently and then the images were merged to show the distribution of particles on the fabric.

In Figures 4.6 - 4.26, the surface structure of fabric layer and the small particles captured by the fabric are clearly shown. For face mask 0-1 (Figures 4.6 and 4.7), small particles were detected on the surfaces of the cover layer and the filtration layer, therefore images of these two layers are shown. Small particles were captured on the fibers, interscies and bonding points of the cover fabric. The filtration layer appeared to capture more small particles than the cover layer.

For face mask 0-2 (Figures 4.8 and 4.9), small particles were also detected on the surfaces of the cover layer and the filtration layer, therefore images of these two layers are shown. Small particles were captured on the fibers, interscies and bonding points of the cover fabric. The filtration layer appeared to capture more small particles than the cover layer.

For face mask 0-3 (Figures 4.10 - 4.12), small particles were detected on the surfaces of the cover layer, support layer and the filtration layer, therefore images of these three layers are shown. Small particles were captured on the fibers, interscies and bonding points of the cover fabric and the support fabric. The filtration layer appeared to capture more small particles than the other two layers while the support layer appeared to capture fewer small particles than the other two layers.

For face mask 6-1 (Figures 4.13 and 4.14), small particles were detected on the surfaces of the cover layer and the filtration layer, therefore images of these two layers are shown. Small particles were captured on the fibers, interscies and bonding points of the cover fabric. The filtration layer appeared to capture more small particles than the cover layer.

For face mask 6-2 (Figures 4.15 and 4.16), small particles were also detected on the surfaces of the cover layer and the filtration layer, therefore images of these two layers are shown. Small particles were captured on the fibers, interscies and bonding points of the cover fabric. The filtration layer appeared to capture more small particles than the cover layer.

For face mask 6-3 (Figures 4.17 - 4.19), small particles were detected on the surfaces of the cover layer, support layer and the filtration layer, therefore images of these three layers are shown. Small particles were captured on the fibers, interscies and bonding points of the cover fabric and the support fabric. The filtration layer appeared to capture more small particles than the other two layers here while the support layer appeared to capture fewer small particles than the other two layers here.

For face mask 12-1 (Figures 4.20 and 4.21), small particles were detected on the surfaces of the cover layer and the filtration layer, therefore images of these two layers are shown. Small particles were captured on the fibers, interscies and bonding points of the cover fabric. The filtration layer appeared to capture more small particles than the cover layer.

For face mask 12-2 (Figures 4.22 and 4.23), small particles were also detected on the surfaces of the cover layer and the filtration layer, therefore images of these two layers are shown. Small particles were captured on the fibers, interscies and bonding points of the cover fabric. The filtration layer appeared to capture more small particles than the cover layer.

For face mask 12-3 (Figures 4.24 - 4.26), small particles were detected on the surfaces of the cover layer, support layer and the filtration layer, therefore images of these three layers are shown. Small particles were captured on the fibers, interscies and bonding points of the cover fabric and the support fabric. The filtration layer appeared to capture more small particles than the other two layers here while the support layer appeared to capture fewer small particles than the other two layers here.

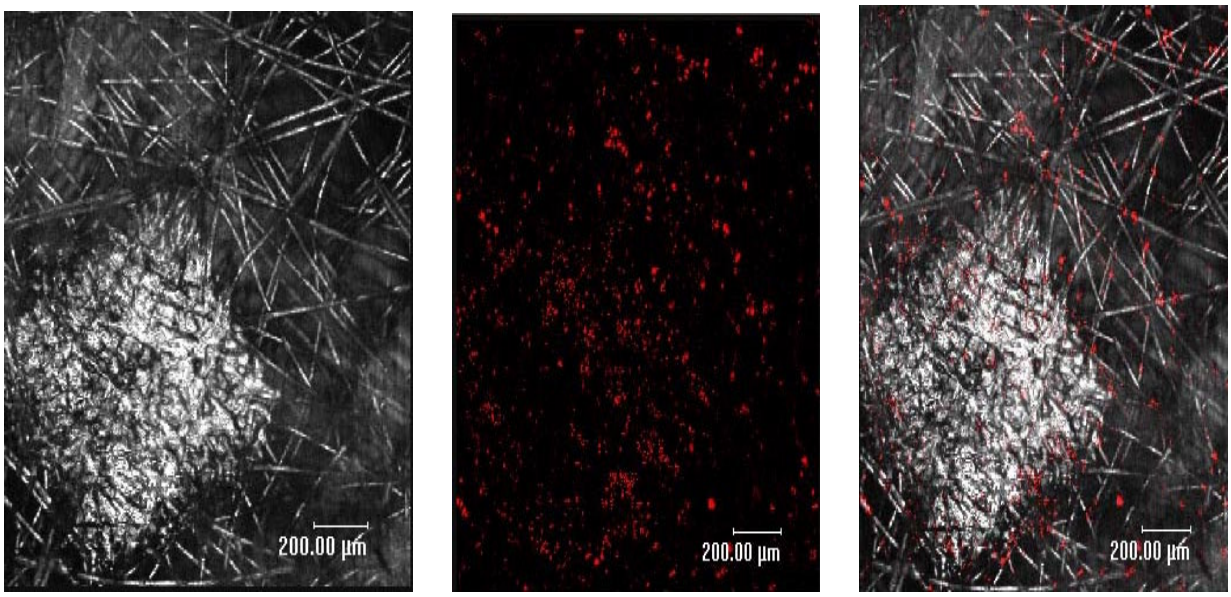

(a) (b) (c)

Figure 4.6 LSCM image of face mask 0-1 exposed to challenge aerosol using modified ASTM F 2101 – cover fabric; (a) image obtained by PMT one, (b) image obtained by PMT two, and (c) merged image

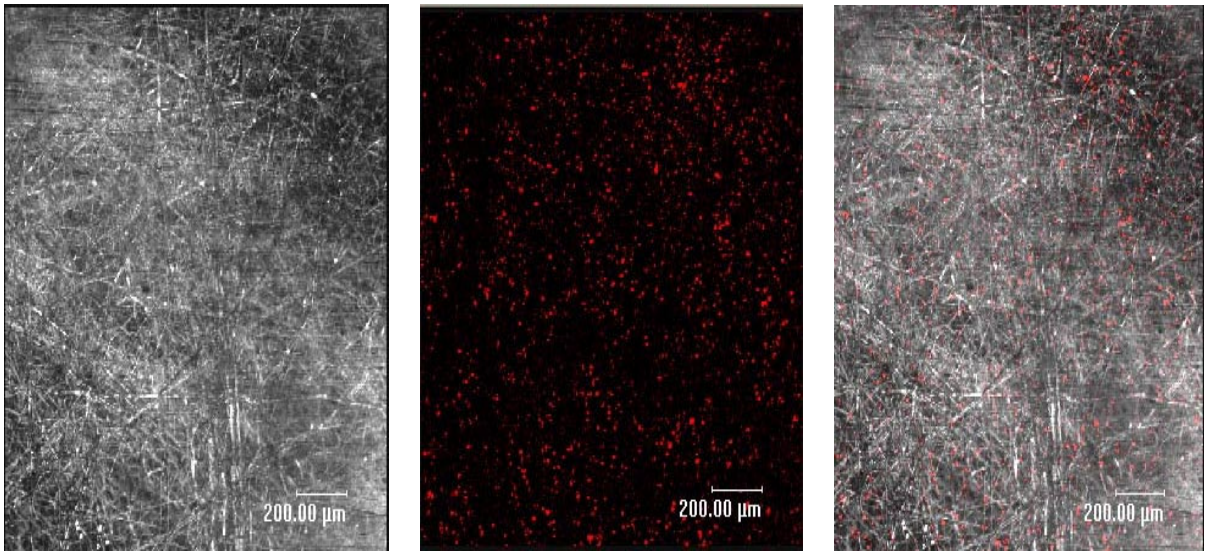

(a) (b) (c)

Figure 4.7 LSCM image of face mask 0-1 exposed to challenge aerosol using modified ASTM F 2101 – filtration fabric; (a) image obtained by PMT one, (b) image obtained by PMT two, and (c) merged image

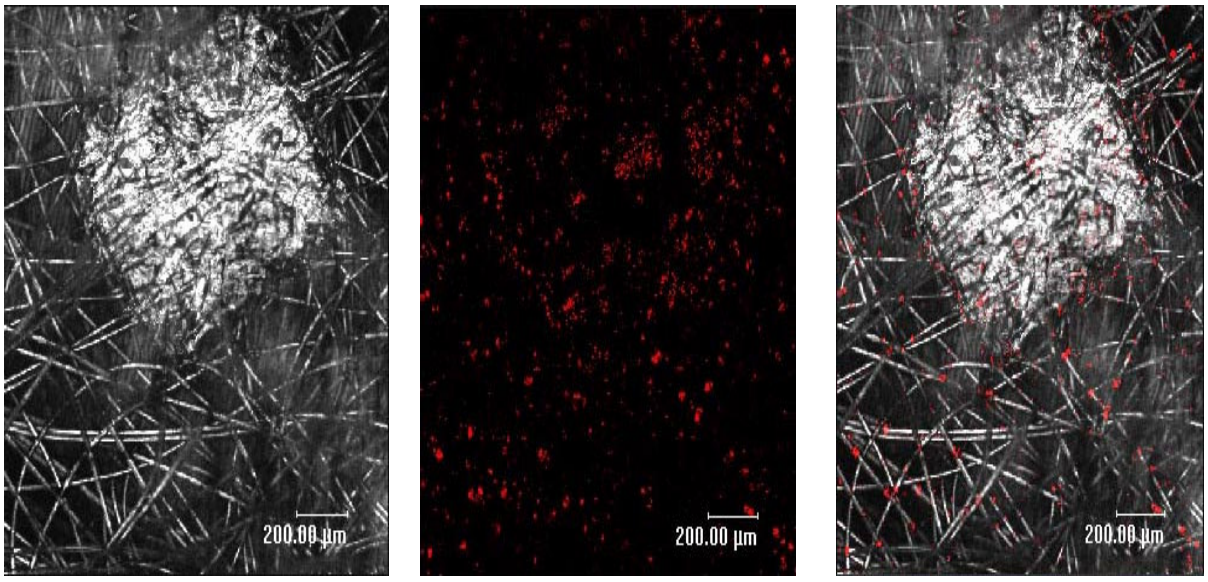

(a) (b) (c)

Figure 4.8 LSCM image of face mask 0-2 exposed to challenge aerosol using modified ASTM F 2101 – cover fabric; (a) image obtained by PMT one, (b) image obtained by PMT two, and (c) merged image

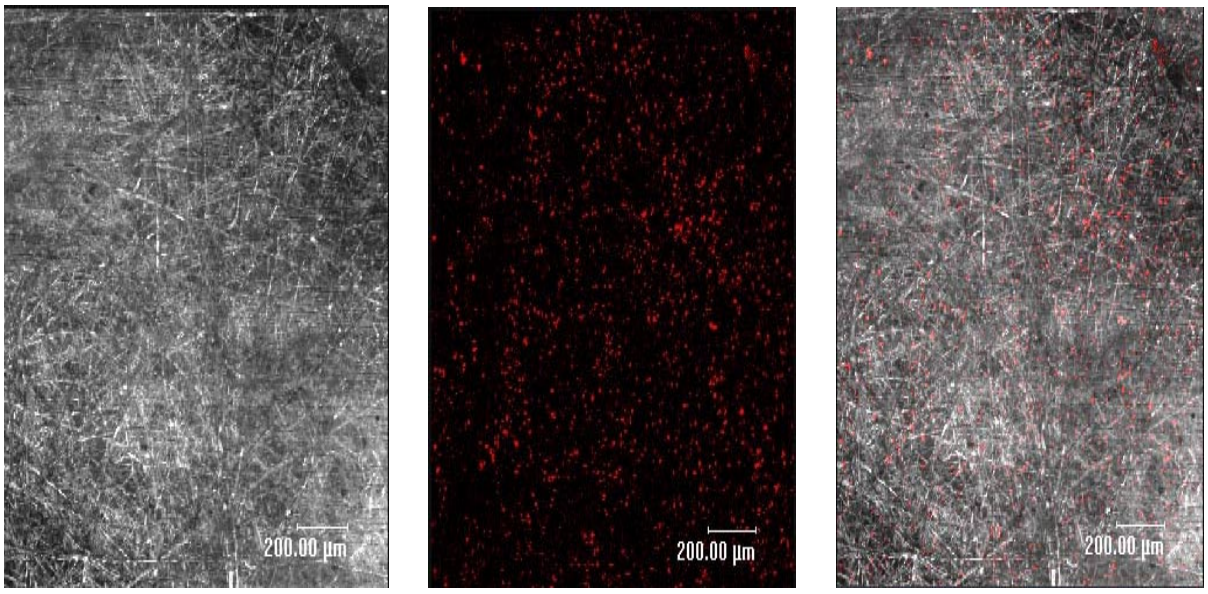

(a) (b) (c)

Figure 4.9 LSCM image of face mask 0-2 exposed to challenge aerosol using modified ASTM F 2101 – filtration fabric; (a) image obtained by PMT one, (b) image obtained by PMT two, and (c) merged image

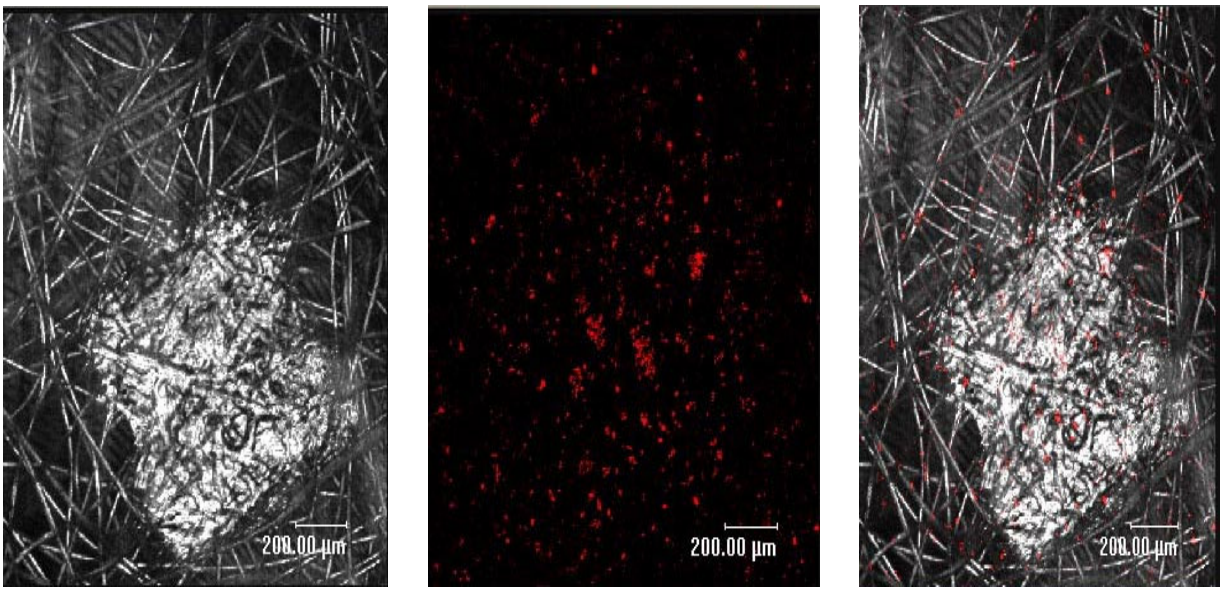

(a) (b) (c)

Figure 4.10 LSCM image of face mask 0-3 exposed to challenge aerosol using modified ASTM F 2101 – cover fabric; (a) image obtained by PMT one, (b) image obtained by PMT two, and (c) merged image

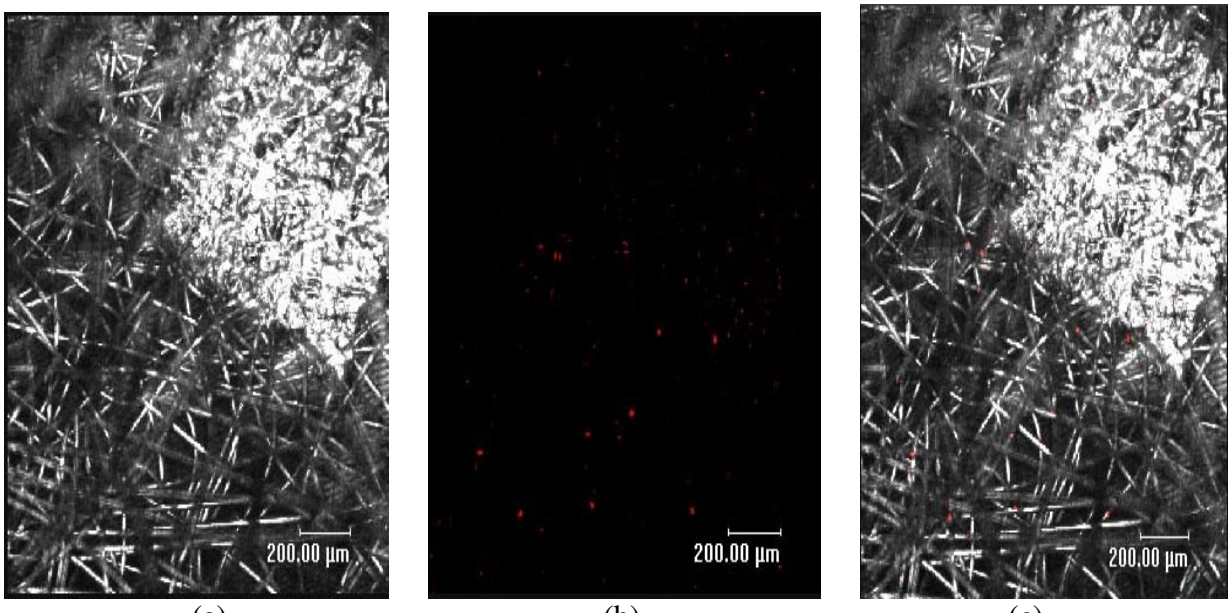

(a) (b) (c)

Figure 4.11 LSCM image of face mask 0-3 exposed to challenge aerosol using modified ASTM F 2101 – support fabric; (a) image obtained by PMT one, (b) image obtained by PMT two, and (c) merged image

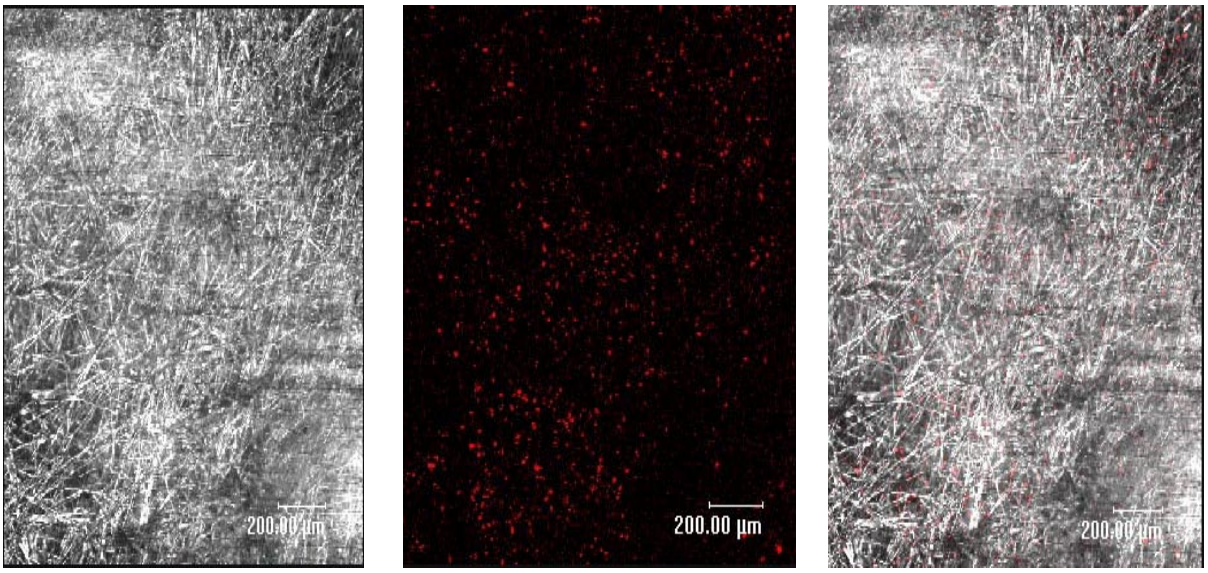

(a) (b) (c)

Figure 4.12 LSCM image of face mask 0-3 exposed to challenge aerosol using modified ASTM F 2101 – filtration fabric; (a) image obtained by PMT one, (b) image obtained by PMT two, and (c) merged image

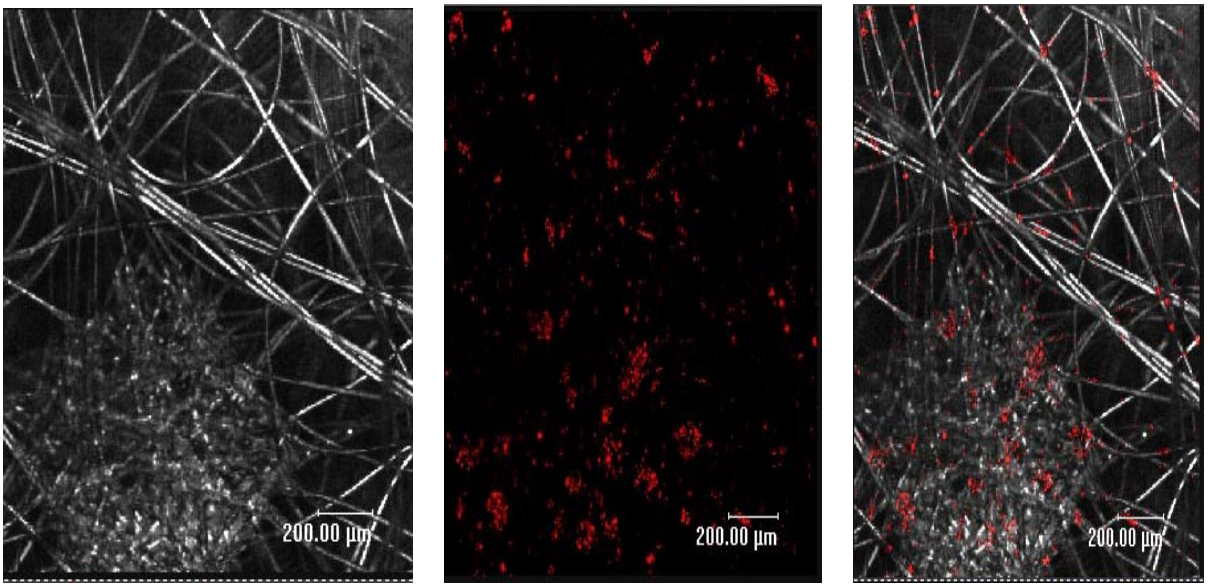

(a) (b) (c)

Figure 4.13 LSCM image of face mask 6-1 exposed to challenge aerosol using modified ASTM F 2101 – cover fabric; (a) image obtained by PMT one, (b) image obtained by PMT two, and (c) merged image

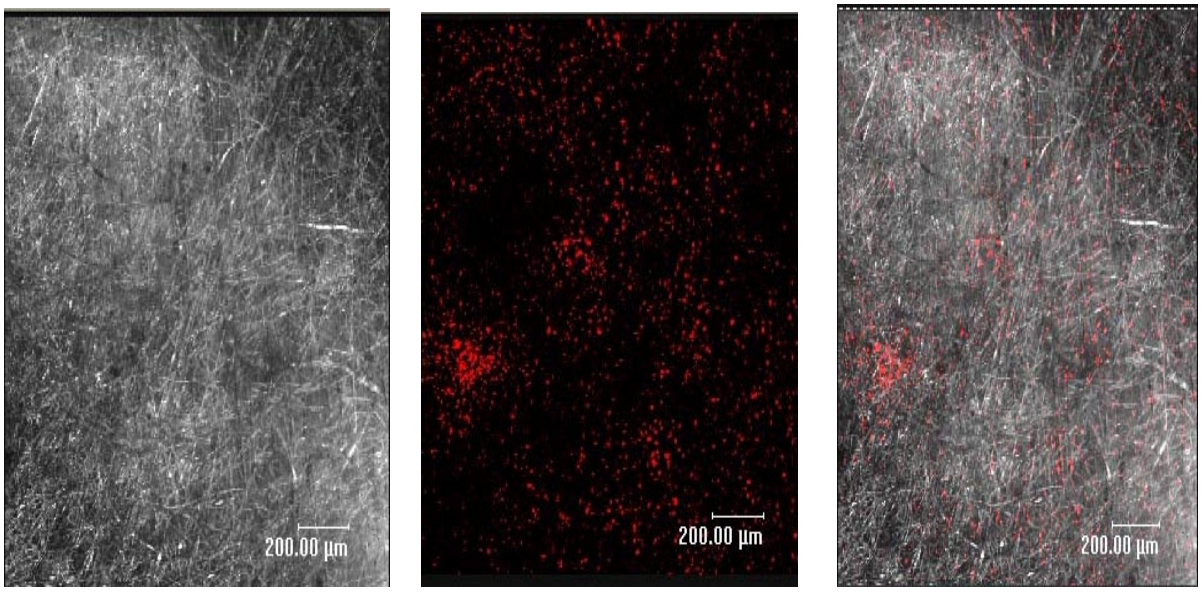

(a) (b) (c)

Figure 4.14 LSCM image of face mask 6-1 exposed to challenge aerosol using modified ASTM F 2101 – filtration fabric; (a) image obtained by PMT one, (b) image obtained by PMT two, and (c) merged image

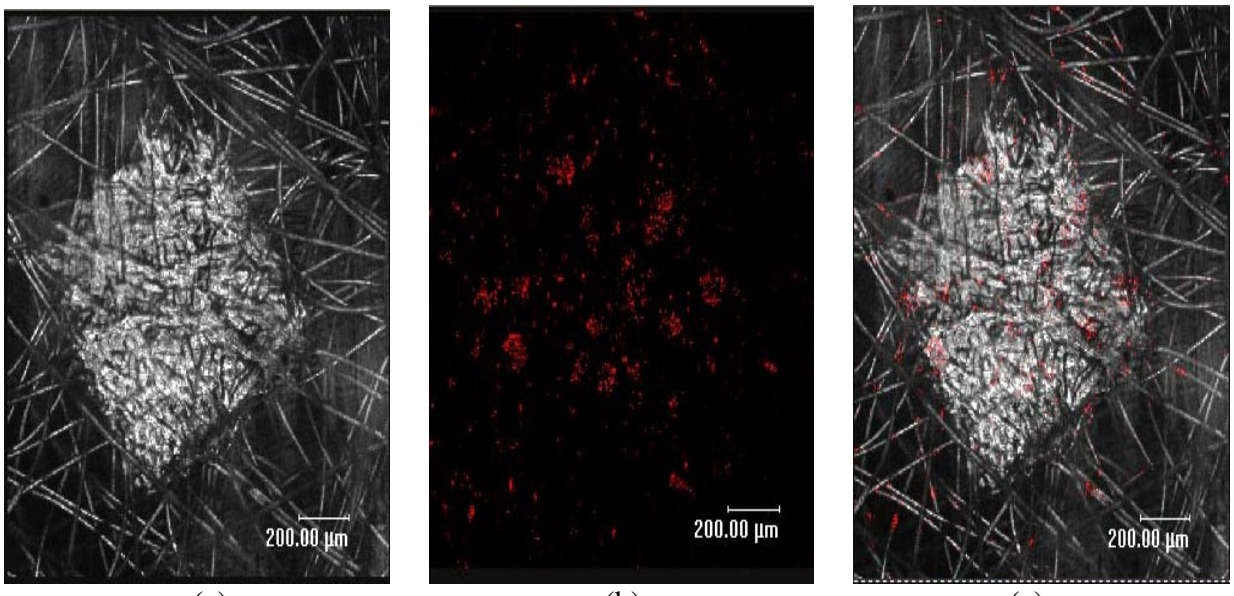

(a) (b) (c)

Figure 4.15 LSCM image of face mask 6-2 exposed to challenge aerosol using modified ASTM F 2101 – cover fabric; (a) image obtained by PMT one, (b) image obtained by PMT two, and (c) merged image

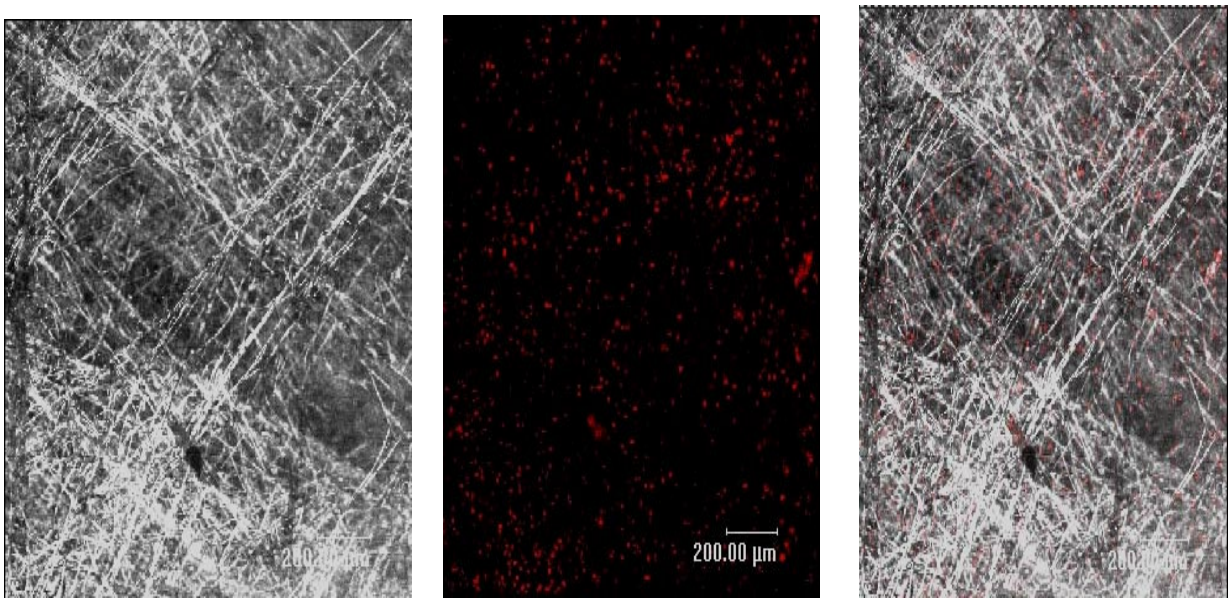

(a) (b) (c)

Figure 4.16 LSCM image of face mask 6-2 exposed to challenge aerosol using modified ASTM F 2101 – filtration fabric; (a) image obtained by PMT one, (b) image obtained by PMT two, and (c) merged image

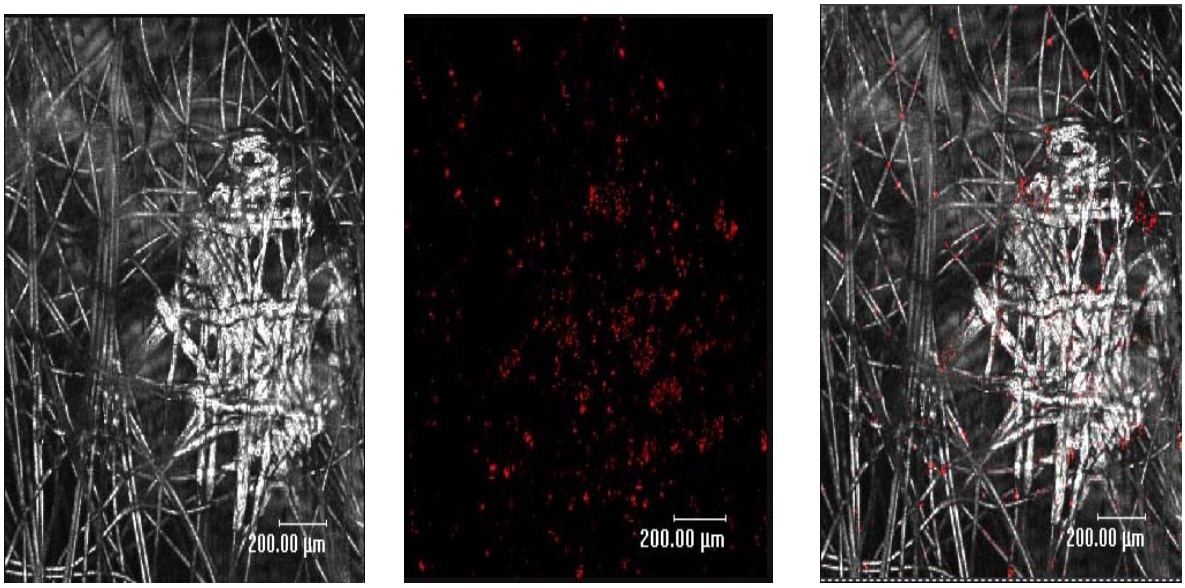

(a) (b) (c)

Figure 4.17 LSCM image of face mask 6-3 exposed to challenge aerosol using modified ASTM F 2101 – cover fabric; (a) image obtained by PMT one, (b) image obtained by PMT two, and (c) merged image

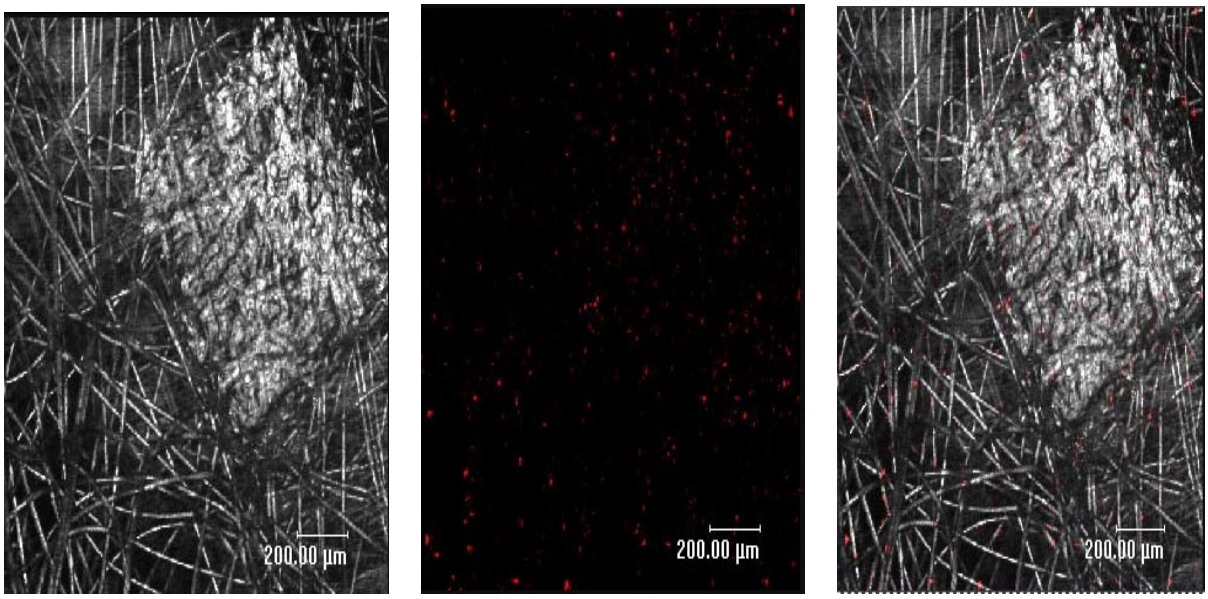

(a) (b) (c)

Figure 4.18 LSCM image of face mask 6-3 exposed to challenge aerosol using modified ASTM F 2101 – support fabric; (a) image obtained by PMT one, (b) image obtained by PMT two, and (c) merged image

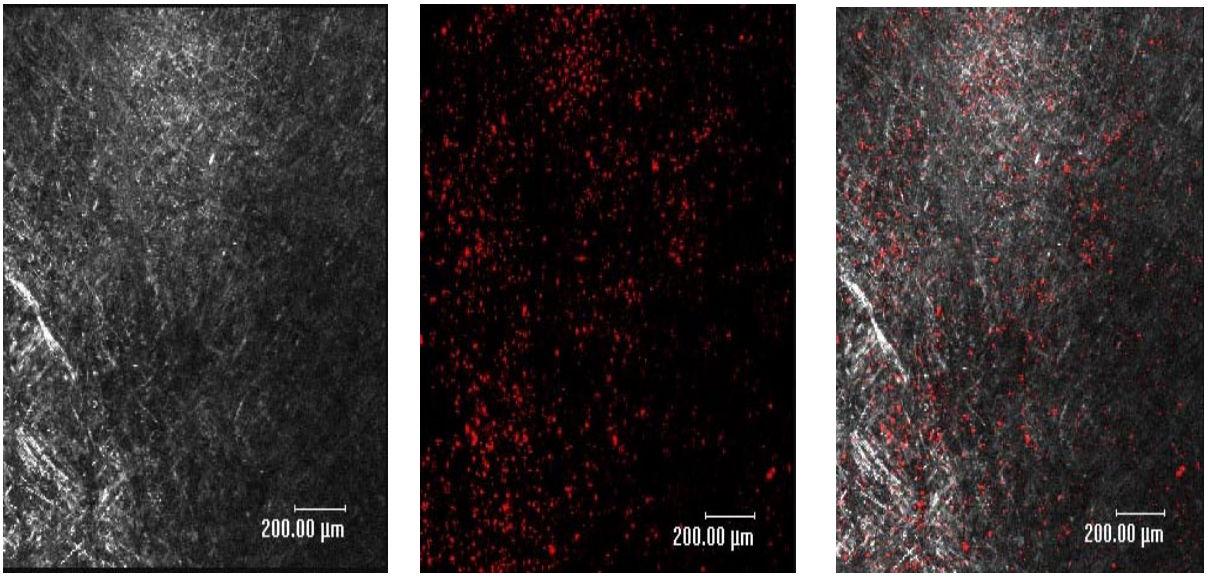

(a) (b) (c)

Figure 4.19 LSCM image of face mask 6-3 exposed to challenge aerosol using modified ASTM F 2101 – filtration fabric; (a) image obtained by PMT one, (b) image obtained by PMT two, and (c) merged image

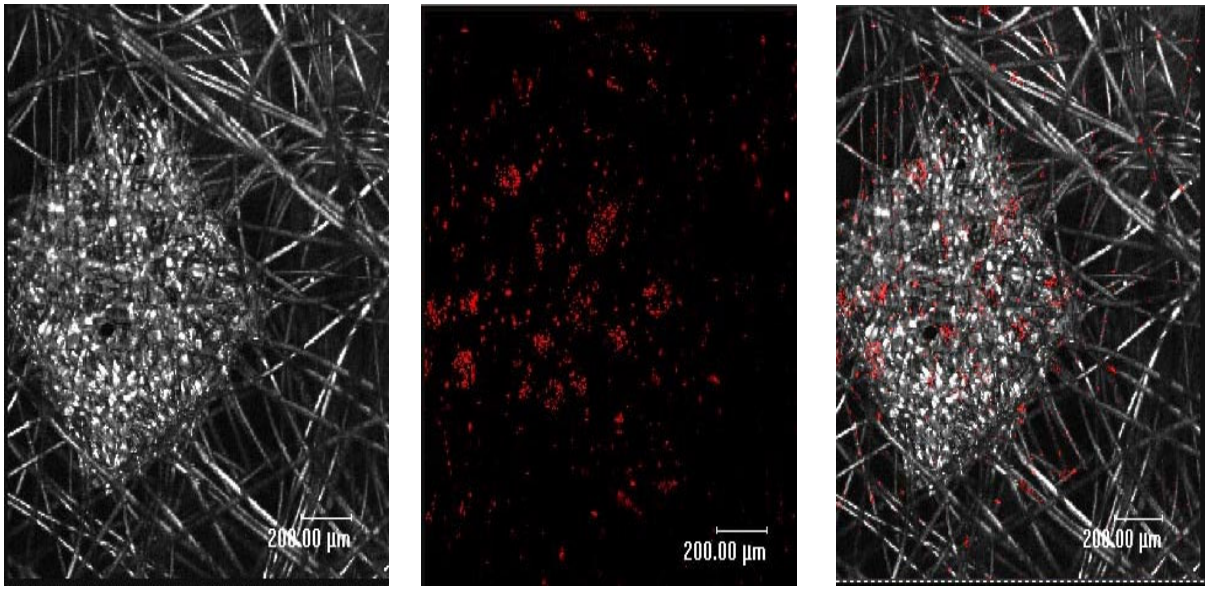

(a) (b) (c)

Figure 4.20 LSCM image of face mask 12-1 exposed to challenge aerosol using modified ASTM F 2101 – cover fabric; (a) image obtained by PMT one, (b) image obtained by PMT two, and (c) merged image

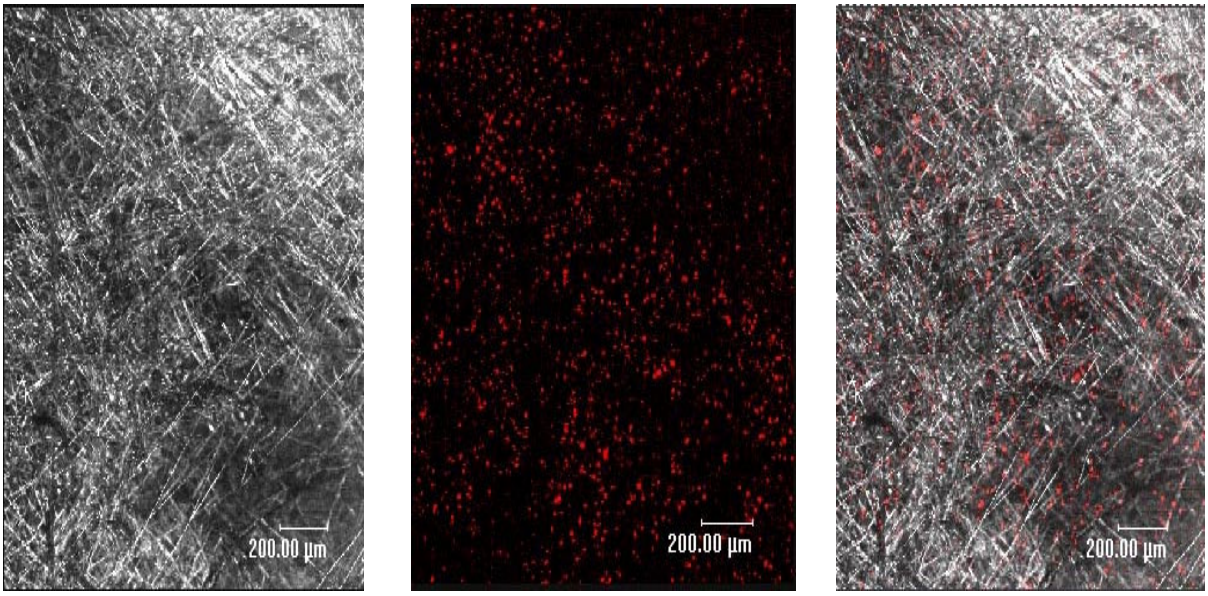

(a) (b) (c)

Figure 4.21 LSCM image of face mask 12-1 exposed to challenge aerosol using modified ASTM F 2101 – filtration fabric; (a) image obtained by PMT one, (b) image obtained by PMT two, and (c) merged image

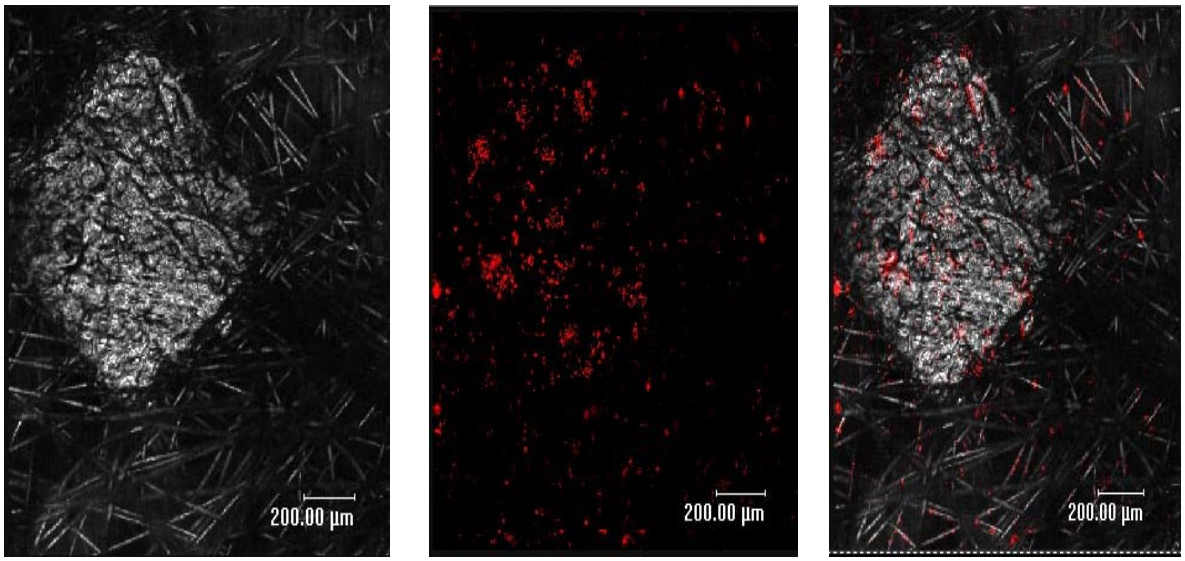

(a) (b) (c)

Figure 4.22 LSCM image of face mask 12-2 exposed to challenge aerosol using modified ASTM F 2101 – cover fabric; (a) image obtained by PMT one, (b) image obtained by PMT two, and (c) merged image

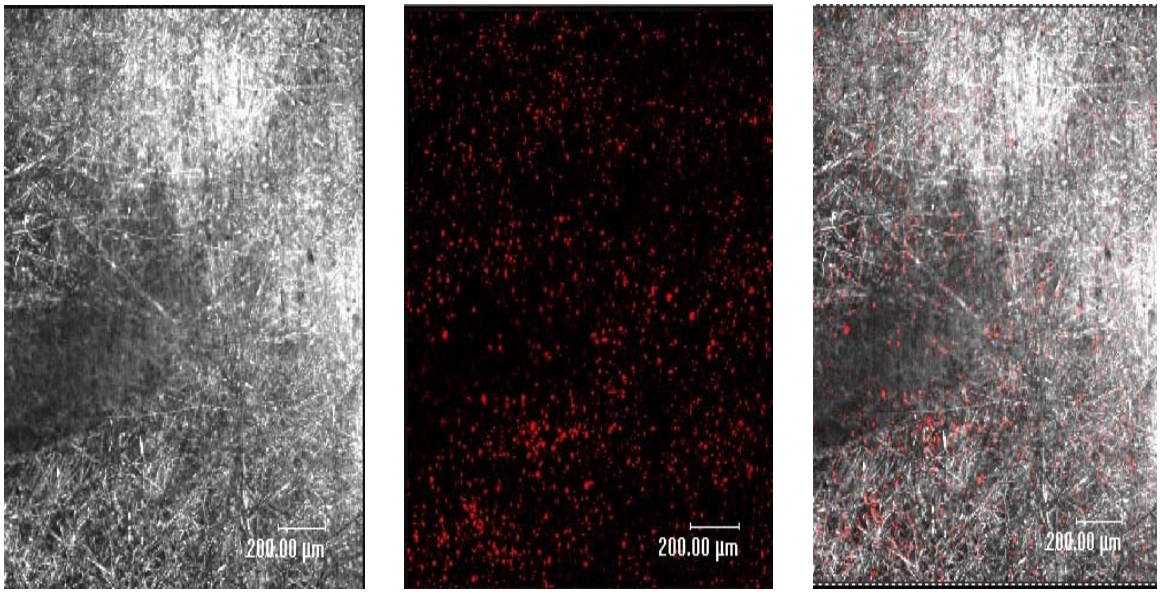

(a) (b) (c)

Figure 4.23 LSCM image of face mask 12-2 exposed to challenge aerosol using modified ASTM F 2101 – filtration fabric; (a) image obtained by PMT one, (b) image obtained by PMT two, and (c) merged image

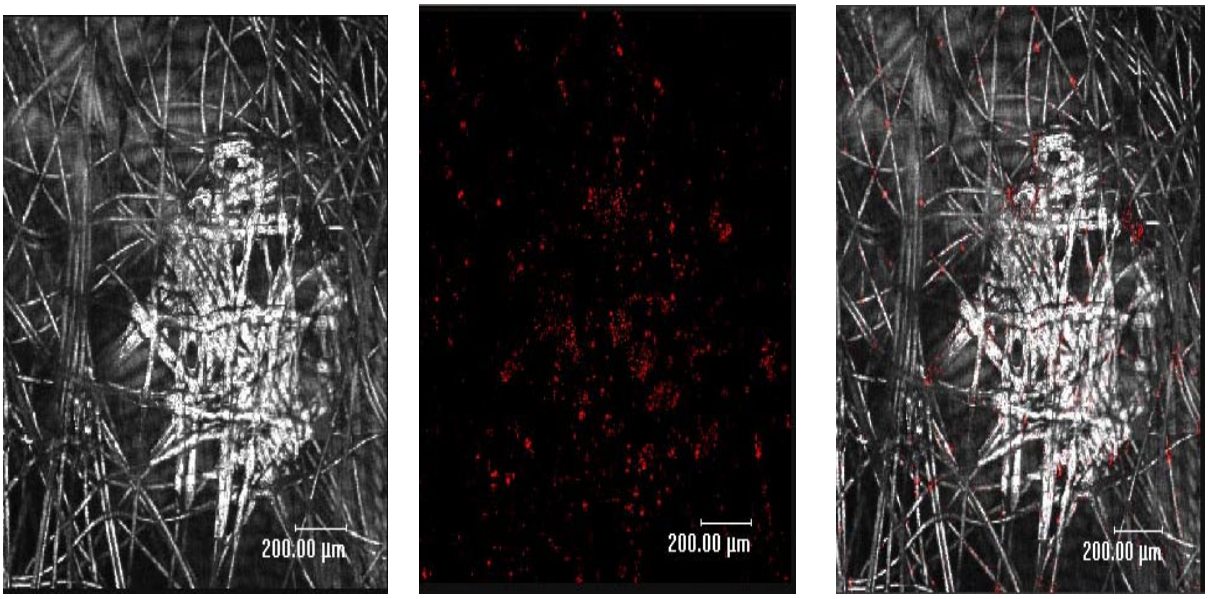

(a) (b) (c)

Figure 4.24 LSCM image of face mask 12-3 exposed to challenge aerosol using modified ASTM F 2101 – cover fabric; (a) image obtained by PMT one, (b) image obtained by PMT two, and (c) merged image

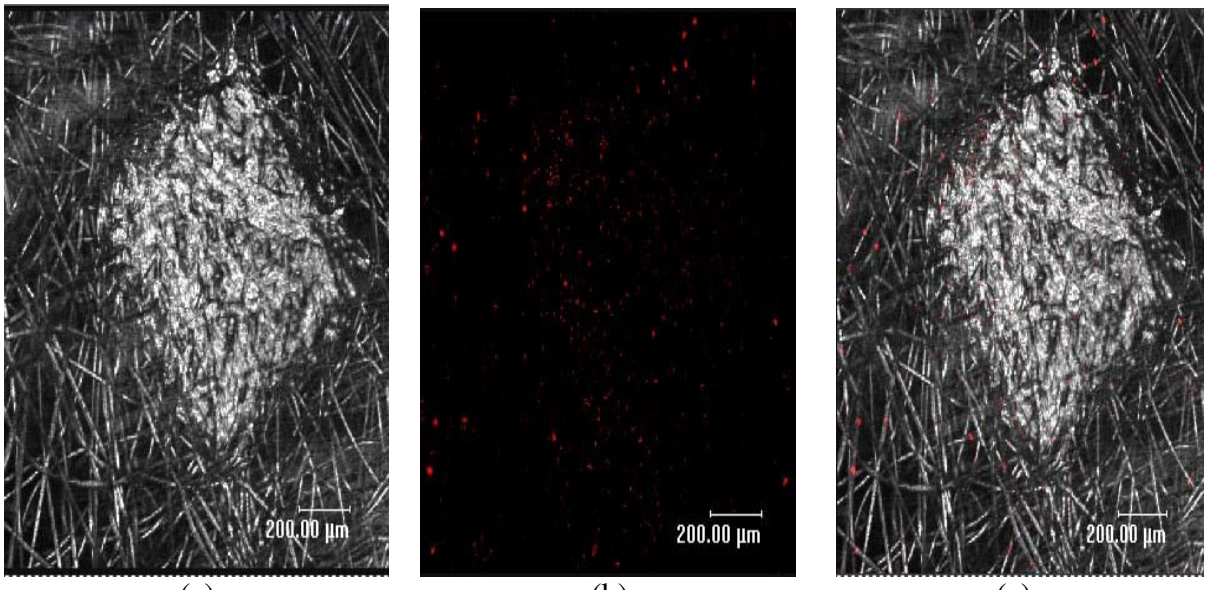

(a) (b) (c)

Figure 4.25 LSCM image of face mask 12-3 exposed to challenge aerosol using modified ASTM F 2101 – support fabric; (a) image obtained by PMT one, (b) image obtained by PMT two, and (c) merged image

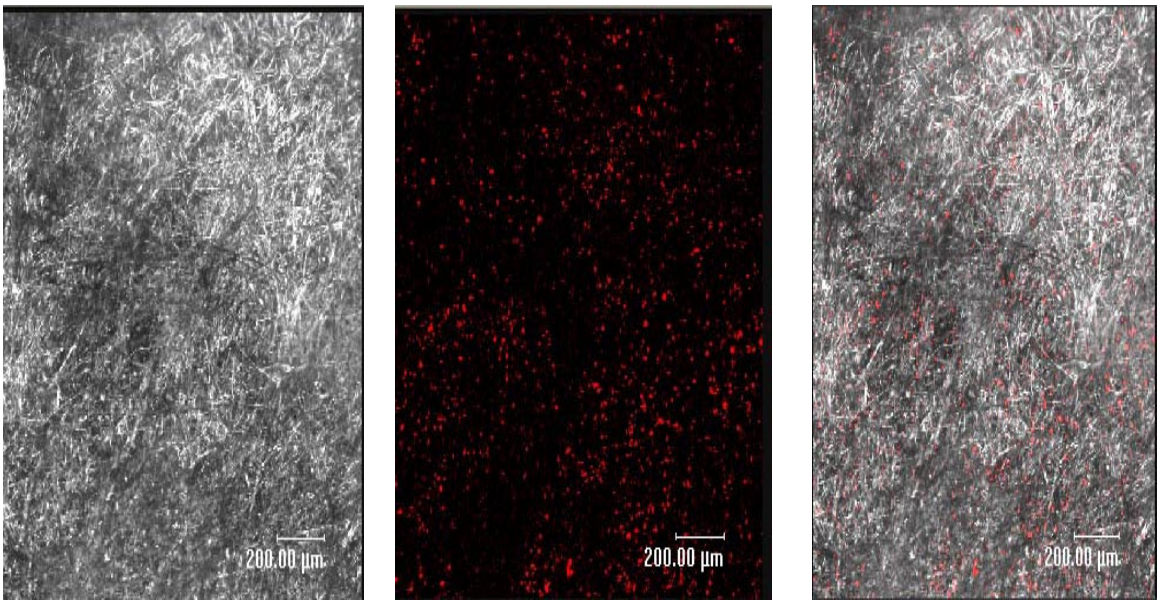

(a) (b) (c)

Figure 4.26 LSCM image of face mask 12-3 exposed to challenge aerosol using modified ASTM F 2101 – filtration fabric; (a) image obtained by PMT one, (b) image obtained by PMT two, and (c) merged image

Image Analysis

ImageJ was used to complete the quantitative analysis of the small particles captured by the surfaces of different layers of face masks. Total area (as determined by square pixels) was used to represent the small particles captured on the surface of individual fabric layers of face masks. The total area was calculated by the product of the number of particle spots with the mean area of all particle spots. Image analysis of the small particles captured by the surfaces of individual layers of all nine face masks was completed. Data have been analyzed and are presented in Tables 4.19 - 4.27. According to these data, a comparison of small particles (represented by total area) captured by the surface of the filtration layer and other fabric layers

were completed. Statistical analysis was also performed to study the effect of repellent finish on the filtration ability of fabric layers within the simulated face mask.

A comparison of small particles (represented by total area) captured by the surface of filtration layer and other fabric layers was prepared and the result is shown in Figure 4.27. In this figure, the x-axis represents the filtration layer and the layers before or after it and the y-axis represents the percent of small particles captured by the surface of this specific layer with reference to all small particles captured by the surfaces of all layers. The figure shows that the percentage of small particles captured by the filtration layer of each face mask is the greatest. This supports the observations previously discussed regarding information obtained from the LSCM images. The filtration layer captured more small particles than the other layers in each face mask. Therefore, the filtration layer is the primary contributor to the filtration ability of the face mask.

To evaluate the importance of surface filtration in surgical face masks, the percentage of the small particles (represented by total area) captured in surface filtration to the small particles (represented by total area) to which the face masks were exposed was calculated for each of nine face masks. The filtration fabric rather than the face masks was exposed to the same challenge aerosol using the modified Standard Test Method ASTM F2101-01, Standard Test Method for Evaluating the Bacterial Filtration Efficiency (BFE) of Medical Face Mask Materials, Using a Biological Aerosol of Staphylococcus aureus under the same test conditions. For each filtration fabric, three specimens were exposed to the challenge aerosol and for each of the specimens, surfaces at five different locations were examined using the LSCM. LSCM images were analyzed using ImageJ and the total area of captured small particles was used to represent the small particles to which the face masks were exposed. Results are presented in Table 4.28. The

percentages of the small particles captured on the surfaces of all layers of a face mask to the small particles to which the face masks were exposed were determined and presented in Table 4.29. The percentage ranged from 81.3% to 98.3%, therefore surface filtration is critical to the filtration ability of the face mask.

Table 4-19 Image analysis of small particles captured in the surface of individual layers of face mask 0-1

Variable		**Number of Particle Spots**		**Mean Area of Particle Spots (Pixel^2)**		**Total Area (Pixel^2)**	
Fabric		Cover Fabric	Filtration Fabric	Cover Fabric	Filtration Fabric	Cover Fabric	Filtration Fabric
Specimen 1	**Location 1**	1496	3373	3.96	3.36	5924.16	11333.3
	Location 2	1589	3464	4.06	3.08	6451.34	10669.1
	Location 3	1602	4082	4.03	3.11	6456.06	12695
	Location 4	1551	4210	3.94	3.16	6110.94	13303.6
	Location 5	1680	3790	3.95	3.07	6636	11635.3
	Mean of Locations	1584	3784	3.99	3.16	6315.7	11927.3
Specimen 2	**Location 1**	1865	3489	4.28	3.16	7982.2	11025.2
	Location 2	1772	3347	4.14	3.32	7336.08	11112
	Location 3	1783	3399	3.9	3.14	6953.7	10672.9
	Location 4	1832	3475	4.27	3.45	7822.64	11988.8
	Location 5	1507	3135	3.74	3.26	5636.18	10220.1
	Mean of Locations	1752	3369	4.07	3.27	7146.16	11003.8
Specimen 3	**Location 1**	1538	3469	4.12	3.33	6336.56	11551.8
	Location 2	1682	3425	4.08	3.13	6862.56	10720.3
	Location 3	1549	4255	4.17	3.14	6459.33	13360.7
	Location 4	1551	3526	4.24	3.34	6576.24	11776.8
	Location 5	1539	3665	3.93	3.28	6048.27	12021.2
	Mean of Locations	1571.8	3668	4.108	3.244	6456.59	11886.2
Mean of Specimens		1635.93	3607	4.056	3.22	6639.48	11605.7

Table 4-20 Image analysis of small particles captured in the surface of individual layers of face mask 0-2

Variable		Number of Particle Spots		Mean Area of Particle Spots (Pixel^2)		Total Area (Pixel^2)	
Fabric		Cover Fabric	Filtration Fabric	Cover Fabric	Filtration Fabric	Cover Fabric	Filtration Fabric
Specimen 1	**Location 1**	1612	3421	4.03	3.22	6496.36	11015.62
	Location 2	1616	3854	3.89	3.26	6286.24	12564.04
	Location 3	1553	3234	4.11	3.42	6382.83	11060.28
	Location 4	1558	3181	4.2	3.12	6543.60	9924.72
	Location 5	1787	3300	4.03	3.53	7201.61	11649.00
	Mean of Locations	1625	3398	4.05	3.31	6582.13	11242.73
Specimen 2	**Location 1**	1690	3566	3.92	3.25	6624.80	11589.50
	Location 2	1507	2935	4.02	3.88	6058.14	11387.80
	Location 3	1493	3522	3.77	3.16	5628.61	11129.52
	Location 4	1510	2559	4.15	3.52	6266.50	9007.68
	Location 5	1773	2808	4.22	3.64	7482.06	10221.12
	Mean of Locations	1595	3078	4.02	3.49	6412.02	10667.12
Specimen 3	**Location 1**	1597	3478	4.34	3.25	6930.98	11303.50
	Location 2	1623	3590	4.26	3.4	6913.98	12206.00
	Location 3	1519	3262	4.19	3.26	6364.61	10634.12
	Location 4	1653	3031	4.18	3.17	6909.54	9608.27
	Location 5	1749	3612	4.21	3.25	7363.29	11739.00
	Mean of Locations	1628.2	3394.6	4.236	3.266	6896.48	11098.18
Mean of Specimens		1616.07	3290.2	4.112	3.35	6630.21	11002.68

Table 4-21 Image analysis of small particles captured in the surface of individual layers of face mask 0-3

Variable		Number of Particle Spots			Mean Area of Particle Spots (Pixel^2)			Total Area (Pixel^2)		
Fabric		Cover Fabric	Support Fabric	Filtration Fabric	Cover Fabric	Support Fabric	Filtration Fabric	Cover Fabric	Support Fabric	Filtration Fabric
Specimen 1	**Location 1**	1525	199	3529	3.89	2.4	2.21	5932.25	477.6	7799.09
	Location 2	1622	156	4343	3.92	2.27	1.93	6358.24	354.12	8381.99
	Location 3	1528	135	4532	4.25	2.48	1.9	6494	334.8	8610.8
	Location 4	1485	102	4536	3.34	3.28	1.66	4959.9	334.56	7529.76
	Location 5	1484	107	2627	3.51	2.92	3.4	5208.84	312.44	8931.8
	Mean of Locations	1528.8	139.8	3913.4	3.782	2.67	2.22	5790.65	362.7	8250.69
Specimen 2	**Location 1**	1553	226	4370	4.17	2.54	1.99	6476.01	574.04	8696.3
	Location 2	1498	191	2904	3.33	2.31	3.68	4988.34	441.21	10686.7
	Location 3	1673	116	2611	5.02	3.11	3.08	8398.46	360.76	8041.88
	Location 4	1611	335	2739	5.3	2.89	3.32	8538.3	968.15	9093.48
	Location 5	1316	304	3339	3.43	3.42	1.92	4513.88	1039.68	6410.88
	Mean of Locations	1530.2	234.4	3192.6	4.25	2.854	2.798	6583	676.77	8585.85
Specimen 3	**Location 1**	1481	338	2618	4.13	1.98	3.17	6116.53	669.24	8299.06
	Location 2	1669	408	3625	3.22	2.45	1.96	5374.18	999.6	7105
	Location 3	1587	368	3898	3.31	2.38	2.11	5252.97	875.84	8224.78
	Location 4	1579	358	4548	4.07	2.53	1.98	6426.53	905.74	9005.04
	Location 5	1646	282	4406	3.88	2.94	1.95	6386.48	829.08	8591.7
	Mean of Locations	1592.4	350.8	3819	3.722	2.456	2.234	5911.34	855.9	8245.12
Mean of Specimens		1550.5	241.6	3641.7	3.92	2.66	2.42	6094.99	631.79	8360.55

Table 4-22 Image analysis of small particles captured in the surface of individual layers of face mask 6-1

Variable		**Number of Particle Spots**		**Mean Area of Particle Spots (Pixel^2)**		**Total Area (Pixel^2)**	
Fabric		Cover Fabric	Filtration Fabric	Cover Fabric	Filtration Fabric	Cover Fabric	Filtration Fabric
Specimen 1	**Location 1**	1034	3203	5.85	4.1	6048.90	13132.30
	Location 2	795	2985	5.34	4.24	4245.30	12656.40
	Location 3	1040	2939	5.81	4.23	6042.40	12431.97
	Location 4	785	2914	5.54	4.44	4348.90	12938.16
	Location 5	964	3427	4.32	4.63	4164.48	15867.01
	Mean of Locations	924	3094	5.37	4.33	4970.00	13405.17
Specimen 2	**Location 1**	866	2857	5.02	4.08	4347.32	11656.56
	Location 2	967	3179	5.33	3.87	5154.11	12302.73
	Location 3	749	3598	4.07	3.96	3048.43	14248.08
	Location 4	984	2586	3.45	4.29	3394.80	11093.94
	Location 5	761	2225	4.41	4.4	3356.01	9790.00
	Mean of Locations	865	2889	4.46	4.12	3860.13	11818.26
Specimen 3	**Location 1**	781	2698	4.43	4.18	3459.83	11277.64
	Location 2	921	2686	5.66	5.17	5212.86	13886.62
	Location 3	914	2911	5.63	5.54	5145.82	16126.94
	Location 4	900	2720	5.2	4.59	4680.00	12484.80
	Location 5	835	2837	4.57	5.06	3815.95	14355.22
	Mean of Locations	870.2	2770.4	5.098	4.908	4462.89	13626.24
Mean of Specimens		886.4	2917.8	4.976	4.45	4431.01	12949.89

Table 4-23 Image analysis of small particles captured in the surface of individual layers of face mask 6-2

Variable		**Number of Particle Spots**		**Mean Area of Particle Spots (Pixel^2)**		**Total Area (Pixel^2)**	
Fabric		Cover Fabric	Filtration Fabric	Cover Fabric	Filtration Fabric	Cover Fabric	Filtration Fabric
Specimen 1	**Location 1**	1038	2407	4.02	4.72	4172.76	11361.04
	Location 2	1110	2760	3.9	4.63	4329.00	12778.80
	Location 3	991	3112	4.34	4.08	4300.94	12696.96
	Location 4	1211	5563	4.26	3.14	5158.86	17467.82
	Location 5	789	2656	4.61	4.68	3637.29	12430.08
	Mean of Locations	1028	3300	4.23	4.25	4319.77	13346.94
Specimen 2	**Location 1**	1037	2539	6.6	4.94	6844.20	12542.66
	Location 2	869	2380	5.23	4.3	4544.87	10234.00
	Location 3	778	2626	4.56	4.42	3547.68	11606.92
	Location 4	967	2628	4.52	4.14	4370.84	10879.92
	Location 5	994	2673	5.06	4.18	5029.64	11173.14
	Mean of Locations	929	2569	5.19	4.40	4867.45	11287.33
Specimen 3	**Location 1**	1092	2975	4.27	4.32	4662.84	12852.00
	Location 2	1030	3022	5.81	4.52	5984.30	13659.44
	Location 3	870	2573	5.59	4.52	4863.30	11629.96
	Location 4	923	2636	6.28	4.55	5796.44	11993.80
	Location 5	1054	2574	5.36	4	5649.44	10296.00
	Mean of Locations	993.8	2756	5.462	4.382	4458.70	12086.24
Mean of Specimens		983.6	2875	4.96	4.34	4548.64	12240.17

Table 4-24 Image analysis of small particles captured in the surface of individual layers of face mask 6-3

Variable		Number of Particle Spots			Mean Area of Particle Spots (Pixel^2)			Total Area (Pixel^2)		
Fabric		Cover Fabric	Support Fabric	Filtration Fabric	Cover Fabric	Support Fabric	Filtration Fabric	Cover Fabric	Support Fabric	Filtration Fabric
Specimen 1	**Location 1**	1267	758	3166	3.53	3.02	4.03	4472.51	2289.16	12758.98
	Location 2	1357	737	2703	3.73	3.35	4.16	5061.61	2468.95	11244.48
	Location 3	1132	833	2118	3.98	2.63	3.72	4505.36	2190.79	7878.96
	Location 4	1165	756	2352	4.44	3.33	3.89	4392.05	2517.48	9149.28
	Location 5	1125	706	1664	3.58	2.51	3.3	4027.50	1772.06	5491.20
	Mean of Locations	1209.2	758	2401	3.85	2.97	3.82	4491.81	2247.69	9304.58
Specimen 2	**Location 1**	1145	882	2181	3.58	3.04	4.8	4099.10	2681.28	10468.80
	Location 2	1314	884	2217	4.57	3.09	3.54	6004.98	2731.56	7848.18
	Location 3	1267	641	1614	3.67	3.04	3.47	4649.89	1948.64	5600.58
	Location 4	1196	577	2537	3.57	2.6	4.18	4269.72	1500.20	10604.66
	Location 5	1062	776	1808	4.53	2.83	3.78	4810.86	2196.08	6834.24
	Mean of Locations	1196.8	752	2071	3.98	2.92	3.95	4766.91	2211.55	8271.29
Specimen 3	**Location 1**	1162	786	1072	3.87	2.86	2.94	4496.94	2247.96	3151.68
	Location 2	1190	716	2402	3.98	2.5	3.76	4736.20	1790.00	9031.52
	Location 3	1108	765	2503	3.71	3.07	3.98	4110.68	2348.55	9961.94
	Location 4	1162	693	2402	3.76	2.8	3.76	4369.12	1940.40	9031.52
	Location 5	1301	711	2681	3.27	2.85	3.91	4254.27	2026.35	10482.71
	Mean of Locations	1184.6	734.2	2212	3.718	2.816	3.67	4393.44	2070.65	8331.87
Mean of Specimens		1197	748.07	2228	3.85	2.9	3.81	4550.72	2176.63	8635.92

Table 4-25 Image analysis of small particles captured in the surface of individual layers of face mask 12-1

Variable		**Number of Particle Spots**		**Mean Area of Particle Spots (Pixel^2)**		**Total Area (Pixel^2)**	
Fabric		Cover Fabric	Filtration Fabric	Cover Fabric	Filtration Fabric	Cover Fabric	Filtration Fabric
Specimen 1	**Location 1**	1167	2903	4.34	4.16	5064.78	12076.48
	Location 2	1164	3158	4.76	3.98	5540.64	12568.84
	Location 3	929	3112	4.6	3.6	4273.40	11203.20
	Location 4	1017	3511	4.55	3.67	4627.35	12885.37
	Location 5	966	3870	4.82	3.97	4656.12	15363.90
	Mean of Locations	1049	3311	4.61	3.88	4832.46	12819.56
Specimen 2	**Location 1**	838	3337	4.85	3.93	4064.30	13114.41
	Location 2	932	3029	5.23	3.75	4874.36	11358.75
	Location 3	863	2712	5.38	4.33	4642.94	11742.96
	Location 4	745	2608	4.57	3.98	3404.65	10379.84
	Location 5	867	2668	5.14	3.9	4456.38	10405.20
	Mean of Locations	849	2871	5.03	3.98	4288.53	11400.23
Specimen 3	**Location 1**	943	2973	4.36	3.97	4111.48	11802.81
	Location 2	932	3138	4.71	4.18	4389.72	13116.84
	Location 3	936	2988	5.32	4.21	4979.52	12579.48
	Location 4	1032	2936	5.04	4.26	5201.28	12507.36
	Location 5	1029	2925	6.03	3.86	6204.87	11290.50
	Mean of Locations	974.4	2992	5.092	4.096	4977.37	12259.40
Mean of Specimens		957.47	3058	4.91	3.98	4699.45	12159.73

Table 4-26 Image analysis of small particles captured in the surface of individual layers of face mask 12-2

Variable		**Number of Particle Spots**		**Mean Area of Particle Spots (Pixel^2)**		**Total Area (Pixel^2)**	
Fabric		Cover Fabric	Filtration Fabric	Cover Fabric	Filtration Fabric	Cover Fabric	Filtration Fabric
Specimen 1	**Location 1**	1146	2818	5.85	4.36	6704.10	12286.48
	Location 2	1059	2986	5.07	4.58	5369.13	13675.88
	Location 3	798	3063	4.09	4.6	3263.82	14089.80
	Location 4	432	3111	4.22	4.75	1823.04	14777.25
	Location 5	816	3000	4.5	4.85	3672.00	14550.00
	Mean of Locations	850	2996	5	4.63	4166.82	13875.88
Specimen 2	**Location 1**	1006	2742	5.11	4.56	5140.66	12503.52
	Location 2	1086	2757	3.63	4.28	3942.18	11799.96
	Location 3	984	2557	4.45	4.08	4378.80	10432.56
	Location 4	826	2484	4.72	3.9	3898.72	9687.60
	Location 5	1036	2421	5.68	3.83	5884.48	9272.43
	Mean of Locations	988	2592	4.72	4.13	4648.97	10739.21
Specimen 3	**Location 1**	883	2554	5.39	4.77	4759.37	12182.58
	Location 2	875	3065	5.94	4.38	5197.50	13424.70
	Location 3	1265	2357	5.46	4.03	6906.90	9498.71
	Location 4	1070	3063	5.56	4.48	5949.20	13722.24
	Location 5	921	2883	5.01	4.64	4614.21	13377.12
	Mean of Locations	1002.8	2784.4	5.472	4.46	5485.44	12441.07
Mean of Specimens		946.93	2790.73	5.06	4.41	4767.08	12352.05

Table 4-27 Image analysis of small particles captured in the surface of individual layers of face mask 12-3

Variable		**Number of Particle Spots**			**Mean Area of Particle Spots (Pixel^2)**			**Total Area (Pixel^2)**		
Fabric		Cover Fabric	Support Fabric	Filtration Fabric	Cover Fabric	Support Fabric	Filtration Fabric	Cover Fabric	Support Fabric	Filtration Fabric
Specimen 1	**Location 1**	1301	762	3334	3.27	2.46	3.28	4254.27	1874.52	10935.52
	Location 2	1351	576	3298	3.52	3.14	3.26	4755.52	1808.64	10751.48
	Location 3	1036	565	2912	3.77	3.39	3.23	3905.72	1915.35	9405.76
	Location 4	1133	521	2756	3.93	2.92	3.39	4452.69	1521.32	9342.84
	Location 5	1141	623	2717	3.72	2.52	3.46	4244.52	1569.96	9400.82
	Mean of Locations	1192	609	3003	3.64	2.89	3.32	4322.54	1737.96	9967.28
Specimen 2	**Location 1**	1231	909	2807	3.72	2.51	3.44	4579.32	2281.59	9656.08
	Location 2	995	418	2780	4.58	3.01	3.3	4557.10	1258.18	9174.00
	Location 3	1191	659	2204	3.19	3.01	3.11	3799.29	1983.59	6854.44
	Location 4	1193	617	2351	3.45	3.58	3.76	4115.85	2208.86	8839.76
	Location 5	1061	628	2623	4.19	3.48	3.86	4445.59	2185.44	10124.78
	Mean of Locations	1134	646	2553	3.83	3.12	3.49	4299.43	1983.53	8929.81
Specimen 3	**Location 1**	1183	787	2347	3.51	2.77	3.36	4152.33	2179.99	7885.92
	Location 2	1285	879	2620	3.57	3.43	3.67	4587.45	3014.97	9615.40
	Location 3	1277	905	1891	3.94	2.72	3.7	5031.38	2461.60	6996.70
	Location 4	1215	857	1667	4.02	3.08	3.46	4884.30	2639.56	5767.82
	Location 5	1261	729	1635	3.16	3.17	3.65	3984.76	2310.93	5967.75
	Mean of Locations	1244.2	831.4	2032	3.64	3.034	3.568	4528.04	2521.41	7246.72
Mean of Specimens		1190	695.47	2529.3	3.7	3.01	3.46	4383.34	2080.97	8714.60

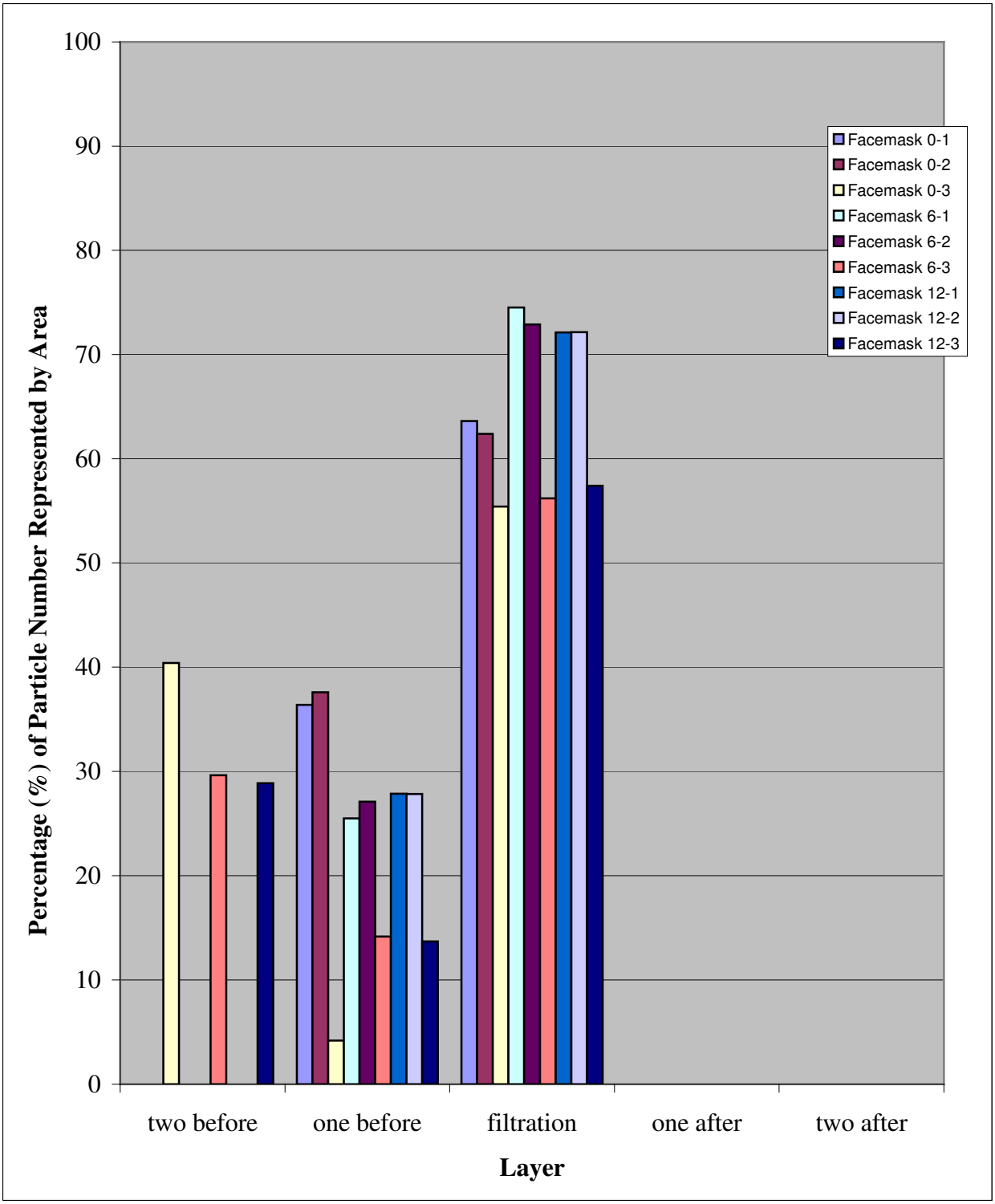

Figure 4.27 Comparison of small particle distribution on the filtration layer and other fabric layers within the face masks exposed to challenge solution

Table 4.28 Image analysis of the number (represented by total area) of small particles to which face masks were exposed

Variable		Number of Particle Spots	Mean Area of Particle Spots (Pixel^2)	Total Area (Pixel^2)
Specimen 1	**Location 1**	6798	2.61	17742.8
	Location 2	7364	2.63	19367.3
	Location 3	7319	2.6	19029.4
	Location 4	7438	2.65	19710.7
	Location 5	7376	2.71	19989
	Mean of Locations	7259	2.64	19167.8
Specimen 2	**Location 1**	7338	2.71	19886
	Location 2	6663	2.79	18589.8
	Location 3	6209	3.02	18751.2
	Location 4	5629	3.03	17055.9
	Location 5	5507	2.97	16355.8
	Mean of Locations	6269.2	2.9	18127.7
Specimen 3	**Location 1**	6786	2.78	18865.1
	Location 2	6052	3.03	18337.6
	Location 3	6745	2.85	19223.3
	Location 4	5799	3.02	17513
	Location 5	6444	2.78	17914.3
	Mean of Locations	6365.2	2.89	18370.6
Mean of Specimens		6631.13	2.81	18555.4

Table 4.29 The percentage of small particles captured by surface filtration

Face Mask	0-1	0-2	0-3	6-1	6-2	6-3	12-1	12-2	12-3
Percentage of Surface Filtration (%)	98.3	95	81.3	93.7	90.5	83.1	90.9	92.3	81.8

Statistical Analysis of the Impact of Repellent Finish on Filtration Ability of Face Masks

Three statistical assumptions were tested first before the One-Way ANOVA was applied. Since individual face masks were selected randomly from the nine independent face masks, the samples are independent. To test whether the samples are approximately normally distributed, Levene's Tests were performed for homogeneity on every layer of the face masks that actually showed presence of small particles. The results are summarized in Table 4.30 and the SAS programs and outputs are presented in the Appendix B. The following null hypothesis was tested:

Hypothesis 4: H_0: The samples are normally distributed and homogeneous.

The results show that the P values of hypothesis test 4 is greater than 0.01. Therefore, the hypothesis was not rejected and it was concluded that the samples are homogeneous and normally distributed.

To test whether the variances of the samples are equal, residues versus small particles on every layer of nine face masks that captured small particles were prepared and analyzed. The results are presented in Figures 4.28 - 4.30. Since all figures show that the residues distribute evenly along the zero axis, the variances of the samples are equal. Therefore, the One-Way ANOVA is appropriate for this study because the samples are independent, normally distributed and the variances of the samples are equal.

Table 4.30 Statistical results of Levene's test

P Value	Order 1		Order 2		Order 3	
	Small Particles on Cover Layers of Face Masks 0-1, 6-1 and 12-1	**Small Particles on Filtration Layers of Face Masks 0-1, 6-1 and 12-1**	**Small Particles on Cover Layers of Face Masks 0-2, 6-2 and 12-2**	**Small Particles on Filtration Layers of Face Masks 0-2, 6-2 and 12-2**	**Small Particles on Cover Layers of Face Masks 0-3, 6-3 and 12-3**	**Small Particles on Filtration Layers of Face Masks 0-3, 6-3 and 12-3**
Levene's Test	0.1977	0.1314	0.0359	0.31	0.0165	0.0247

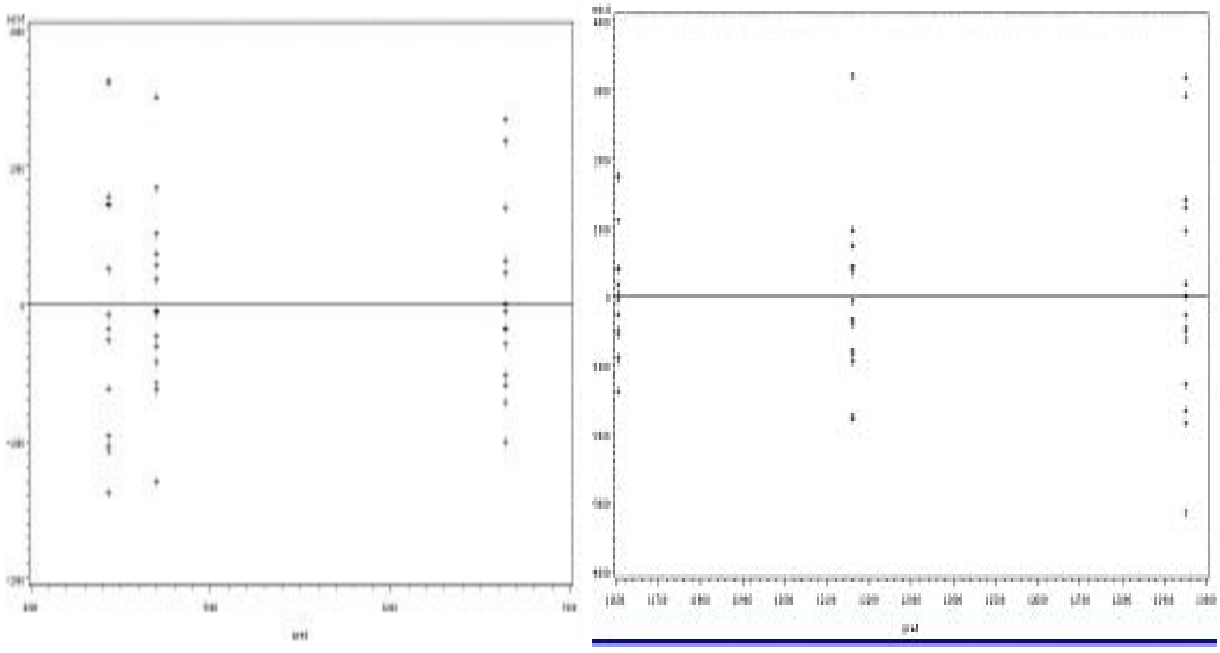

(a) (b)

Figure 4.28 Residues plot of face masks with layering order one; (a) cover layer and (b) filtration layer

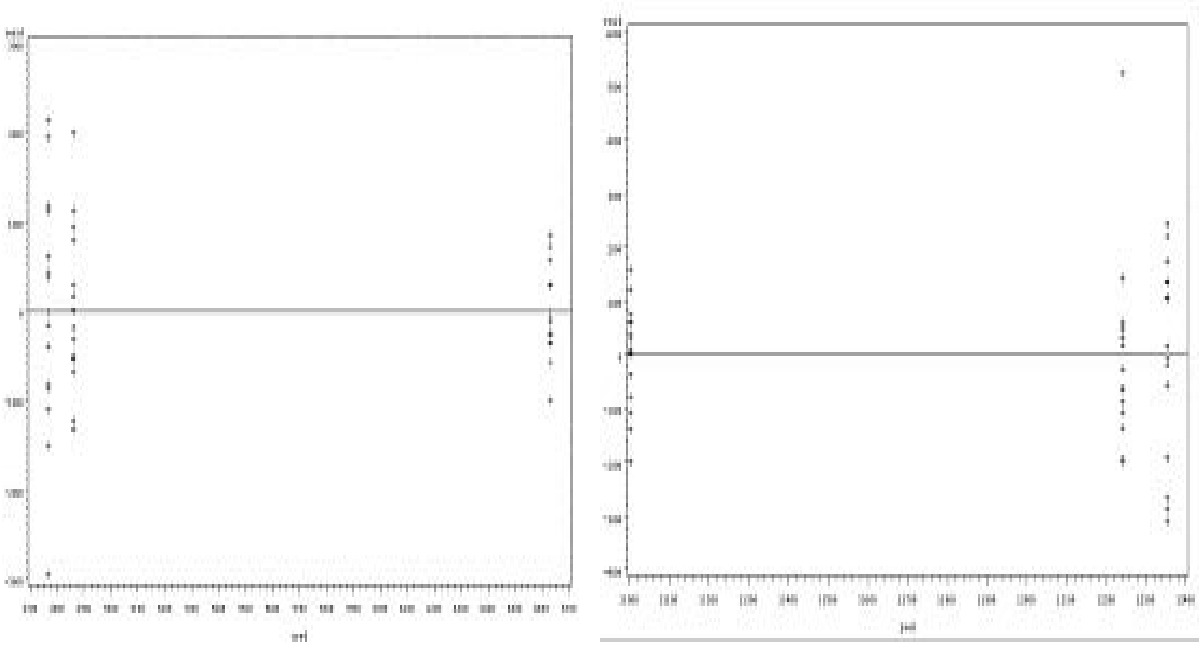

(a) (b)

Figure 4.29 Residues plot of face masks with layering order two; (a) cover layer, and (b) filtration layer

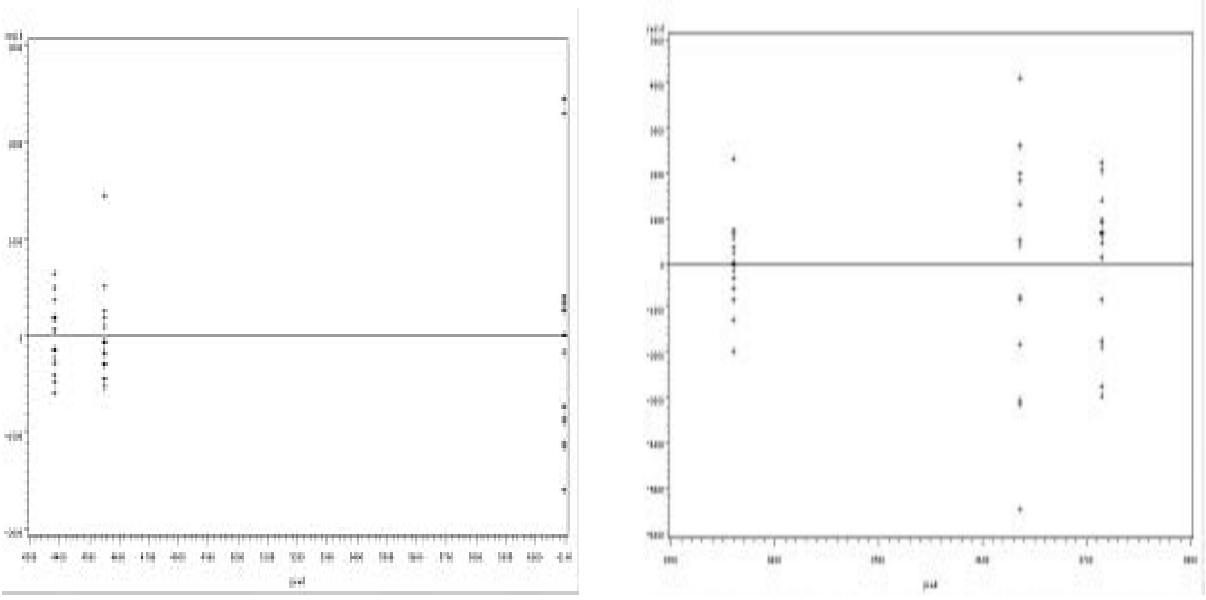

(a) (b)

Figure 4.30 Residues plot of face masks with layering order three; (a) cover layer, and (b) filtration layer

One-Way ANOVA SAS programs (Appendix B) were prepared and used to complete the analysis. Repellent finish was applied to the cover fabric to increase the fluid resistance of face mask. However, filtration ability of the cover fabric was studied to determine whether repellent finish affected this property. Table 4.31 shows that both cover fabric and filtration fabric capture small particles. Although repellent finish was only applied to the cover fabric, small particles had to penetrated the treated cover fabric before they were captured by the filtration layer. Therefore, the effect of repellent finish on the filtration ability of filtration layers of the nine simulated face masks were also studied. The statistical results are shown in Table 4.31. Null hypotheses were tested on small particles (represented by total area) captured by cover layers and filtration layers of simulated face masks with three layering orders:

Hypothesis 5: H_0: Repellent finished cover layers did not capture significantly fewer small particles than control cover layers in face masks with layering order one,

Hypothesis 6: H_0: There were no significant differences of small particles captured by the cover layers of face masks with layering order one between finish add-on levels 6% and 12%.

The results show that the P value of the hypothesis test 5 is smaller than 0.0001. Therefore, the hypothesis 5 was rejected and it was concluded that repellent finished cover layers captured significant fewer small particles than control cover layers in face masks with layering order one. The P value of the hypothesis test 6 is 0.3454. Therefore, the hypothesis 6 was not rejected and it was concluded that there were no significant differences of small particles captured by the cover layers of face masks with layering order one between finish add-on levels 6% and 12%.

Hypothesis 7: H_0: There were no significant differences of small particle captured by the filtration layers of face masks with layering order one when the cover layers were finished with add-on levels 0% and 6%, 12%,

Hypothesis 8: H_0: There were no significant differences of small particle captured by the filtration layers of face masks with layering order one when the cover layers were finished with add-on levels 6% and 12%.

The results show that the P value of the hypothesis test 7 is 0.0317 and the P value of the hypothesis test 8 is 0.1166. Therefore, both hypotheses were not rejected and it was concluded that the repellent finish did not influence the filtration ability of the filtration layer of face masks with layering order one when the cover layers were finished with all three add-on levels.

Table 4.31 Statistical results of one-way ANOVA analysis

	Order 1		**Order 2**		**Order 3**	
P Value	**Small Particles on Cover Layers of Face Masks 0-1, 6-1 and 12-1**	**Small Particles on Filtration Layers of Face Masks 0-1, 6-1 and 12-1**	**Small Particles on Cover Layers of Face Masks 0-2, 6-2 and 12-2**	**Small Particles on Filtration Layers of Face Masks 0-2, 6-2 and 12-2**	**Small Particles on Cover Layers of Face Masks 0-3, 6-3 and 12-3**	**Small Particles on Filtration Layers of Face Masks 0-3, 6-3 and 12-3**
Effect of Finish	<0.0001	0.0317	<0.0001	0.0433	<0.0001	0.8579
Contrast Finish 2 VS 3	0.3454	0.1166	0.7975	0.8468	0.5484	0.9071

Hypothesis 9: H_0: Repellent finished cover layers did not capture significantly fewer small particles than control cover layers in face masks with layering order two,

Hypothesis 10: H_0: There were no significant differences of small particle captured by the cover layers of face masks with layering order two between finish add-on levels 6% and 12%.

The results show that the P value of the hypothesis test 9 is smaller than 0.0001. Therefore, the hypothesis 9 was rejected and it was concluded that repellent finished cover layers captured significant fewer small particles than control cover layers in face masks with layering order two. The P value of the hypothesis test 10 is 0.7975. Therefore, the hypothesis 10 was not rejected and it was concluded there were no significant differences of small particle captured by the cover layers of face masks with layering order two between finish add-on levels 6% and 12%.

Hypothesis 11: H_0: There were no significant differences of small particle captured by the filtration layers of face masks with layering order two when the cover layers were finished with add-on levels 0% and 6%, 12%,

Hypothesis 12: H_0: There were no significant differences of small particle captured by the filtration layers of face masks with layering order two when the cover layers were finished with add-on levels 6% and 12%.

The results show that the P value of the hypothesis test 11 is 0.0433 and the P value of the hypothesis test 12 is 0.8468. Therefore, both hypotheses were not rejected and it was concluded that the repellent finish did not influence the filtration ability of the filtration layer of face masks with layering order two when the cover layers were finished with all three add-on levels.

Hypothesis 13: H_0: Repellent finished cover layers did not capture significantly fewer small particles than control cover layers in face masks with layering order three,

Hypothesis 14: H_0: There were no significant differences of small particle captured by the cover layers of face masks with layering order three between finish add-on levels 6% and 12%.

The results show that the P value of the hypothesis test 13 is smaller than 0.0001. Therefore, the hypothesis 13 was rejected and it was concluded that repellent finished cover layers captured significant fewer small particles than control cover layers in face masks with layering order three. The P value of the hypothesis test 14 is 0.5484. Therefore, the hypothesis 14 was not rejected and it was concluded that there were no significant differences of small particle captured by the cover layers of face masks with layering order three between finish add-on levels 6% and 12%.

Hypothesis 15: H_0: There were no significant differences of small particle captured by the filtration layers of face masks with layering order three when the cover layers were finished with add-on levels 0% and 6%, 12%,

Hypothesis 16: H_0: There were no significant differences of small particle captured by the filtration layers of face masks with layering order three when the cover layers were finished with add-on levels 6% and 12%.

The results show that the P value of the hypothesis test 15 is 0.8579 and the P value of the hypothesis test 16 is 0.9071. Therefore, both hypotheses were not rejected and it was concluded that the repellent finish did not influence the filtration ability of the filtration layer of face masks with layering order three when the cover layers were finished with all three add-on levels.

In summary, repellent finished cover layers captured significantly fewer small particles than control cover layers in face masks with all three layering orders. However, there were no significant differences of small particle captured by the finished cover layers of face masks between add-on levels 6% and 12%. Cover layer is the fabric comes in direct contact with the fluid, therefore the filtration mechanism, interception, predominates the particle capture of the

fabric. Interception involves a particle following a stream and then being captured if this results in it coming into contact with the fiber. Therefore, the stream determines the interception of particles greatly. Repellent finished cover fabrics provide significantly better ability to resist the fluid than the control fabrics, therefore less fluid can wet out the fabric. As a result, fewer particles are intercepted by the fabric. However, compared with 6% add-on level, 12% add-on level does not increase the fabric's ability to resist fluid significantly, therefore there were no significant differences of small particle captured by the finished cover layers of face masks between add-on levels 6% and 12%.

Repellent finish on the cover fabric did not influence the filtration ability of the filtration layer within the face mask. Of the layers within the face mask, the filtration layer is the primary contributor to the filtration ability of the face mask. The filtration layer captures particles by combined capture mechanisms including interception, inertial impaction, diffusion and gravity. Because the filtration layer does not contact the fluid directly, interception is not the primary particle capture mechanism. Most of particles are captured by inertial impaction, diffusion and gravity. Although fewer particles are intercepted by the filtration layer, the change is not significant. Therefore, repellent finish on the cover fabric did not influence the filtration ability of the filtration layer within the face mask significantly.

LSCM Cross Sectional Examination

To study the effect of layering order on the filtration ability of the entire face mask, the transmission of small particles through the face mask as a whole is as necessary. However, LSCM surface examination did not provide appropriate information for this component of the

study. Therefore, LSCM cross sectional examination was used to study the impact of layering order on filtration ability.

LSCM cross sectional examination was first used to observe the cross sections of all control face masks. The cross section of each face mask was prepared and then observed using LSCM. Then all face masks were exposed to the challenge aerosol using the modified Standard Test Method ASTM F2101-01. Results are presented in Figures 4.31 - 4.48. In these color micrographs*, the microspheres are represented by red and the fabrics are represented by shades of gray in color.

Figures 4.31, 4.33, 4.35, 4.37, 4.39, 4.41, 4.43, 4.45 and 4.47 show the cross sections of nine simulated face masks. In these figures, the layered fabric orders are clearly shown. Each of the face masks has a relatively flat layered structure and pockets of air are found between each layer. Face masks 0-1, 6-1 and 12-1 have three layers and all other face masks have four layers. When all of these images are evaluated, it is apparent that the cross sections of the face masks are clearly identified by detector one while nothing is identified by detector two and the merged images are the same as the image obtained by detector one only. This was expected as control face masks were examined.

Figures 4.32, 4.34, 4.36, 4.38, 4.40, 4.42, 4.44, 4.46 and 4.48 show the cross sections of nine face masks after exposure to the challenge aerosol using the modified ASTM F 2101. Figures 4.32, 4.34 and 4.36 show those face masks with varying layering orders and no repellent finish. Figure 4.32 shows that for face mask 0-1, small particles have penetrated through the first layer, the cover layer. Although small particles have penetrated into the second layer, the filtration layer, they have not penetrated through this layer and have not reached the third layer, the shell layer. Therefore, the filtration layer stopped the penetration of small particles.

Figure 4.34 shows that for face mask 0-2, small particles have penetrated through the first layer, the cover layer. Although small particles have penetrated into the second layer, the filtration layer, they have not penetrated through this layer and have not reached the third layer, the support layer or the fourth layer, the shell layer. Therefore, the filtration layer stopped the penetration of small particles.

Figure 4.36 shows that for face mask 0-3, small particles have penetrated through the first layer, the cover layer, and the second layer, the support layer. Although small particles have penetrated into the third layer, the filtration layer, they have not penetrated through this layer and have not reached the fourth layer, the shell layer. Therefore, the filtration layer stopped the penetration of small particles.

Figures 4.38, 4.40 and 4.42 show those face masks with varying layering orders and 6% add-on level of repellent finish. Figure 4.38 shows that for face mask 6-1, small particles have penetrated through the first layer, the cover layer. Although small particles have penetrated into the second layer, the filtration layer, they have not penetrated through this layer and have not reached the third layer, the shell layer. Therefore, the filtration layer stopped the penetration of small particles.

Figure 4.40 shows that for face mask 6-2, small particles have penetrated through the first layer, the cover layer. Although small particles have penetrated into the second layer, the filtration layer, they have not penetrated through this layer and have not reached the third layer, the support layer or the fourth layer, the shell layer. Therefore, the filtration layer stopped the penetration of small particles.

Figure 4.42 shows that face mask 6-3, small particles have penetrated through the first layer, the cover layer, and the second layer, the support layer. Although small particles have

penetrated into the third layer, the filtration layer, they have not penetrated through this layer and have not reached the fourth layer, the shell layer. Therefore, the filtration layer stopped the penetration of small particles.

Figures 4.44, 4.46 and 4.48 show those face masks with varying layering orders and 12% add-on level of repellent finish. Figure 4.44 shows that for face mask 12-1, small particles have penetrated through the first layer, the cover layer. Although small particles have penetrated into the second layer, the filtration layer, they have not penetrated through this layer and have not reached the third layer, the shell layer. Therefore, the filtration layer stopped the penetration of small particles.

Figure 4.46 shows that for face mask 12-2, small particles have penetrated through the first layer, the cover layer. Although small particles have penetrated into the second layer, the filtration layer, they have not penetrated through this layer and have not reached the third layer, the support layer or the fourth layer, the shell layer. Therefore, the filtration layer stopped the penetration of small particles.

Figure 4.48 shows that for face mask 12-3, small particles have penetrated through the first layer, the cover layer, and the second layer, the support layer. Although small particles have penetrated into the third layer, the filtration layer, they have not penetrated through this layer and have not reached the fourth layer, the shell layer. Therefore, the filtration layer stopped the penetration of small particles.

In each of these nine face masks examined, the filtration layer stopped the penetration of small particles through face masks no matter whether the filtration is the second layer of a three-layer face mask or the second layer of a four-layer face mask or the third layer of a four-layer

face mask. In summary, although its location changed in the three layering orders, the filtration layer always stopped the penetration of small particles.

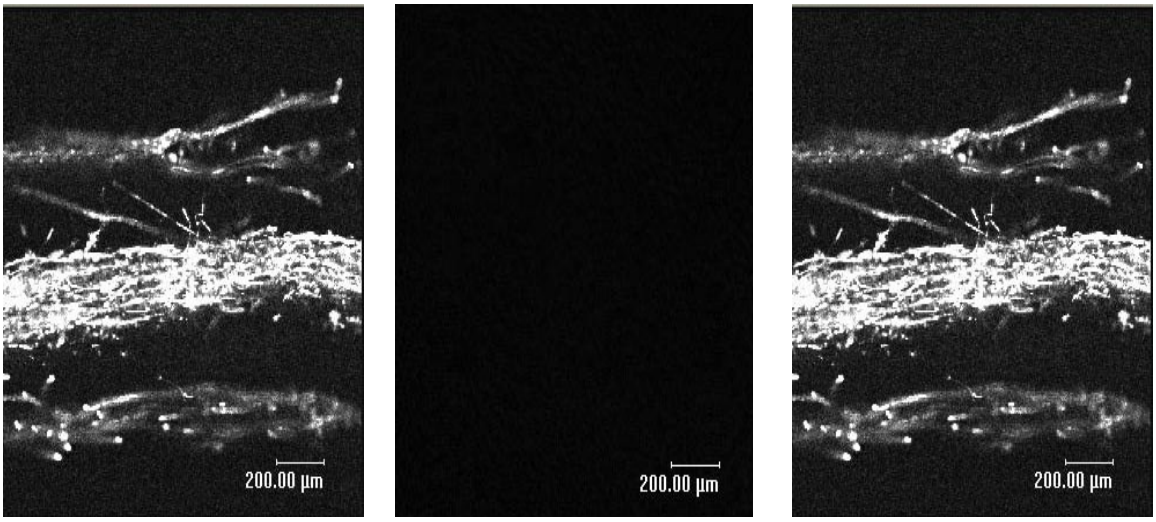

(a) (b) (c)

Figure 4.31 LSCM cross sectional image of control face mask 0-1; (a) image obtained by PMT one, (b) image obtained by PMT two, and (c) merged image

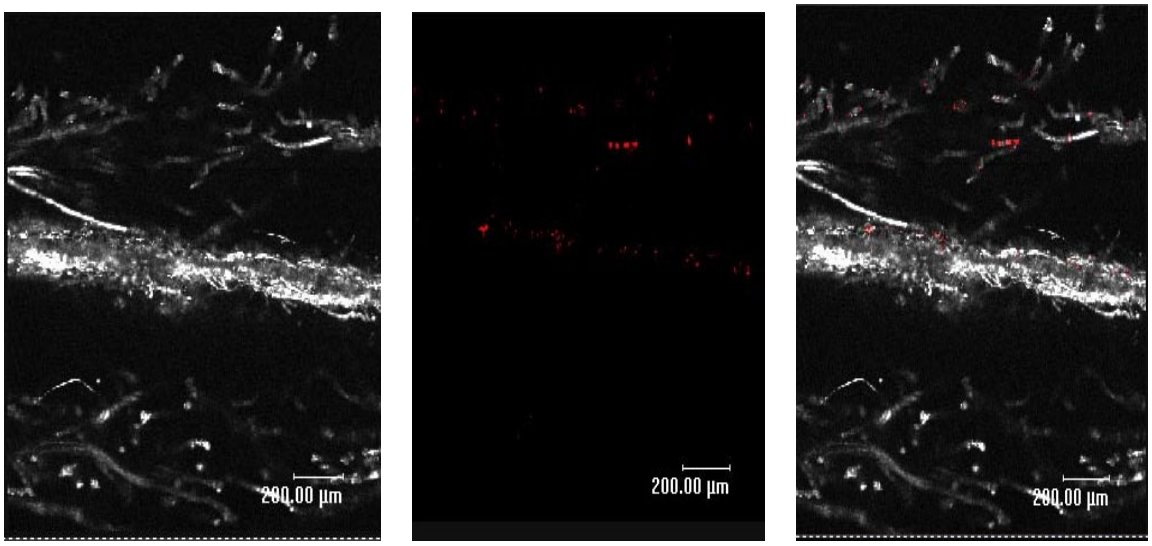

(a) (b) (c)

Figure 4.32 LSCM cross sectional image of face mask 0-1 exposed to challenge aerosol using modified ASTM F 2101; (a) image obtained by PMT one, (b) image obtained by PMT two, and (c) merged image

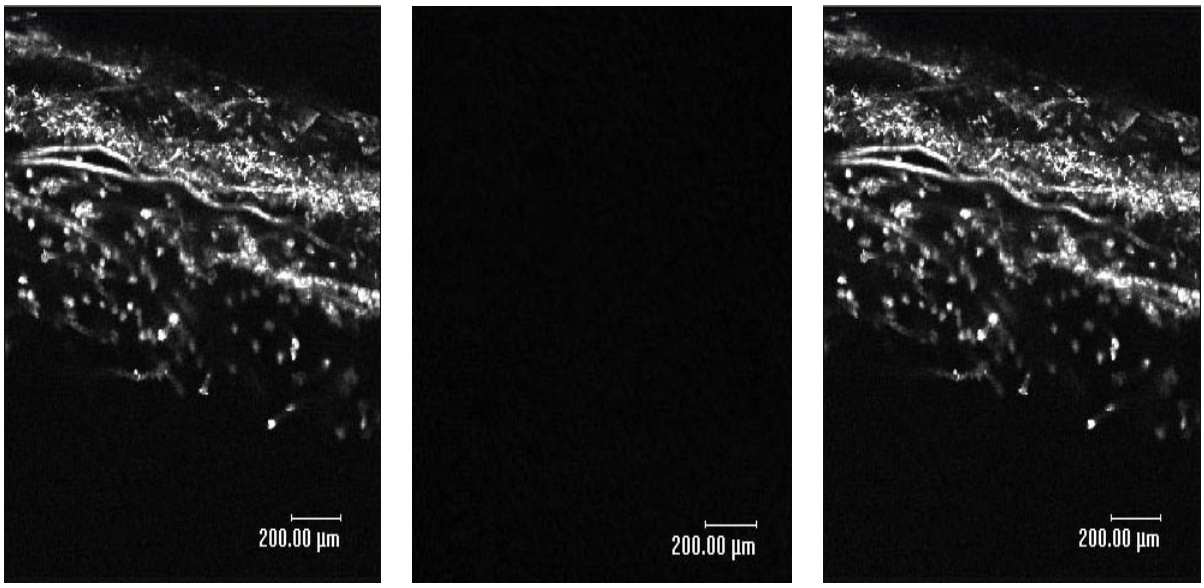

(a) (b) (c)

Figure 4.33 LSCM cross sectional image of control face mask 0-2; (a) image obtained by PMT one, (b) image obtained by PMT two, and (c) merged image

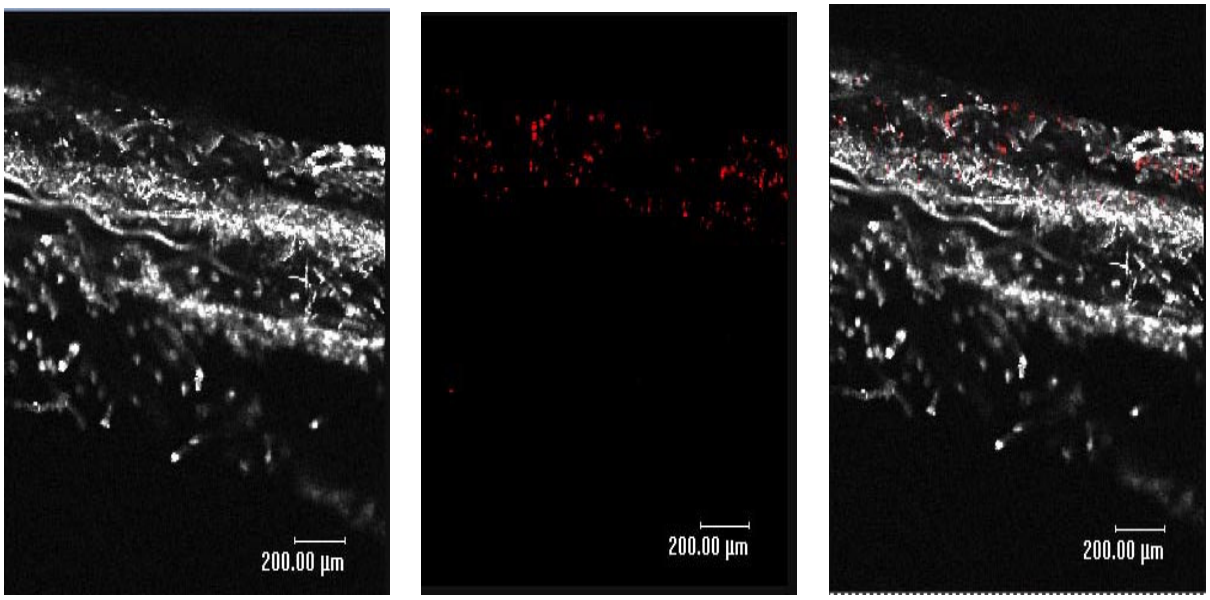

(a) (b) (c)

Figure 4.34 LSCM cross sectional image of face mask 0-2 exposed to challenge aerosol using modified ASTM F 2101; (a) image obtained by PMT one, (b) image obtained by PMT two, and (c) merged image

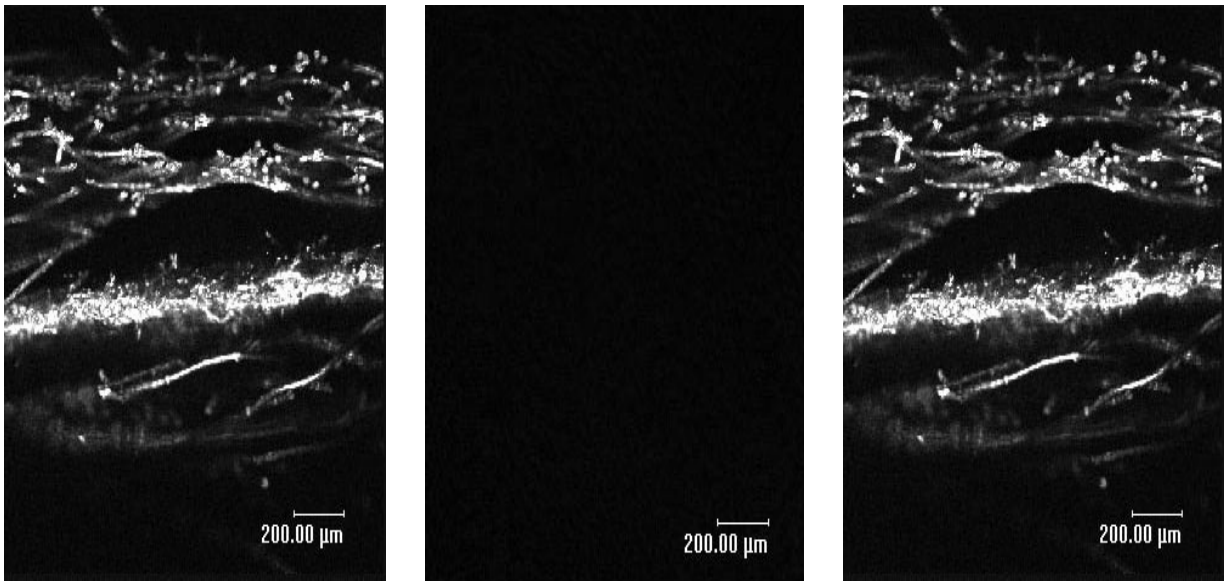

(a) (b) (c)

Figure 4.35 LSCM cross sectional image of control face mask 0-3; (a) image obtained by PMT one, (b) image obtained by PMT two, and (c) merged image

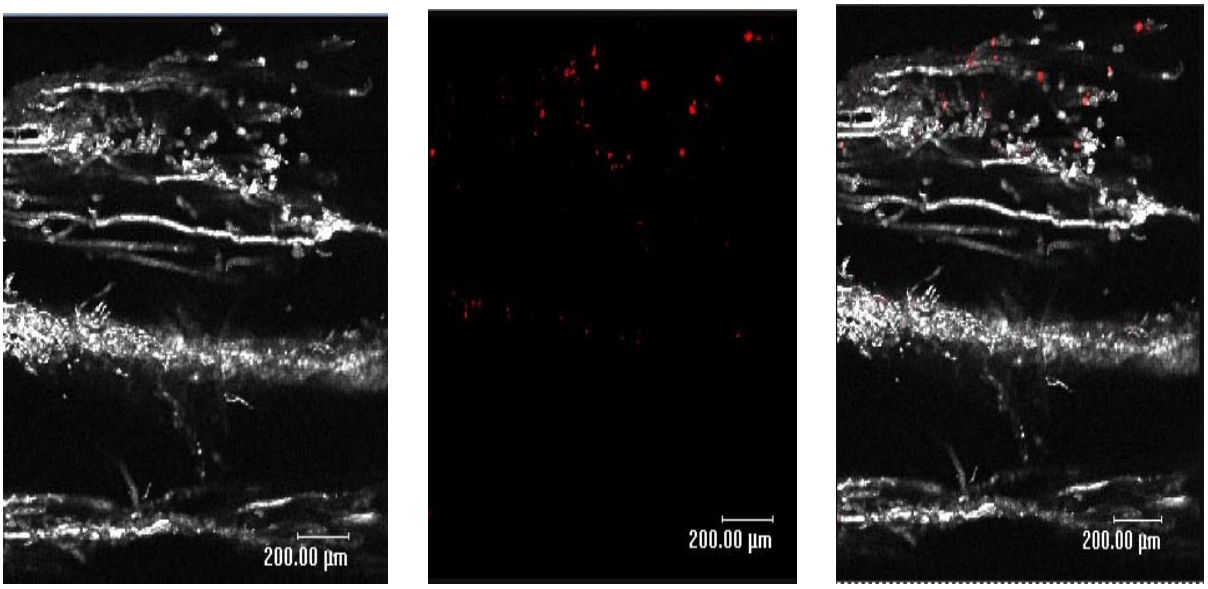

(a) (b) (c)

Figure 4.36 LSCM cross sectional image of face mask 0-3 exposed to challenge aerosol using modified ASTM F 2101; (a) image obtained by PMT one, (b) image obtained by PMT two, and (c) merged image

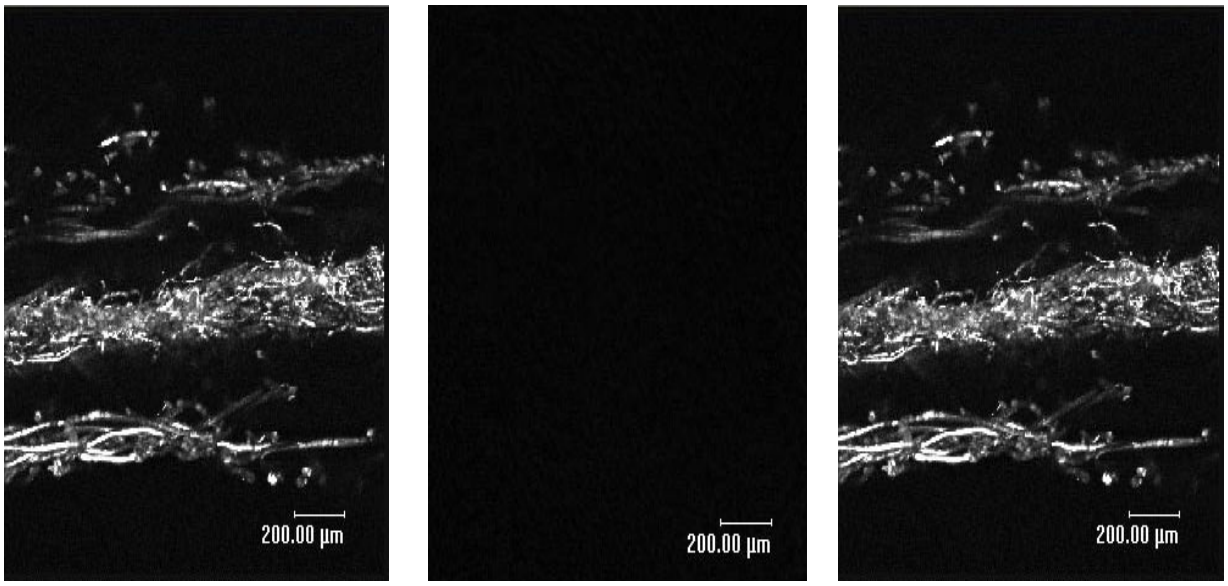

(a) (b) (c)

Figure 4.37 LSCM cross sectional image of control face mask 6-1; (a) image obtained by PMT one, (b) image obtained by PMT two, and (c) merged image

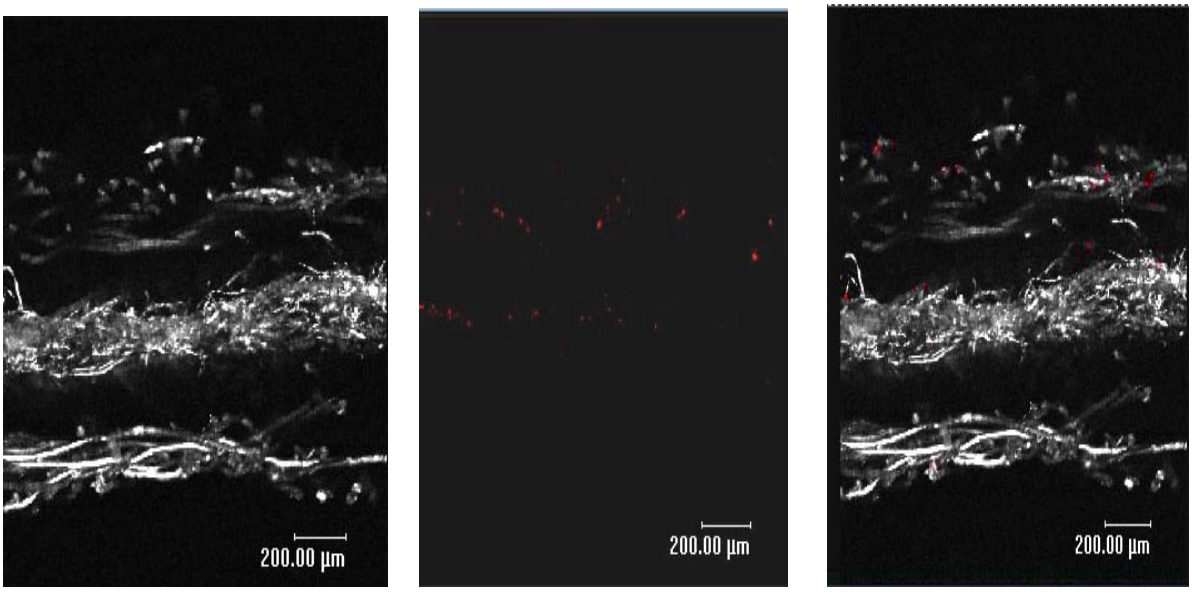

(a) (b) (c)

Figure 4.38 LSCM cross sectional image of face mask 6-1 exposed to challenge aerosol using modified ASTM F 2101; (a) image obtained by PMT one, (b) image obtained by PMT two, and (c) merged image

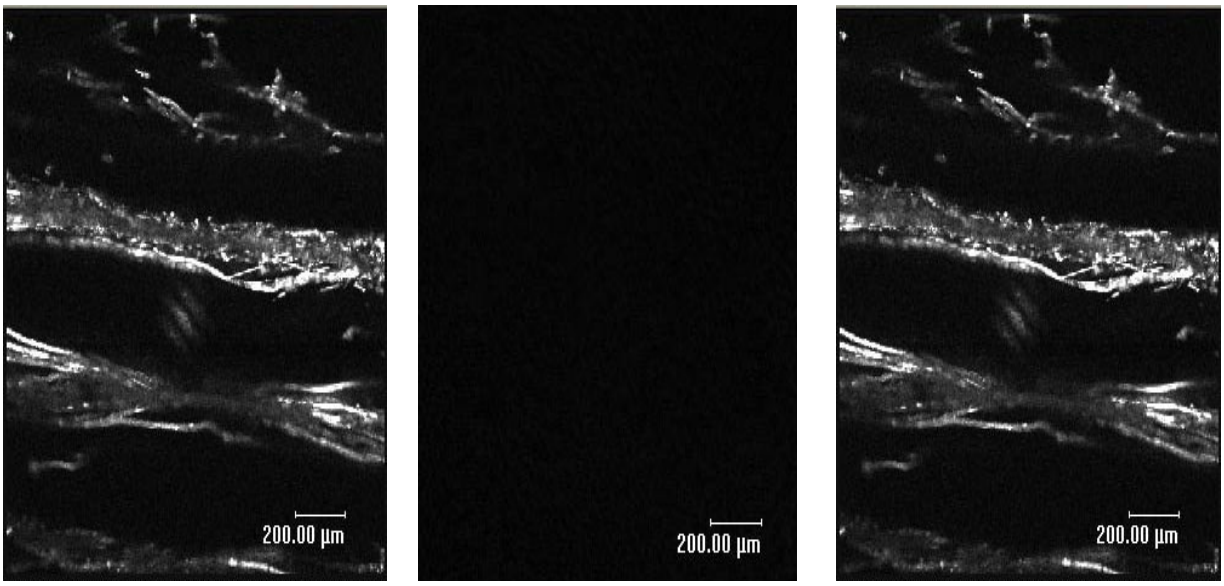

(a) (b) (c)

Figure 4.39 LSCM cross sectional image of control face mask 6-2; (a) image obtained by PMT one, (b) image obtained by PMT two, and (c) merged image

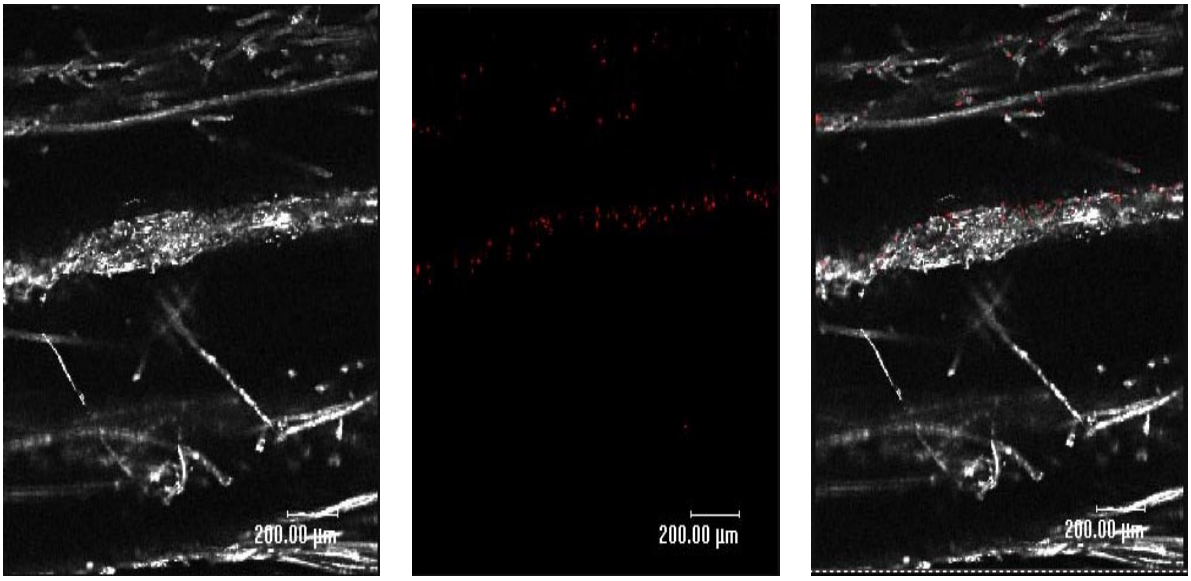

(a) (b) (c)

Figure 4.40 LSCM cross sectional image of face mask 6-2 exposed to challenge aerosol using modified ASTM F 2101; (a) image obtained by PMT one, (b) image obtained by PMT two, and (c) merged image

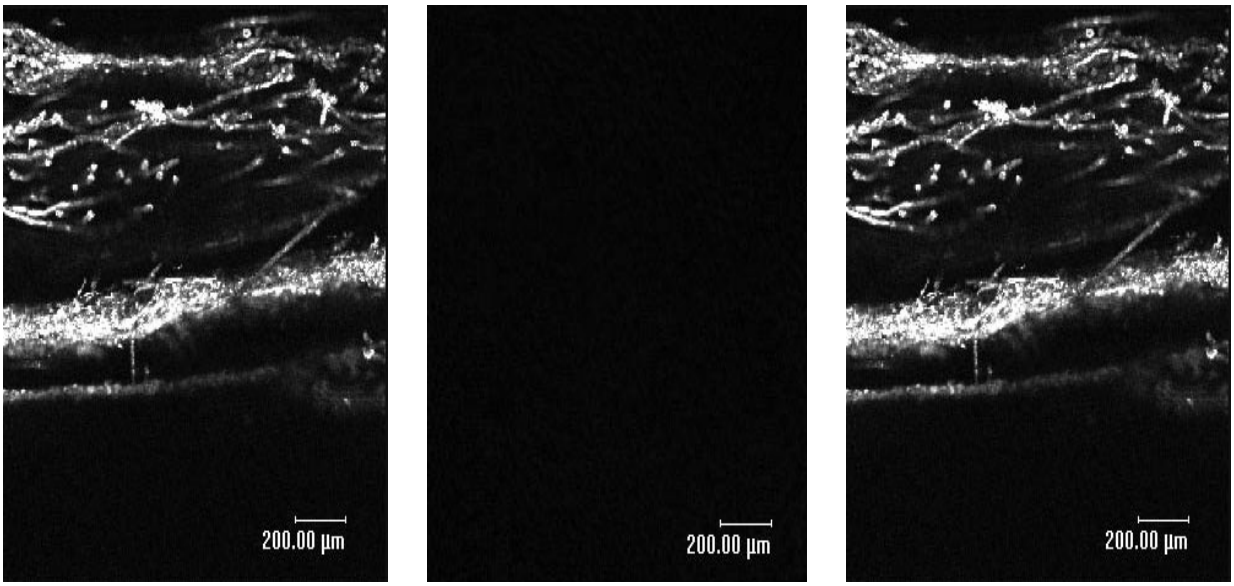

(a) (b) (c)

Figure 4.41 LSCM cross sectional image of control face mask 6-3; (a) image obtained by PMT one, (b) image obtained by PMT two, and (c) merged image

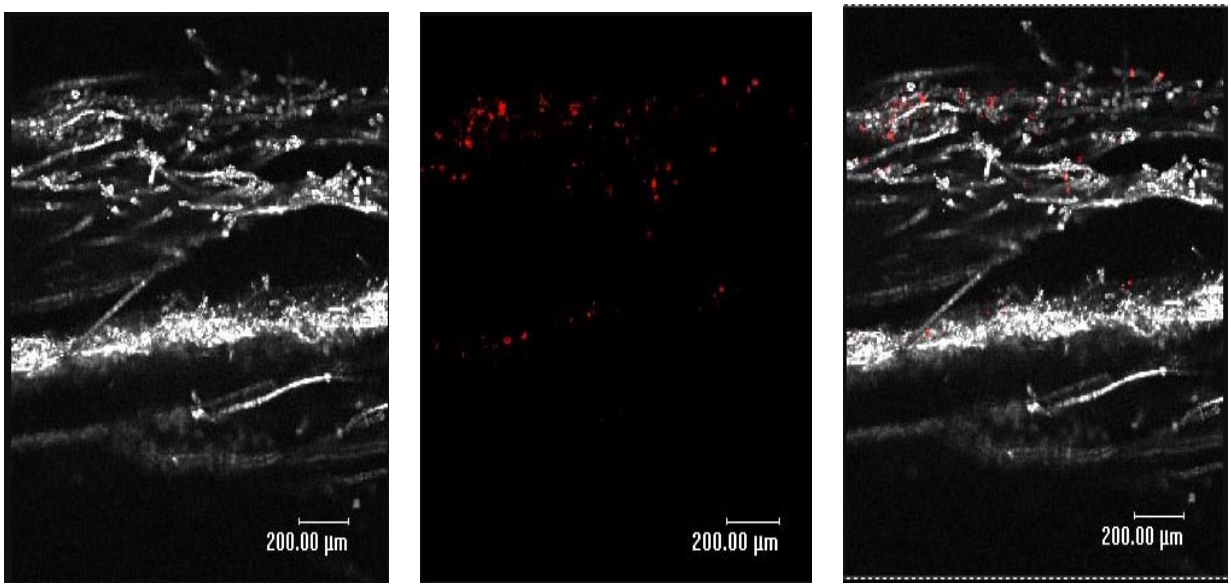

(a) (b) (c)

Figure 4.42 LSCM cross sectional image of face mask 6-3 exposed to challenge aerosol using modified ASTM F 2101; (a) image obtained by PMT one, (b) image obtained by PMT two, and (c) merged image

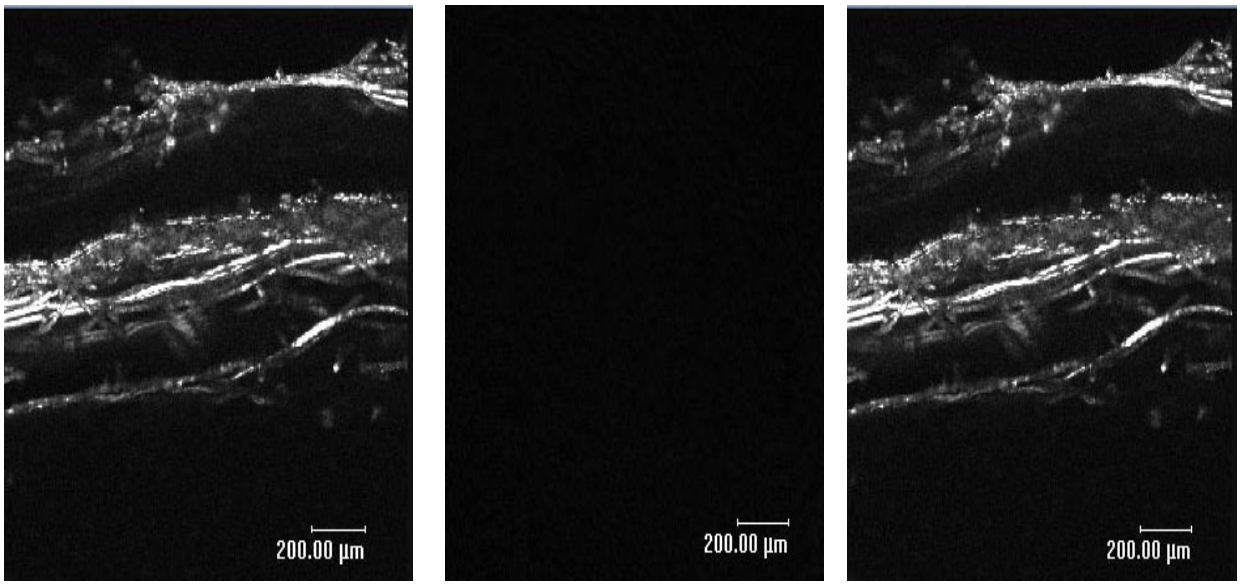

(a) (b) (c)

Figure 4.43 LSCM cross sectional image of control face mask 12-1; (a) image obtained by PMT one, (b) image obtained by PMT two, and (c) merged image

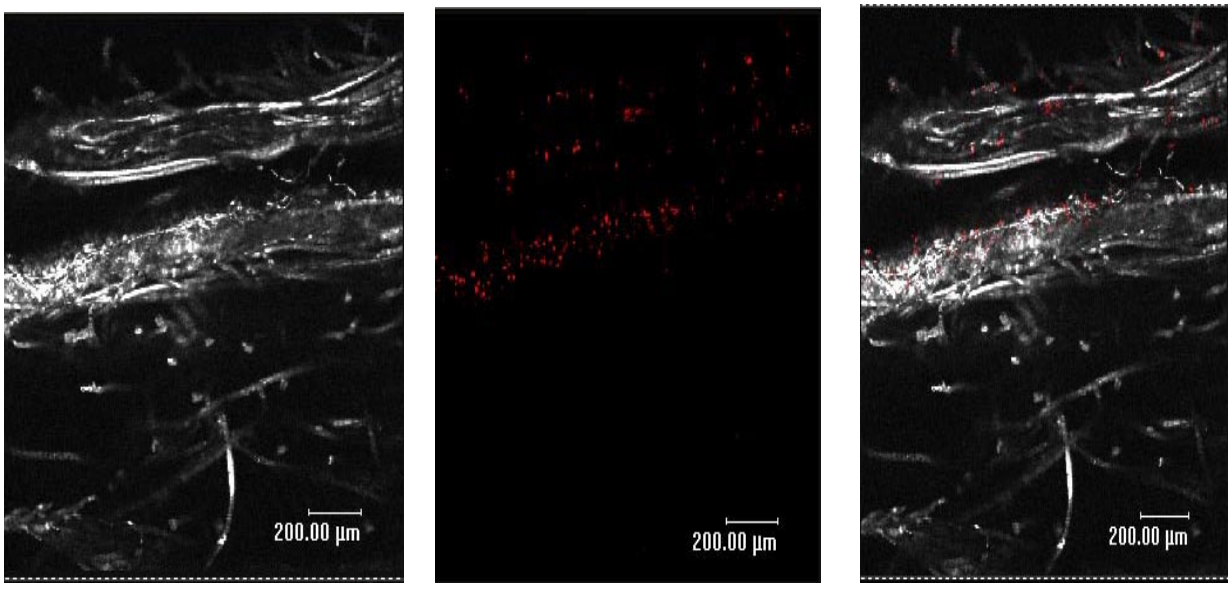

(a) (b) (c)

Figure 4.44 LSCM cross sectional image of face mask 12-1 exposed to challenge aerosol using modified ASTM F 2101; (a) image obtained by PMT one, (b) image obtained by PMT two, and (c) merged image

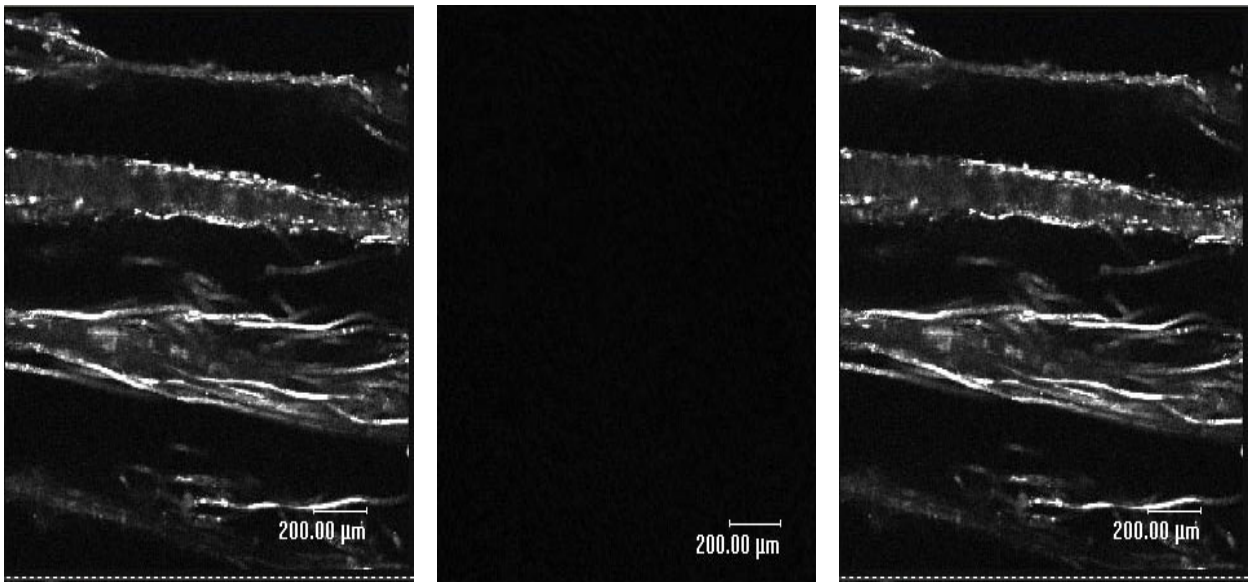

(a) (b) (c)

Figure 4.45 LSCM cross sectional image of control face mask 12-2; (a) image obtained by PMT one, (b) image obtained by PMT two, and (c) merged image

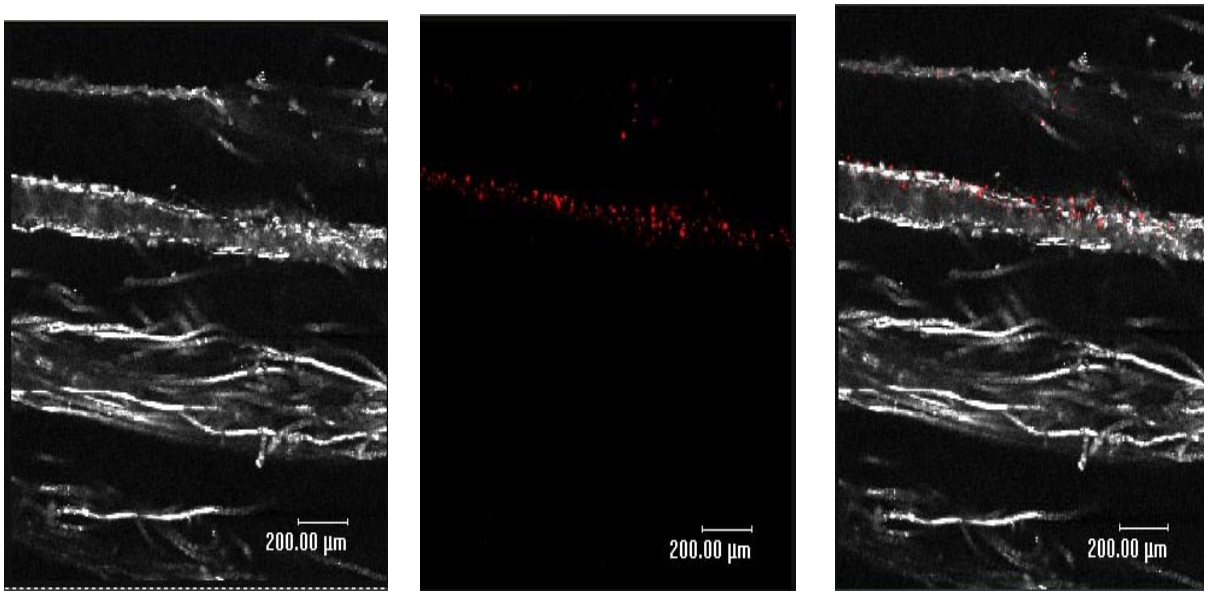

(a) (b) (c)

Figure 4.46 LSCM cross sectional image of face mask 12-2 exposed to challenge aerosol using modified ASTM F 2101; (a) image obtained by PMT one, (b) image obtained by PMT two, and (c) merged image

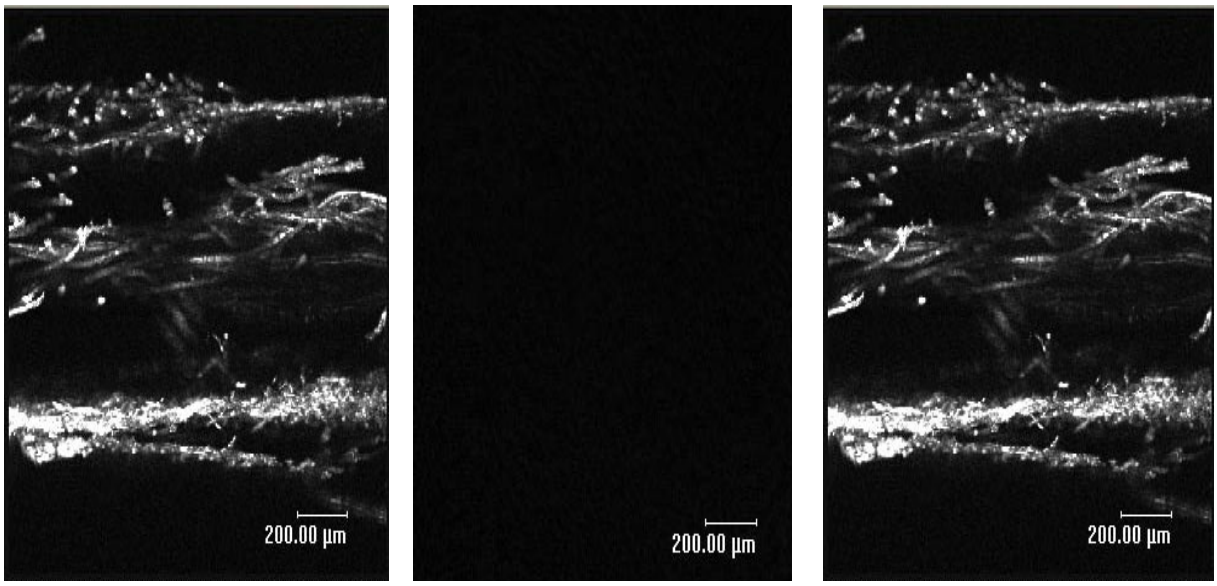

(a) (b) (c)

Figure 4.47 LSCM cross sectional image of control face mask 12-3; (a) image obtained by PMT one, (b) image obtained by PMT two, and (c) merged image

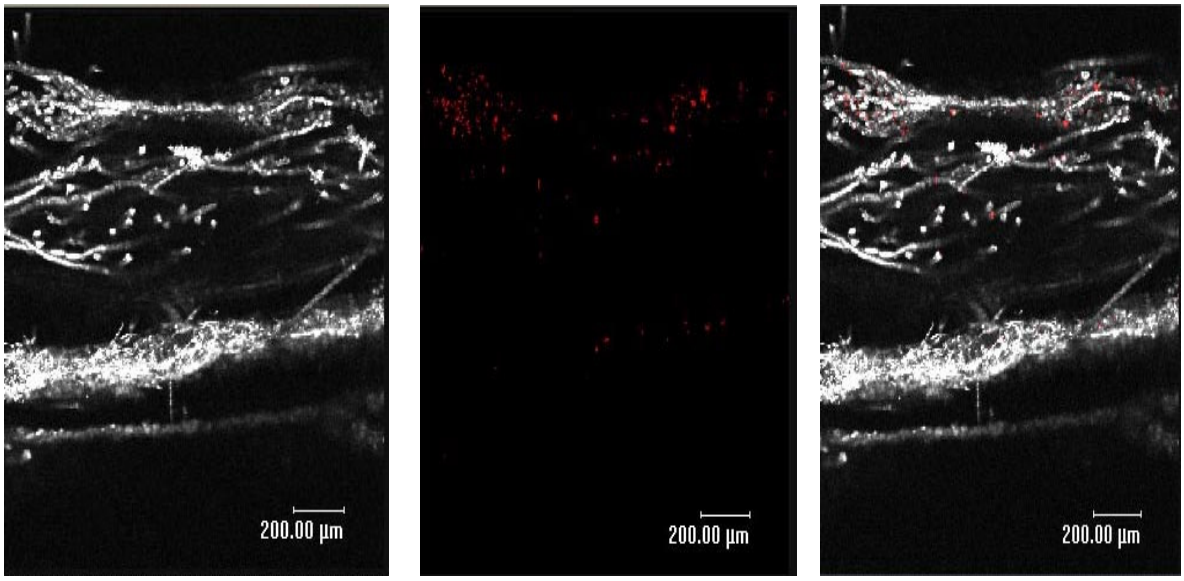

(a) (b) (c)

Figure 4.48 LSCM cross sectional image of face mask 12-3 exposed to challenge aerosol using modified ASTM F 2101; (a) image obtained by PMT one, (b) image obtained by PMT two, and (c) merged image

Evaluation of Differential Pressure of Simulated Face Masks

Differential Pressures of the nine simulated face masks were determined at Nelson Laboratory, Salt Lake City, Utah and the results are presented in Table 4.32. To study the impacts of repellent finish and layering order on differential pressure of face masks, Shapiro-Wilk (Appendix C) was first performed to test whether the differential pressures of the samples are approximately normally distributed. Since the results show that the p-value is 0.0035, the hypothesis that the differential pressures of the samples are normally distributed was rejected. Therefore, Nonparametric Two-way ANOVA tests (Appendix C) were performed and the following hypotheses were tested:

Hypothesis 17: H_0: There were no significant differences of differential pressures of face masks when the cover fabrics were finished with add-on levels 0%, 6% and 12%.

The results show that the P value of the hypothesis test 17 is 0.3518. Therefore, the hypothesis 17 was not rejected and it was concluded that the repellent finish on the cover fabric did not influence the differential pressure of the face mask. Actually repellent finish affects neither the structure of the face mask nor the airflow, therefore the breathability of the face mask will not change due to the repellent finish.

Hypothesis 18: H_0: There were no significant differences of differential pressures of face masks among three different layering orders.

The results show that the P value of the hypothesis test 18 is smaller than 0.0002. Therefore, the hypothesis 18 was rejected and it was concluded that the layering order affected the differential pressure of the face mask significantly. The bar chart in Figure 4.49 shows the differences between these layering order levels. It is obvious that face masks with layering order one provide lower differential pressures, however there are no significant differences of

differential pressures between face masks with layering orders two and three. Compared with the face masks with layering order two and three, there is no support layer in the face masks with layering order one. Therefore, face masks with layering order one provide less ability to resist airflow and offer better breathability. Although fabric arrangement changes in layering orders two and three, the layer numbers are the same. Therefore, face masks with layering order two provide the same breathability as face masks with layering order three.

In summary, the repellent finish did not affect the breathing resistance of the face masks while the layering order influenced the breathing resistance significantly. Face masks with layering order one (cover fabric, filtration fabric and then shell fabric) provide better breathability than the face masks with the other two layering orders. However, according to the ASTM F 2100 Standard Specification for Performance of Materials Used in Medical Face Masks [55], the breathing resistance of an acceptable face mask should be lower than 4.0 mmH_2O/cm^2. Therefore, although face masks with layering order one provide better breathability, all three layering order can offer acceptable breathability.

Table 4.32 Differential pressures of face masks

Face Mask		**0-1**	**0-2**	**0-3**	**6-1**	**6-2**	**6-3**	**12-1**	**12-2**	**12-3**
Differential Pressure (mmH_2O/cm^2)	**Replication 1**	1.9	2.4	2.3	2.0	2.1	2.3	2.1	2.4	2.3
	Replication 2	2.1	2.3	2.3	2.1	2.3	2.3	2.1	2.3	2.3

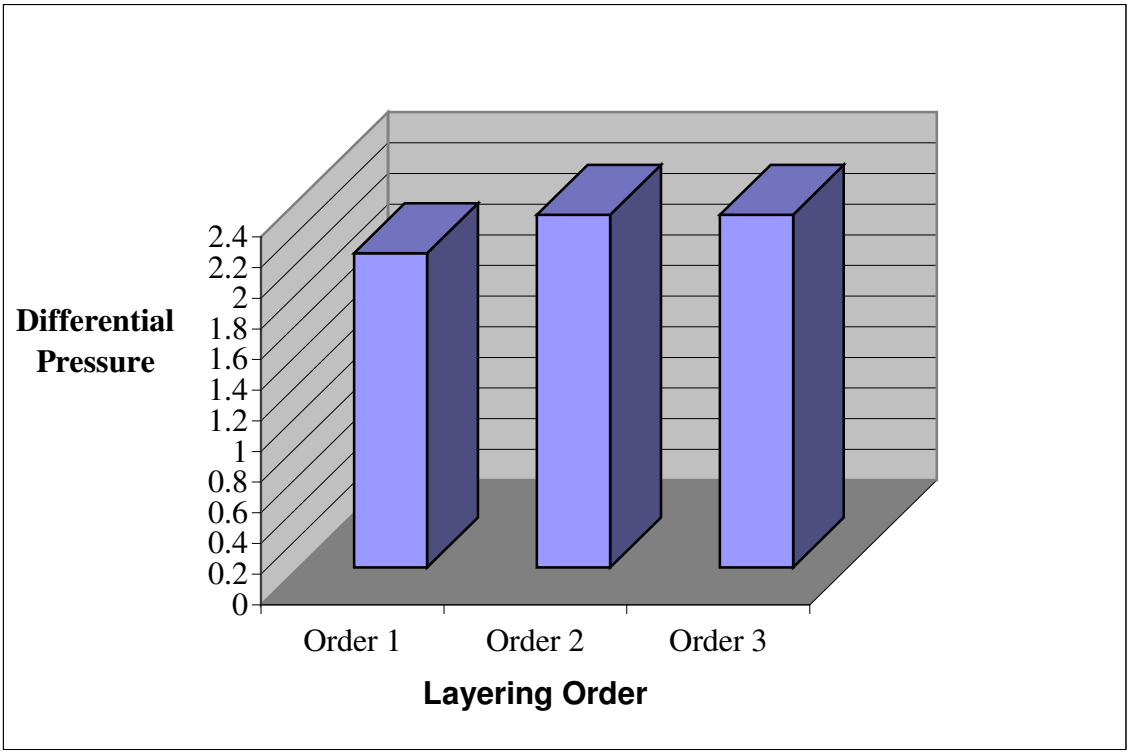

Figure 4.49 Impact of layering order on differential pressures of face masks

CHAPTER 5

CONCLUSIONS AND FUTURE WORK

The primary objective of this dissertation is to study the effects of repellent finish and layering order on fluid resistance, filtration ability and differential pressure of surgical face masks. To carry out this research, four nonwoven fabrics were selected as a cover fabric, a filtration fabric, a support fabric and a shell fabric. Three levels of repellent finish, 0%, 6% and 12%, were applied to the cover fabric. Then the nonwoven fabrics were ordered to simulate face masks according to three different layering orders. Fluid resistance and differential pressure of those face masks were evaluated. In determining the filtration ability of face masks, techniques using LSCM were used to determine particle capture. Small particles present on/in nonwoven fabrics were located using LSCM to determine that the particles were captured. Then, image analysis was used to quantify the small particles by total area to evaluate the filtration ability. Finally, statistical analysis was performed to analyze the impacts of repellent finish and layering order on these performances.

Repellent finish, fluid pressure and layering order all affected fluid resistance of the face masks significantly. The fluid resistance of face masks increased with increasing add-on level of repellent finish. The higher the add-on level of repellent finished cover fabric, the better the fluid resistance of the face mask. In this study, when the cover fabrics were finished with 12% add-on level, the face masks provided the maximum fluid resistance. The fluid resistance of face masks decreased with increasing fluid pressure. Therefore, face masks provided the minimum fluid resistance at the pressure of 160 mmHg among those three pressures identified in ASTM F 1862.

The face masks with layering order of cover fabric, support fabric, filtration fabric and shell fabric provided the best fluid resistance and the face masks with layering order of cover fabric, filtration fabric and shell fabric provided the lowest fluid resistance. A statistical model, ln (P/Q) = 18.6602 + 0.9267 Finish – 0.1959 Pressure + 4.1486 (Order 2 –Order 1) + 13.1485 (Order 3 – Order 1), was developed and used to describe the relationship between these parameters qualitatively as well as quantitatively. This model can also be used to predict the fluid resistance of any face mask with specific parameters and the optimum parameters.

Filtration abilities of both entire face masks and different layers of face masks were studied. First, the face mask was exposed to a challenge aerosol containing latex microspheres using the modified Standard Test Method ASTM F2101-01, Standard Test Method for Evaluating the Bacterial Filtration Efficiency (BFE) of Medical Face Mask, Using a Biological Aerosol of Staphylococcus aureus. To locate the small particles on/in nonwoven fabrics, two detectors were used to identify different components by selective signal detection. Results show that LSCM is an effective method to locate the small particles captured on and/or in the structure of the face masks. LSCM surface examination was performed to observe the small particles captured on the surface of fabric layers. Image analysis was used to quantify the small particles by total area to evaluate the filtration ability. Results show that the filtration layer captured greater number of small particles than other layers. Therefore, the filtration layer is the primary contributor to the filtration ability of the face mask. Statistical analysis was also performed to determine whether repellent finish had effect on the filtration ability of fabric layers. The results show that repellent finish only affects the filtration ability of the cover fabric. Repellent finished cover layers captured significantly fewer small particles than control cover layers in all face masks. However, there were no significant differences of small particle captured by the finished

cover layers of face masks between add-on levels 6% and 12%. Repellent finish on the cover fabric did not influence the filtration ability of the filtration layer of all face masks.

To study the effect of layering order on the filtration ability of the entire face mask, LSCM cross sectional examination was performed to evaluate the cross sections of the face masks and the penetration of small particles through the face masks. The results show that the filtration layer halts the penetration of small particles through face masks no matter whether the filtration is the second layer of a three-layer face mask or the second layer of a four-layer face mask or the third layer of a four-layer face mask. Although its location changed in the three layering orders, the filtration layer always stopped the penetration of the small particles.

Differential Pressures of face masks were determined by Nelson Laboratory and statistical analysis was performed to determine whether repellent finish and layering order had effects on the breathing resistance of the face masks. The results show that repellent finish does not affect the breathing resistance of the face mask while the layering order influences the breathing resistance significantly. Face masks with layering order one (cover fabric, filtration fabric and then shell fabric) provided better breathability than the face masks with the other two layering orders. However, according to the standard specification for performance of face masks, all three layering order could offer acceptable breathability.

According to the above analysis, parameters of the face mask can be optimized based on repellent finish and layering order. This would be a face mask treated with 4.5% add-on level of Zonyl® PPR protector on the cover fabric and a layering order of cover fabric, support fabric, filtration fabric and shell fabric. The repellent finish and layering order of this face mask would offer it the best fluid resistance with the lowest cost. Although 4.5% of repellent finish changes the filtration ability of the cover fabric, it does not affect the filtration ability of the filtration

layer that is the primary contributor to the barrier effectiveness of the face mask. In addition, the filtration layer used here halted the penetration of small particles through the face mask formed here. Therefore, this proposed face mask has superior filtration ability. Moreover, it still has a differential pressure lower than 4 mmH_2O/cm^2, offering a good breathability.

FUTURE WORK

Effects of repellent finish and layering order on the properties of surgical face masks were studied and a statistically designed face mask that has optimum fluid resistance, filtration ability and breathability was achieved based on repellent finish and layering order. Further research in the area would be recommended as following:

(1) Fluorochemicals may be applied in the spunbonded method to offer the fiber inherent repellent, then the effect can be studied to determine whether the treatment can offer better fluid resistance to the face mask,

(2) The filtration ability of face mask against bacteria and virus may be evaluated,

(3) Antimicrobial finish may be applied to the face mask to determine whether it offers the product with better filtration ability against bacterial and virus,

(4) Face fitting of the face mask may be studied to determine its effect on breathability,

(5) A face mask based on the predicted model may be generated and its properties evaluated.

REFERENCE

1. Geoff, F., Medical and hygiene textiles-continuing in good health, Technical Textiles International, April, 2002; 10-15.
2. Occupational Safety & Health Administration, Federal Register, 56, 64004-64182 (29 CFR Part 1910.1030), December, 1991.
3. Association of periOperative Registered Nurses, Recommended Practices for Standard and Transmission-based Precautions in the Preoperative Practice Setting, AORN Journal, Feb, 1999.
4. Centers for Disease Control. Morbidity and Mortality Weekly Report, Recommendations and Reports, Vol. 43, No. RR-13, October, 1994; 42.
5. ASTM, Annual Book of Standards (2000), American Society for Testing and Materials, Philadelphia, Pennsylvania.
6. ASTM, Annual Book of Standards (2001), American Society for Testing and Materials, Philadelphia, Pennsylvania.
7. Huang, W. and Leonas, K.K., One-Bath Application of Repellent and Antimicrobial Finishes to Nonwoven Surgical Gown Fabrics, Textile Chemist and Colorist, March, 1999; 11-16.
8. Huang, W. and Leonas, K.K., Evaluation a one-bath process for imparting antimicrobial activity and repellency to nonwoven surgical gown fabrics, Textile Research Journal, 70(9): 2000; 774-782.
9. Personal Communication, Michael M. Thomason, BBA Fiberweb, January 2003.
10. Shooter, R.A., Smith, M.A. and Hunter C.J.W., A study of surgical Masks, British Journal Surgery, Vol. 62, 1975; 246-249.

11. Madsen, P.O. and Madsen, R.E., A study of disposal surgical masks, American Journal of Surgery, Vol.114, 1967; 431-435.
12. Hogan, B., and Samaranayake, L.P., The surgical mask unmasked: A review, Oral Surgery, Vol.70, 1990; 34-36.
13. Leonas, K.K. Nonwovens Cooperative Research Center Project: Surgical Face Mask Barrier Effectiveness: Influence of Finish and Construction.
14. Ayliffe, G.A.J., Masks in surgery, Journal of Hospital Infection, Vol.18, 1991; 165-166.
15. Tunevall, T.G., Postoperative wound infections and surgical face masks: a controlled study, World Journal of Surgery, Vol.15, 1991; 383-388.
16. Greene, V.W. and Vesley, D., Method for evaluating effectiveness of surgical masks, Journal of Bacteriology, Vol. 83, 1962; 663-667.
17. Madsen, P.O. and Madsen, R.E., A study of disposal surgical masks, American Journal of Surgery, Vol.114, 1967; 431-435.
18. Quesnel, L.B., The efficiency of surgical masks of varying design and composition, British Journal of Surgery, Vol.62, 1975; 936-940.
19. Ford, C.R. and Peterson, D.E., The efficiency of surgical face masks, American Journal of Surgery, Vol.106, 1963; 954-957.
20. Ford, C.R., Peterson, D.E. and Mitchell C.R., An appraisal of the role of surgical face masks, American Journal of Surgery, Vol.113, 1967; 787-790.
21. Rogers, K.B., An investigation into the efficiency of disposable face masks, Journal of Clinical Pathology, Vol.33, 1980; 1086-1091.
22. Mil-M-36945C 4.4.1.1.1 Military Specifications: Surgical Mask, disposable.

23. ASTM, Annual Book of Standards (2004), American Society for Testing and Materials, Philadelphia, Pennsylvania.

24. Turbak, A.F., Introduction to nonwovens, TAPPI Press, Atlanta, Georgia, 1998.

25. Albrecht W., Fuchs, H., Kittelmann W., Nonwoven Fabrics, Weinheim, Cambridge: Wiley-VCH, 2003.

26. Tomasino, C., Chemistry and Technology of Fabric Preparation and Finish, North Carolina State University, Raleigh, North Carolina, 1996.

27. Contact angle website, http://www.ksvinc.com/contact_angle.htm.

28. Hinds, W.C., Aerosol Technology: Properties, Behavior, and Measurement of Airborne Particles, John Wiley and Sons, Inc., NY, 1999.

29. Weber, A., Willeke, K., Marchioni, R., Myojo, T., McKay, R., Donnelly, J. and Liebhaber, F., Aerosol penetration and leakage characteristics of mask used in the health care industry, American Journal of Infection Control. Vol.21, No.4, 1993; 167-173.

30. Chen, S., Vesley, D., Brosseau, L.M. and Vincent, J.H., Evaluation of single-use masks and respirators for protection of health care workers against mycobacterial aerosols, American Journal of Infection Control, Vol.22, No.2, 1994; 65-74.

31. Willeke, K., Qian, Y., Donnelly, J., Grinshpun, S. and Ulevicius, V., Penetration of Airborne Microorganisms Through a Surgical Mask and a Dust/Mist Respirator, American Industrial Hygiene Association Journal, Vol.57, 1996; 348-355.

32. National Institute for Occupational Safety and Health (NIOSH) Regulation 42 CFR Part 84, 1995.

33. Qian, Y., Willeke, K., Grinshpun, S.A., Donnelly, J. and Coffey, C.C., Performance of N95 Respirators: Filtration Efficiency for Airborne Microbial and Inert Particles, American Industrial Hygiene Association Journal, Vol.59, 1998; 128-132.

34. Qian, Y., Willeke, K., Grinshpun, S.A. and Donnelly, J., Performance of N95 Respirators: Reaerosolization of Bacteria and Solid Particles, American Industrial Hygiene Association Journal, Vol.58, 1997; 876-880.

35. Brosseau, L.M., McCullough N.V. and Vesley, D., Mycobacterial Aerosol Collection Efficiency of Respirator and Surgical Mask Filters Under Varying Conditions of Flow and Humidity, Applied Occupational Environmental Hygiene, Vol.12, No.6, 1997; 435-445.

36. McCullough N.V., Brosseau L.M. and Vesley D., Collection of Three Bacterial Aerosol by Respirator and Surgical Mask Filters Under Varying Conditions of Flow and Relative Humidity, Annual Occupational Hygiene, Vol.41, No.6, 1997; 677-690.

37. Anderson, A.A., New sampler for the collection, sizing, and enumeration of viable airborne particles. Journal of Bacteriology, Vol.6, 1992; 471-484.

38. Wadsworth L.C. and Davis W.T., A rapid latex filtration efficiency test method for simulating bacterial filtration efficiency, Particulate Microb Control, Vol. 2, 1983; 30-37.

39. Spurny K.R., Advances in Aerosol Filtration, CRC Press LLC, NY, 1998.

40. Brown R.C., Air filtration, Pergamon Press, Oxford 1993.

41. Davis, C.N., Aerosol Science, Academic Press, London and New York, 1966.

42. Davis, C.N., Air Filtration, Academic Press, Inc., NY, 1973.

43. Foldes-Papp, Z., Demel, U. and Tilz, G.P., Laser scanning confocal fluorescence microscopy: an overview, International Immunopharmacology, Vol.3, 2003; 1715–1729.

44. Leonas, K.K., Confocal Scanning Laser Microscopy: A Method To Evaluate Textile Structures, American Dyestuff Reporter, March, 1999; 15-18.

45. Pawley, B., Handbook of Biological Confocal Microscopy, Plenum Press, New York, 1995.

46. Confocal Microscopy Web Resources: http://www.mwrn.com/guide/light_microscopy/laser.htm

47. Leonas, K.K. and Huang, W., Transmission of Small Particles Through Selected Surgical Gown Fabrics, International Nonwovens Journal, March, 1999; 18-23.

48. Zonyl® PPR Protector Technical Bulletin.

49. Ciba Specialty Chemicals Website, http://www.cibasc.com

50. ASTM, Annual Book of Standards (1996), American Society for Testing and Materials, Philadelphia, Pennsylvania.

51. ASTM, Annual Book of Standards (1997), American Society for Testing and Materials, Philadelphia, Pennsylvania.

52. Technical Manual of the American Association of Textile Chemists and Colorists, 2000.

53. ImageJ website, http://rsb.info.nih.gov/ij/

54. Longnecker, M., An introduction to Statistical Methods and Data Analysis, Duxbury, 2001.

55. ASTM, Annual Book of Standards (2004), American Society for Testing and Materials, Philadelphia, Pennsylvania.

APPENDICES

APPENDIX A. Fluid Resistance Logistic Model

SAS Program

```
options ls=78;
data resistance;
   input finishing order pressure y n;
   cards;

0 1 80 10 10
0 1 120 0 10
0 1 160 0 10
0 2 80 10 10
0 2 120 2 10
0 2 160 0 10
0 3 80 10 10
0 3 120 9 10
0 3 160 7 10
6 1 80 10 10
6 1 120 8 10
6 1 160 0 10
6 2 80 10 10
6 2 120 10 10
6 2 160 1 10
6 3 80 10 10
6 3 120 10 10
6 3 160 10 10
12 1 80 10 10
12 1 120 10 10
12 1 160 0 10
12 2 80 10 10
12 2 120 10 10
12 2 160 10 10
12 3 80 10 10
12 3 120 10 10
12 3 160 10 10
3 2 120 . 10
4.5 3 160 10 10
;
run;
proc logistic data=resistance;
  class order/param=reference ref=first;
  model y/n=finishing order pressure;
  contrast 'order 2 vs 3' order 1 -1;
  output out=C p=pred l=lbp u=ubp/alpha=.05;
  proc print data=c;
  run;
```

SAS Output

The LOGISTIC Procedure

Model Information

Data Set	WORK.RESISTANCE
Response Variable (Events)	y
Response Variable (Trials)	n
Number of Observations	28
Model	binary logit
Optimization Technique	Fisher's scoring

Response Profile

Ordered Value	Binary Outcome	Total Frequency
1	Event	207
2	Nonevent	73

NOTE: 1 observation was deleted due to missing values for the response or explanatory variables.

Class Level Information

Class	Value	Design Variables 1	2
order	1	0	0
	2	1	0
	3	0	1

Model Convergence Status

Convergence criterion (GCONV=1E-8) satisfied.

Model Fit Statistics

Criterion	Intercept Only	Intercept and Covariates
AIC	323.330	74.658
SC	326.964	92.832
-2 Log L	321.330	64.658

The LOGISTIC Procedure

Testing Global Null Hypothesis: BETA=0

Test	Chi-Square	DF	Pr > ChiSq

Likelihood Ratio	256.6715	4	<.0001
Score	147.0206	4	<.0001
Wald	27.1974	4	<.0001

Type III Analysis of Effects

Effect	DF	Wald Chi-Square	Pr > ChiSq
finishing	1	21.5636	<.0001
order	2	25.6027	<.0001
pressure	1	25.9681	<.0001

Analysis of Maximum Likelihood Estimates

Parameter		DF	Estimate	Standard Error	Wald Chi-Square	Pr > ChiSq
Intercept		1	18.6602	3.7286	25.0456	<.0001
finishing		1	0.9267	0.1996	21.5636	<.0001
order	2	1	4.1486	1.1896	12.1609	0.0005
order	3	1	13.1485	2.6545	24.5343	<.0001
pressure		1	-0.1959	0.0385	25.9681	<.0001

Odds Ratio Estimates

Effect		Point Estimate	95% Wald Confidence Limits	
finishing		2.526	1.708	3.735
order	2 vs 1	63.343	6.153	652.109
order	3 vs 1	>999.999	>999.999	>999.999
pressure		0.822	0.762	0.886

Association of Predicted Probabilities and Observed Responses

Percent Concordant	97.9	Somers' D	0.971
Percent Discordant	0.8	Gamma	0.985
Percent Tied	1.3	Tau-a	0.376
Pairs	15111	c	0.986

The LOGISTIC Procedure

Contrast Test Results

Contrast	DF	Wald Chi-Square	Pr > ChiSq
order 2 vs 3	1	24.8014	<.0001

Obs	finishing	order	pressure	y	n	pred	lbp	ubp
1	0.0	1	80	10	10	0.95187	0.74893	0.99243
2	0.0	1	120	0	10	0.00774	0.00068	0.08175
3	0.0	1	160	0	10	0.00000	0.00000	0.00053
4	0.0	2	80	10	10	0.99920	0.98299	0.99996
5	0.0	2	120	2	10	0.33076	0.12978	0.62092
6	0.0	2	160	0	10	0.00019	0.00001	0.00583
7	0.0	3	80	10	10	1.00000	0.99996	1.00000
8	0.0	3	120	9	10	0.99975	0.99402	0.99999
9	0.0	3	160	7	10	0.61238	0.31289	0.84570
10	6.0	1	80	10	10	0.99981	0.99423	0.99999
11	6.0	1	120	8	10	0.66965	0.42532	0.84738
12	6.0	1	160	0	10	0.00080	0.00004	0.01499
13	6.0	2	80	10	10	1.00000	0.99949	1.00000
14	6.0	2	120	10	10	0.99227	0.92983	0.99920
15	6.0	2	160	1	10	0.04821	0.01050	0.19472
16	6.0	3	80	10	10	1.00000	1.00000	1.00000
17	6.0	3	120	10	10	1.00000	0.99981	1.00000
18	6.0	3	160	10	10	0.99757	0.96908	0.99981
19	12.0	1	80	10	10	1.00000	0.99981	1.00000
20	12.0	1	120	10	10	0.99810	0.97337	0.99987
21	12.0	1	160	0	10	0.17203	0.04945	0.45349
22	12.0	2	80	10	10	1.00000	0.99998	1.00000
23	12.0	2	120	10	10	0.99997	0.99741	1.00000
24	12.0	2	160	10	10	0.92938	0.62233	0.99058
25	12.0	3	80	10	10	1.00000	1.00000	1.00000
26	12.0	3	120	10	10	1.00000	0.99999	1.00000
27	12.0	3	160	10	10	0.99999	0.99890	1.00000
28	3.0	2	120	.	10	0.88847	0.66588	0.96955
29	4.5	3	160	10	10	0.99031	0.92755	0.99878

APPENDIX B Statistic Analysis of the Impact of Repellent Finishing on Filtration Ability of Face Masks

1. Cover layers of face masks with order one

SAS Program

```
options ls=78;

data filtraionorder1cover;
   input filtrationcover finishing;
   cards;
5924.16 0
6451.34 0
6456.06 0
6110.94 0
6636.00 0
7982.20 0
7336.08 0
6953.70 0
7822.64 0
5636.18 0
6336.56 0
6862.56 0
6459.33 0
6576.24 0
6048.27 0
6048.90 6
4245.30 6
6042.40 6
4348.90 6
4164.48 6
4347.32 6
5154.11 6
3048.43 6
3394.80 6
3356.01 6
3459.83 6
5212.86 6
5145.82 6
4680.00 6
3815.95 6
5064.78 12
5540.64 12
4273.40 12
4627.35 12
4656.12 12
4064.30 12
4874.36 12
4642.94 12
3404.65 12
4456.38 12
4111.48 12
4389.72 12
4979.52 12
```

```
5201.28 12
6204.87 12
;
run;

proc glm data=filtraionorder1cover;
  class finishing;
  model filtrationcover=finishing;
  output out=out1 p=pred  r=resid;
  means finishing/hovtest welch;
  contrast 'finishing 1 vs 2,3' finishing 2 -1 -1;
  contrast 'finishing 2 vs 3' finishing 0 -1 1;
  run;

proc gplot data=out1;
    plot resid*pred/vref=0;
run;
```

SAS Output

The GLM Procedure

Class Level Information

Class	Levels	Values
finishing	3	0 6 12

Number of observations 45

The GLM Procedure

Dependent Variable: filtrationcover

Source	DF	Sum of Squares	Mean Square	F Value	Pr > F
Model	2	43565768.29	21782884.15	36.71	<.0001
Error	42	24924518.57	593440.92		
Corrected Total	44	68490286.86			

R-Square	Coeff Var	Root MSE	filtrationcover Mean
0.636087	14.65480	770.3512	5256.648

Source	DF	Type I SS	Mean Square	F Value	Pr > F
finishing	2	43565768.29	21782884.15	36.71	<.0001

Source	DF	Type III SS	Mean Square	F Value	Pr > F
finishing	2	43565768.29	21782884.15	36.71	<.0001

The GLM Procedure

Levene's Test for Homogeneity of filtrationcover Variance
ANOVA of Squared Deviations from Group Means

Source	DF	Sum of Squares	Mean Square	F Value	Pr > F
finishing	2	1.76E12	8.798E11	1.68	0.1977
Error	42	2.193E13	5.222E11		

Welch's ANOVA for filtrationcover

Source	DF	F Value	Pr > F
finishing	2.0000	41.21	<.0001
Error	27.4424		

The GLM Procedure

Level of finishing	N	filtrationcover Mean	filtrationcover Std Dev
0	15	6639.48400	664.452403
6	15	4431.00733	945.020926
12	15	4699.45267	667.653510

The GLM Procedure

Dependent Variable: filtrationcover

Contrast	DF	Contrast SS	Mean Square	F Value	Pr > F
finishing 1 vs 2,3	1	43025296.57	43025296.57	72.50	<.0001
finishing 2 vs 3	1	540471.73	540471.73	0.91	0.3454

2. Filtration layers of face masks with order one

SAS Program

```
options ls=78;

data filtraionorder1;
   input filtration1 finishing;
   cards;
11333.28 0
10669.12 0
12695.02 0
13303.60 0
11635.30 0
11025.24 0
11112.04 0
10672.86 0
11988.75 0
10220.10 0
11551.77 0
10720.25 0
13360.70 0
11776.84 0
12021.20 0
13132.30 6
12656.40 6
12431.97 6
12938.16 6
15867.01 6
11656.56 6
12302.73 6
14248.08 6
11093.94 6
9790.00 6
11277.64 6
13886.62 6
16126.94 6
12484.80 6
14355.22 6
12076.48 12
12568.84 12
11203.20 12
12885.37 12
15363.90 12
13114.41 12
11358.75 12
11742.96 12
10379.84 12
10405.20 12
11802.81 12
13116.84 12
12579.48 12
12507.36 12
11290.50 12
;
run;
```

```
proc glm data=filtraionorder1;
  class finishing;
  model filtration1=finishing;
  output out=out1 p=pred  r=resid;
  means finishing/hovtest welch;
  contrast 'finishing 1 vs 2,3' finishing 2 -1 -1;
  contrast 'finishing 2 vs 3' finishing 0 -1 1;
  run;

proc gplot data=out1;
    plot resid*pred/vref=0;
run;
```

SAS Output

The GLM Procedure

Class Level Information

Class	Levels	Values
finishing	3	0 6 12

Number of observations 45

The GLM Procedure

Dependent Variable: filtration1

Source	DF	Sum of Squares	Mean Square	F Value	Pr > F
Model	2	13690052.84	6845026.42	3.75	0.0317
Error	42	76622139.35	1824336.65		
Corrected Total	44	90312192.19			

R-Square	Coeff Var	Root MSE	filtration1 Mean
0.151586	11.03636	1350.680	12238.45

Source	DF	Type I SS	Mean Square	F Value	Pr > F
finishing	2	13690052.84	6845026.42	3.75	0.0317

Source	DF	Type III SS	Mean Square	F Value	Pr > F

finishing	2	13690052.84	6845026.42	3.75	0.0317

The GLM Procedure

Levene's Test for Homogeneity of filtration1 Variance
ANOVA of Squared Deviations from Group Means

Source	DF	Sum of Squares	Mean Square	F Value	Pr > F
finishing	2	3.021E13	1.51E13	2.13	0.1314
Error	42	2.977E14	7.088E12		

Welch's ANOVA for filtration1

Source	DF	F Value	Pr > F
finishing	2.0000	3.58	0.0421
Error	26.5865		

The GLM Procedure

Level of finishing	N	filtration1 Mean	filtration1 Std Dev
0	15	11605.7380	948.98731
6	15	12949.8913	1733.33781
12	15	12159.7293	1252.18731

The GLM Procedure

Dependent Variable: filtration1

Contrast	DF	Contrast SS	Mean Square	F Value	Pr > F
finishing 1 vs 2,3	1	9007382.939	9007382.939	4.94	0.0317
finishing 2 vs 3	1	4682669.897	4682669.897	2.57	0.116

3. Cover layers of face masks with order two

SAS Program

```
options ls=78;
data order2cover;
   input cover2 finishing;
   cards;
6496.36 0
6286.24 0
6382.83 0
6543.60 0
7201.61 0
6624.80 0
6058.14 0
5628.61 0
6266.50 0
7482.06 0
6930.98 0
6913.98 0
6364.61 0
6909.54 0
7363.29 0
4172.76 6
4329.00 6
4300.94 6
5158.86 6
3637.29 6
6844.20 6
4544.87 6
3547.68 6
4370.84 6
5029.64 6
4662.84 6
5984.30 6
4863.30 6
5796.44 6
5649.44 6
6704.10 12
5369.13 12
3263.82 12
1823.04 12
3672.00 12
5140.66 12
3942.18 12
4378.80 12
3898.72 12
5884.48 12
4759.37 12
5197.50 12
6906.90 12
5949.20 12
4614.21 12
;
run;
proc glm data=order2cover;
  class finishing;
```

```
  model cover2=finishing;
  output out=out1 p=pred  r=resid;
  means finishing/hovtest welch;
  contrast 'finishing 1 vs 2,3' finishing 2 -1 -1;
  contrast 'finishing 2 vs 3' finishing 0 -1 1;
  run;

proc gplot data=out1;
    plot resid*pred/vref=0;
run;
```

SAS Output

```
                          The SAS System                              11
                                                 22:15 Monday, February 21, 2005

                          The GLM Procedure

                     Class Level Information

                Class         Levels    Values

                finishing          3    0 6 12


                 Number of observations    45

                          The SAS System                              12
                                                 22:15 Monday, February 21, 2005

                          The GLM Procedure

Dependent Variable: cover2

                                   Sum of
Source                     DF       Squares    Mean Square   F Value   Pr > F

Model                       2    33078880.59    16539440.30     17.17   <.0001

Error                      42    40456840.37      963258.10

Corrected Total            44    73535720.96


           R-Square     Coeff Var      Root MSE    cover2 Mean

           0.449834      18.11180      981.4571       5418.881


Source                     DF      Type I SS    Mean Square   F Value   Pr > F

finishing                   2    33078880.59    16539440.30     17.17   <.0001


Source                     DF    Type III SS    Mean Square   F Value   Pr > F

finishing                   2    33078880.59    16539440.30     17.17   <.0001
```

The GLM Procedure

Levene's Test for Homogeneity of cover2 Variance
ANOVA of Squared Deviations from Group Means

Source	DF	Sum of Squares	Mean Square	F Value	Pr > F
finishing	2	1.628E13	8.138E12	3.60	0.0359
Error	42	9.485E13	2.258E12		

Welch's ANOVA for cover2

Source	DF	F Value	Pr > F
finishing	2.0000	28.85	<.0001
Error	24.4090		

The GLM Procedure

Level of finishing	N	cover2 Mean	cover2 Std Dev
0	15	6630.21000	505.45732
6	15	4859.49333	905.57028
12	15	4766.94067	1346.93343

The GLM Procedure

Dependent Variable: cover2

Contrast	DF	Contrast SS	Mean Square	F Value	Pr > F
finishing 1 vs 2,3	1	33014635.62	33014635.62	34.27	<.0001
finishing 2 vs 3	1	64244.97	64244.97	0.07	0.797

4. Filtration layers of face masks with order two

SAS Program

```
options ls=78;

data filtraionorder2;
   input filtration2 finishing;
   cards;
11015.62 0
12564.04 0
11060.28 0
9924.72 0
11649.00 0
11589.50 0
11387.80 0
11129.52 0
9007.68 0
10221.12 0
11303.50 0
12206.00 0
10634.12 0
9608.27 0
11739.00 0
11361.04 6
12778.80 6
12696.96 6
17467.82 6
12430.08 6
12542.66 6
10234.00 6
11606.92 6
10879.92 6
11173.14 6
12852.00 6
13659.44 6
11629.96 6
11993.80 6
10296.00 6
12286.48 12
13675.88 12
14089.80 12
14777.25 12
14550.00 12
12503.52 12
11799.96 12
10432.56 12
9687.60 12
9272.43 12
12182.58 12
13424.70 12
9498.71 12
13722.24 12
13377.12 12
;
run;
```

```
proc glm data=filtraionorder2;
  class finishing;
  model filtration2=finishing;
  output out=out1 p=pred  r=resid;
  means finishing/hovtest welch;
  contrast 'finishing 1 vs 2,3' finishing 2 -1 -1;
  contrast 'finishing 2 vs 3' finishing 0 -1 1;
  run;

proc gplot data=out1;
    plot resid*pred/vref=0;
run;
```

SAS Output

The GLM Procedure

Class Level Information

Class	Levels	Values
finishing	3	0 6 12

Number of observations 45

The GLM Procedure

Dependent Variable: filtration2

Source	DF	Sum of Squares	Mean Square	F Value	Pr > F
Model	2	16823612.3	8411806.2	3.39	0.0433
Error	42	104358905.1	2484735.8		
Corrected Total	44	121182517.4			

R-Square	Coeff Var	Root MSE	filtration2 Mean
0.138829	13.28537	1576.304	11864.97

Source	DF	Type I SS	Mean Square	F Value	Pr > F
finishing	2	16823612.32	8411806.16	3.39	0.0433

Source	DF	Type III SS	Mean Square	F Value	Pr > F
finishing	2	16823612.32	8411806.16	3.39	0.0433

The GLM Procedure

Levene's Test for Homogeneity of filtration2 Variance
ANOVA of Squared Deviations from Group Means

Source	DF	Sum of Squares	Mean Square	F Value	Pr > F
finishing	2	4.729E13	2.364E13	1.20	0.3100
Error	42	8.244E14	1.963E13		

Welch's ANOVA for filtration2

Source	DF	F Value	Pr > F
finishing	2.0000	4.75	0.0177
Error	25.4620		

The GLM Procedure

Level of finishing	N	filtration2 Mean	filtration2 Std Dev
0	15	11002.6780	974.00266
6	15	12240.1693	1747.31653
12	15	12352.0553	1858.06654

The GLM Procedure

Dependent Variable: filtration2

Contrast	DF	Contrast SS	Mean Square	F Value	Pr > F
finishing 1 vs 2,3	1	16729723.75	16729723.75	6.73	0.0130
finishing 2 vs 3	1	93888.58	93888.58	0.04	0.846

5. Cover layers of face masks with order three

SAS Program

```
options ls=78;

data order3cover;
   input cover3 finishing;
   cards;
5932.25 0
6358.24 0
6494.00 0
4959.90 0
5208.84 0
6476.01 0
4988.34 0
8398.46 0
8538.30 0
4513.88 0
6116.53 0
5374.18 0
5252.97 0
6426.53 0
6386.48 0
4472.51 6
5061.61 6
4505.36 6
4392.05 6
4027.50 6
4099.10 6
6004.98 6
4649.89 6
4269.72 6
4810.86 6
4496.94 6
4736.20 6
4110.68 6
4369.12 6
4254.27 6
4254.27 12
4755.52 12
3905.72 12
4452.69 12
4244.52 12
4579.32 12
4557.10 12
3799.29 12
4115.85 12
4445.59 12
4152.33 12
4587.45 12
5031.38 12
4884.30 12
3984.76 12
;
run;
```

```
proc glm data=order3cover;
  class finishing;
  model cover3=finishing;
  output out=out1 p=pred  r=resid;
  means finishing/hovtest welch;
  contrast 'finishing 1 vs 2,3' finishing 2 -1 -1;
  contrast 'finishing 2 vs 3' finishing 0 -1 1;
  run;

proc gplot data=out1;
    plot resid*pred/vref=0;
run;
```

SAS Output

```
                          The SAS System                              21
                                                 22:15 Monday, February 21, 2005

                          The GLM Procedure

                     Class Level Information

                Class          Levels    Values

                finishing           3    0 6 12


                 Number of observations    45

                          The SAS System                              22
                                                 22:15 Monday, February 21, 2005

                          The GLM Procedure

Dependent Variable: cover3

                                    Sum of
Source                      DF       Squares    Mean Square   F Value   Pr > F

Model                        2    26712810.04    13356405.02     23.27   <.0001

Error                       42    24110635.65      574062.75

Corrected Total             44    50823445.69


           R-Square     Coeff Var      Root MSE    cover3 Mean

           0.525600      15.12409      757.6693       5009.684


Source                      DF      Type I SS    Mean Square   F Value   Pr > F

finishing                    2    26712810.04    13356405.02     23.27   <.0001


Source                      DF    Type III SS    Mean Square   F Value   Pr > F

finishing                    2    26712810.04    13356405.02     23.27   <.0001
```

The GLM Procedure

Levene's Test for Homogeneity of cover3 Variance
ANOVA of Squared Deviations from Group Means

Source	DF	Sum of Squares	Mean Square	F Value	Pr > F
finishing	2	1.188E13	5.94E12	4.53	0.0165
Error	42	5.504E13	1.311E12		

Welch's ANOVA for cover3

Source	DF	F Value	Pr > F
finishing	2.0000	14.47	<.0001
Error	25.1092		

The GLM Procedure

Level of finishing	N	cover3 Mean	cover3 Std Dev
0	15	6094.99400	1161.83648
6	15	4550.71933	492.45819
12	15	4383.33933	360.29042

The GLM Procedure

Dependent Variable: cover3

Contrast	DF	Contrast SS	Mean Square	F Value	Pr > F
finishing 1 vs 2,3	1	26502689.56	26502689.56	46.17	<.0001
finishing 2 vs 3	1	210120.48	210120.48	0.37	0.548

6. Filtration layers of face masks with order three

SAS Program

```
options ls=78;

data filtraionorder3;
   input filtration3 finishing;
   cards;
7799.09 0
8381.99 0
8610.80 0
7529.76 0
8931.80 0
8696.30 0
10686.72 0
8041.88 0
9093.48 0
6410.88 0
8299.06 0
7105.00 0
8224.78 0
9005.04 0
8591.70 0
12758.98 6
11244.48 6
7878.96 6
9149.28 6
5491.20 6
10468.80 6
7848.18 6
5600.58 6
10604.66 6
6834.24 6
3151.68 6
9031.52 6
9961.94 6
9031.52 6
10482.71 6
10935.52 12
10751.48 12
9405.76 12
9342.84 12
9400.82 12
9656.08 12
9174.00 12
6854.44 12
8839.76 12
10124.78 12
7885.92 12
9615.40 12
6996.70 12
5767.82 12
5967.75 12
;
run;
```

```
proc glm data=filtraionorder3;
  class finishing;
  model filtration3=finishing;
  output out=out1 p=pred  r=resid;
  means finishing/hovtest welch;
  contrast 'finishing 1 vs 2,3' finishing 2 -1 -1;
  contrast 'finishing 2 vs 3' finishing 0 -1 1;
  run;

proc gplot data=out1;
    plot resid*pred/vref=0;
run;
```

SAS Output

The GLM Procedure

Class Level Information

Class	Levels	Values
finishing	3	0 6 12

Number of observations 45

The GLM Procedure

Dependent Variable: filtration3

Source	DF	Sum of Squares	Mean Square	F Value	Pr > F
Model	2	1036851.3	518425.7	0.15	0.8579
Error	42	141494714.3	3368921.8		
Corrected Total	44	142531565.6			

R-Square	Coeff Var	Root MSE	filtration3 Mean
0.007275	21.41640	1835.462	8570.357

Source	DF	Type I SS	Mean Square	F Value	Pr > F
finishing	2	1036851.336	518425.668	0.15	0.8579

Source	DF	Type III SS	Mean Square	F Value	Pr > F
finishing	2	1036851.336	518425.668	0.15	0.8579

The GLM Procedure

Levene's Test for Homogeneity of filtration3 Variance
ANOVA of Squared Deviations from Group Means

Source	DF	Sum of Squares	Mean Square	F Value	Pr > F
finishing	2	2.065E14	1.033E14	4.05	0.0247
Error	42	1.072E15	2.552E13		

Welch's ANOVA for filtration3

Source	DF	F Value	Pr > F
finishing	2.0000	0.28	0.7546
Error	24.7675		

The GLM Procedure

Level of finishing	N	filtration3 Mean	filtration3 Std Dev
0	15	8360.55200	979.28632
6	15	8635.91533	2541.14864
12	15	8714.60467	1640.22170

The GLM Procedure

Dependent Variable: filtration3

Contrast	DF	Contrast SS	Mean Square	F Value	Pr > F
finishing 1 vs 2,3	1	990411.2526	990411.2526	0.29	0.5905
finishing 2 vs 3	1	46440.0839	46440.0839	0.01	0.907

APPENDIX C. Statistic Analysis of the Impact of Repellent Finishing and Layering order on Differential Pressure

1. Test of Normality

SAS Program

```
options ls=78;

data p;
   input finishing order p;
   cards;
0 1 1.9
0 1 2.1
0 2 2.4
0 2 2.3
0 3 2.3
0 3 2.3
6 1 2.1
6 1 2.0
6 2 2.1
6 2 2.3
6 3 2.3
6 3 2.3
12 1 2.1
12 1 2.1
12 2 2.4
12 2 2.3
12 3 2.3
12 3 2.3
;
run;

proc glm data=p;
  class order;
  model p=finishing order;
  output out=out1 p=pred  rstudent=resid;
  lsmeans order;
  contrast 'order 1 vs 2,3' order 2 -1 -1;
  contrast 'order 2 vs 3' order 0 -1 1;
  run;

proc gplot data=out1;
    plot resid*pred/vref=0;
run;

proc univariate data=out1 normal plot;
   var resid;
run;
```

SAS Output

The GLM Procedure

Class Level Information

Class	Levels	Values
order	3	1 2 3

Number of observations 18

The GLM Procedure

Dependent Variable: p

Source	DF	Sum of Squares	Mean Square	F Value	Pr > F
Model	3	0.25333333	0.08444444	12.90	0.0003
Error	14	0.09166667	0.00654762		
Corrected Total	17	0.34500000			

R-Square	Coeff Var	Root MSE	p Mean
0.734300	3.650407	0.080917	2.216667

Source	DF	Type I SS	Mean Square	F Value	Pr > F
finishing	1	0.00333333	0.00333333	0.51	0.4873
order	2	0.25000000	0.12500000	19.09	0.0001

Source	DF	Type III SS	Mean Square	F Value	Pr > F
finishing	1	0.00333333	0.00333333	0.51	0.4873
order	2	0.25000000	0.12500000	19.09	0.0001

The GLM Procedure
Least Squares Means

order	p LSMEAN
1	2.05000000
2	2.30000000
3	2.30000000

The GLM Procedure

Dependent Variable: p

Contrast	DF	Contrast SS	Mean Square	F Value	Pr > F
order 1 vs 2,3	1	0.25000000	0.25000000	38.18	<.0001
order 2 vs 3	1	0.00000000	0.00000000	0.00	1.0000

The UNIVARIATE Procedure
Variable: resid

Moments

N	18	Sum Weights	18
Mean	-0.0576369	Sum Observations	-1.0374636
Std Deviation	1.23564235	Variance	1.52681202
Skewness	-1.7755964	Kurtosis	4.5251414
Uncorrected SS	26.0156006	Corrected SS	25.9558044
Coeff Variation	-2143.8403	Std Error Mean	0.2912437

Basic Statistical Measures

Location		Variability	
Mean	-0.05764	Std Deviation	1.23564
Median	0.11482	Variance	1.52681
Mode	-0.22965	Range	5.57161
		Interquartile Range	0.69177

NOTE: The mode displayed is the smallest of 3 modes with a count of 3.

Tests for Location: Mu0=0

Test	-Statistic-		-----p Value------	
Student's t	t	-0.1979	Pr > |t|	0.8455
Sign	M	1.5	Pr >= |M|	0.6072
Signed Rank	S	11	Pr >= |S|	0.5510

Tests for Normality

Test	--Statistic---		-----p Value------	
Shapiro-Wilk	W	0.825051	Pr < W	0.0035
Kolmogorov-Smirnov	D	0.277976	Pr > D	<0.0100
Cramer-von Mises	W-Sq	0.227202	Pr > W-Sq	<0.0050
Anderson-Darling	A-Sq	1.236513	Pr > A-Sq	<0.0050

Quantiles (Definition 5)

Quantile	Estimate
100% Max	1.791387
99%	1.791387
95%	1.791387
90%	1.208584
75% Q3	0.462117

The UNIVARIATE Procedure
Variable: resid

Quantiles (Definition 5)

Quantile	Estimate
50% Median	0.114824
25% Q1	-0.229648
10%	-2.129333
5%	-3.780222
1%	-3.780222
0% Min	-3.780222

Extreme Observations

------Lowest------		------Highest-----	
Value	Obs	Value	Obs
-3.780222	9	0.462117	14
-2.129333	1	0.663212	7
-0.663212	8	0.947886	2
-0.229648	18	1.208584	15
-0.229648	17	1.791387	3

Stem	Leaf	#	Boxplot
1	28	2	0
0	0002225579	10	+-----+
-0	7222	4	+--+--+
-1			
-2	1	1	0
-3	8	1	*

----+----+----+----+

Normal Probability Plot

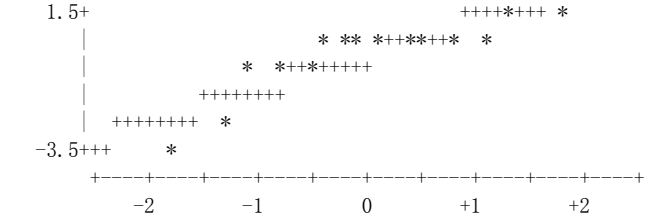

2. Nonparametric Test of Finishing

SAS Program

```
options ls=78;

data p;
   input finishing order p;
   cards;
0 1 1.9
0 1 2.1
0 2 2.4
0 2 2.3
0 3 2.3
0 3 2.3
6 1 2.1
6 1 2.0
6 2 2.1
6 2 2.3
6 3 2.3
6 3 2.3
12 1 2.1
12 1 2.1
12 2 2.4
12 2 2.3
12 3 2.3
12 3 2.3
;
run;
** Nonparametric 2-way ANOVA **;
proc sort data=p;
   by order;
   run;
PROC RANK data = p;
    BY order;    * Treat finishing as block ;
    VAR p;
    RANKS rp;
 RUN;

PROC ANOVA;
   CLASS  finishing order;
   MODEL rp = finishing order;
   TITLE2 'FRIEDMAN''S TWO-WAY NON-PARAMETRIC ANOVA';
RUN;
```

SAS Output

The SAS System 48
FRIEDMAN'S TWO-WAY NON-PARAMETRIC ANOVA
22:15 Monday, February 21, 2005

The ANOVA Procedure

Class Level Information

Class	Levels	Values
finishing	3	0 6 12
order	3	1 2 3

Number of observations 18

The SAS System 49
FRIEDMAN'S TWO-WAY NON-PARAMETRIC ANOVA
22:15 Monday, February 21, 2005

The ANOVA Procedure

Dependent Variable: rp Rank for Variable p

Source	DF	Sum of Squares	Mean Square	F Value	Pr > F
Model	4	4.08333333	1.02083333	0.57	0.6913
Error	13	23.41666667	1.80128205		
Corrected Total	17	27.50000000			

R-Square	Coeff Var	Root MSE	rp Mean
0.148485	38.34624	1.342118	3.500000

Source	DF	Anova SS	Mean Square	F Value	Pr > F
finishing	2	4.08333333	2.04166667	1.13	0.3518
order	2	0.00000000	0.00000000	0.00	1.000

3. Nonparametric Test of Layering Order

SAS Program

```
options ls=78;

data p;
   input finishing order p;
   cards;
0 1 1.9
0 1 2.1
0 2 2.4
0 2 2.3
0 3 2.3
0 3 2.3
6 1 2.1
6 1 2.0
6 2 2.1
6 2 2.3
6 3 2.3
6 3 2.3
12 1 2.1
12 1 2.1
12 2 2.4
12 2 2.3
12 3 2.3
12 3 2.3
;
run;

** Nonparametric 2-way ANOVA **;
PROC RANK data = p;
    BY finishing;    * Treat finishing as block ;
    VAR p;
    RANKS rp;
 RUN;

PROC ANOVA;
   CLASS  finishing order;
   MODEL rp = finishing order;
   TITLE2 'FRIEDMAN''S TWO-WAY NON-PARAMETRIC ANOVA';
RUN;
```

SAS Output

The ANOVA Procedure

Class Level Information

Class	Levels	Values
finishing	3	0 6 12
order	3	1 2 3

Number of observations 18

The ANOVA Procedure

Dependent Variable: rp Rank for Variable p

Source	DF	Sum of Squares	Mean Square	F Value	Pr > F
Model	4	33.25000000	8.31250000	8.82	0.0011
Error	13	12.25000000	0.94230769		
Corrected Total	17	45.50000000			

R-Square	Coeff Var	Root MSE	rp Mean
0.730769	27.73501	0.970725	3.500000

Source	DF	Anova SS	Mean Square	F Value	Pr > F
finishing	2	0.00000000	0.00000000	0.00	1.0000
order	2	33.25000000	16.62500000	17.64	0.0002